THE UNIVERSITY OF TEXAS AT AUSTIN

Dynamic Modeling and Optimal Scheduling of Chemical Processes Participating in Fast-Changing Electricity Markets: A Data-Driven Approach

Morgan Kelley
2022 Howes Scholar

Day-to-day capacity, load, and pricing in a deregulated market

- Increased capacity from renewables exacerbates variability issues
- Can lead to reliability problems

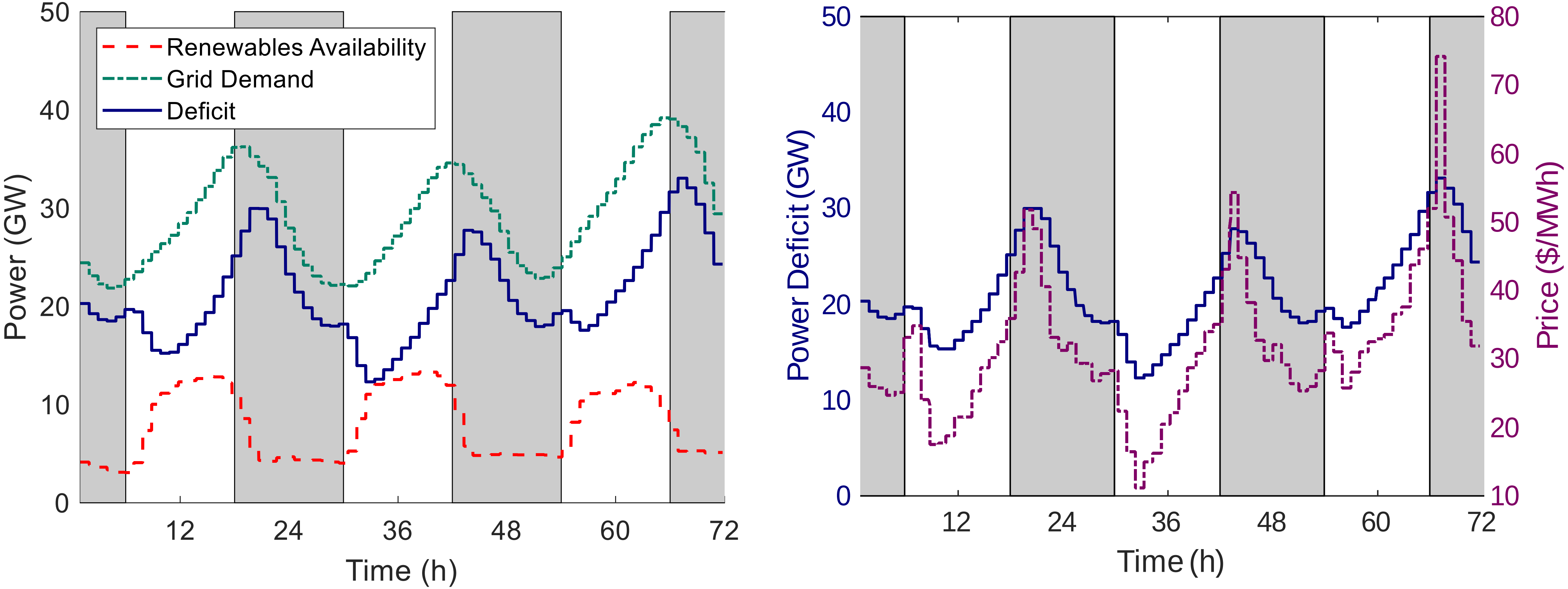

Renewables contribution, grid demand, and prices for July 3-5 2017 from data supplied by CAISO

CAISO. (2017). California Independent System Operator. Retrieved from http://www.caiso.com/Pages/default.aspx

Extreme example: Central Texas “does” winter

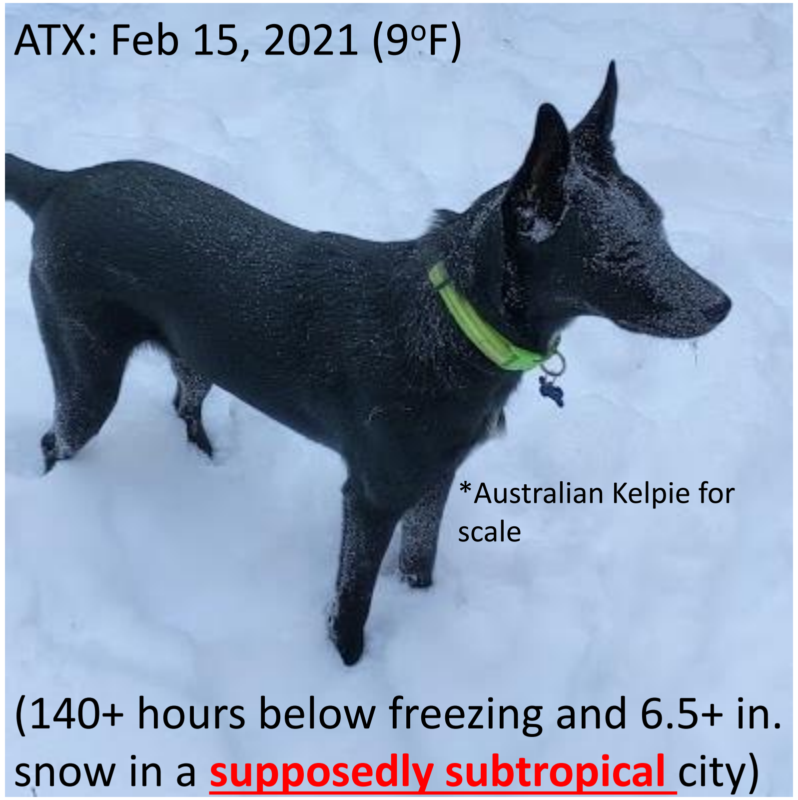

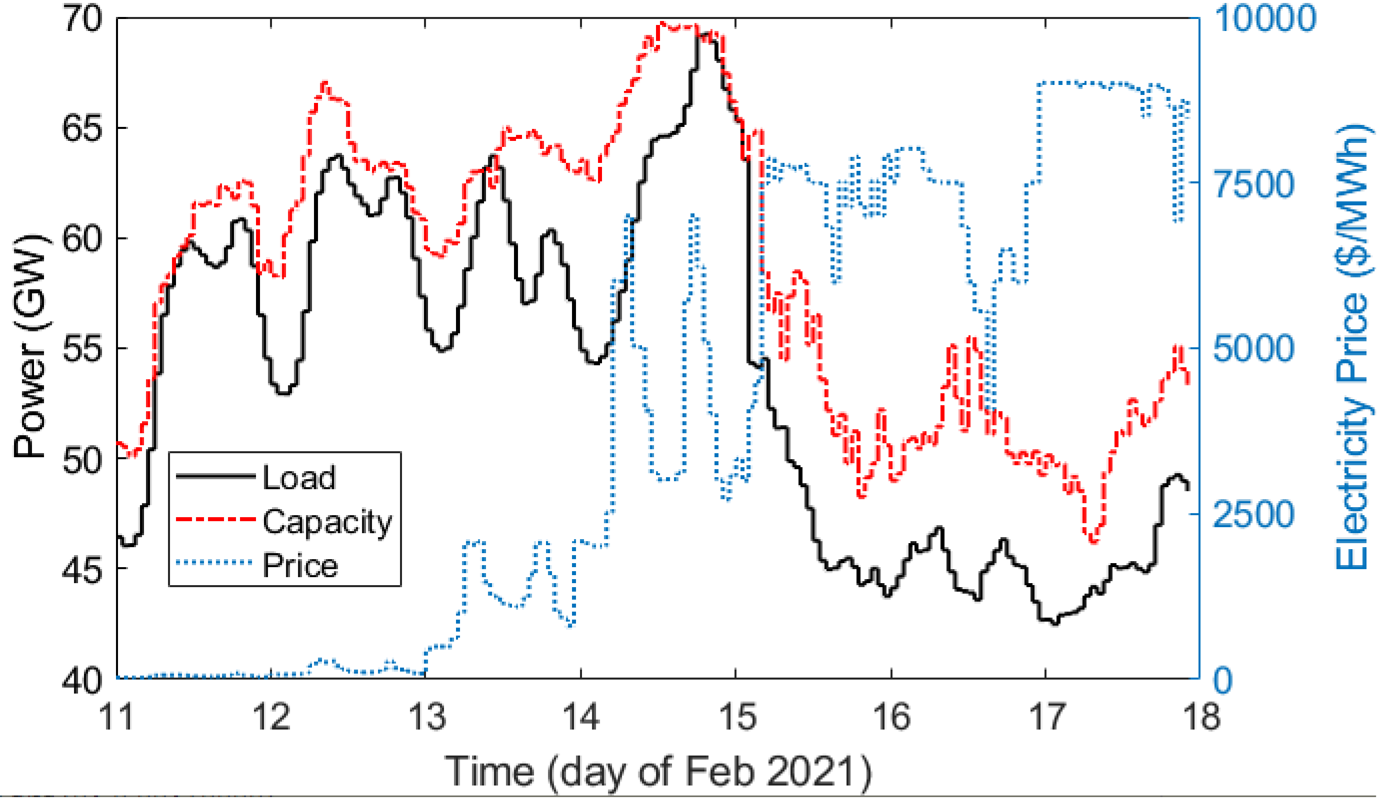

The case for integrated scheduling and control

- Competitive global markets place heightened emphasis on information exchange between all layers of the chemical supply chain
- E.g., fast-changing markets, distributed energy systems

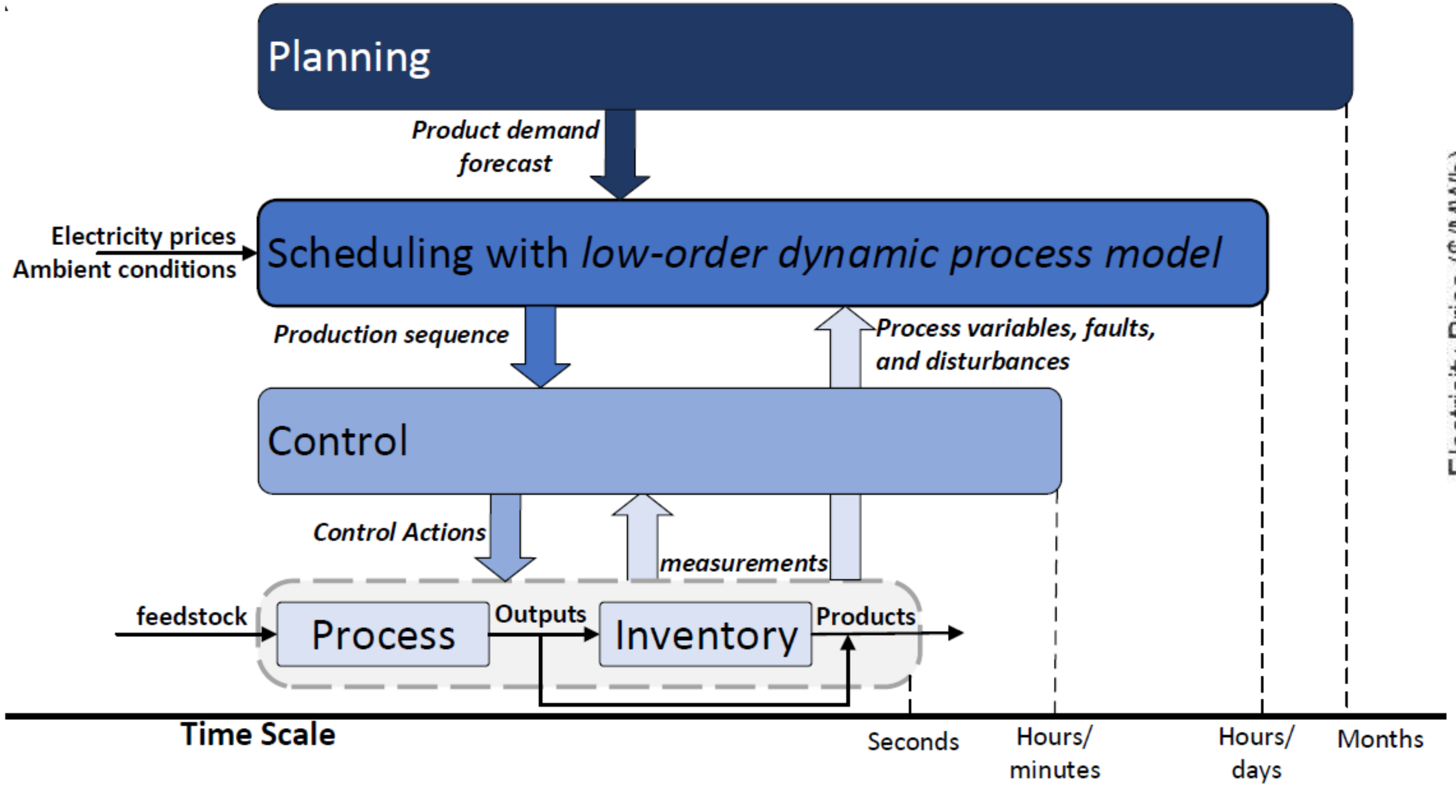

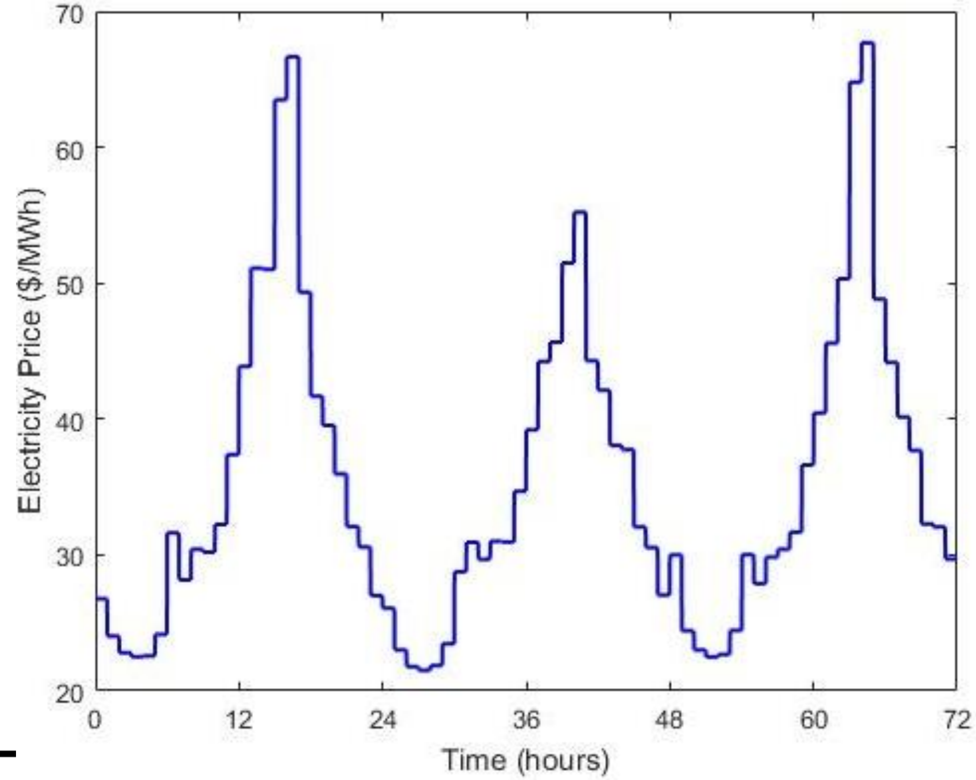

ERCOT. (2017). Energy Reliability Council of Texas. Retrieved April 3, 2017, from http://www.ercot.com/

Load Shifting: Industrial Participation

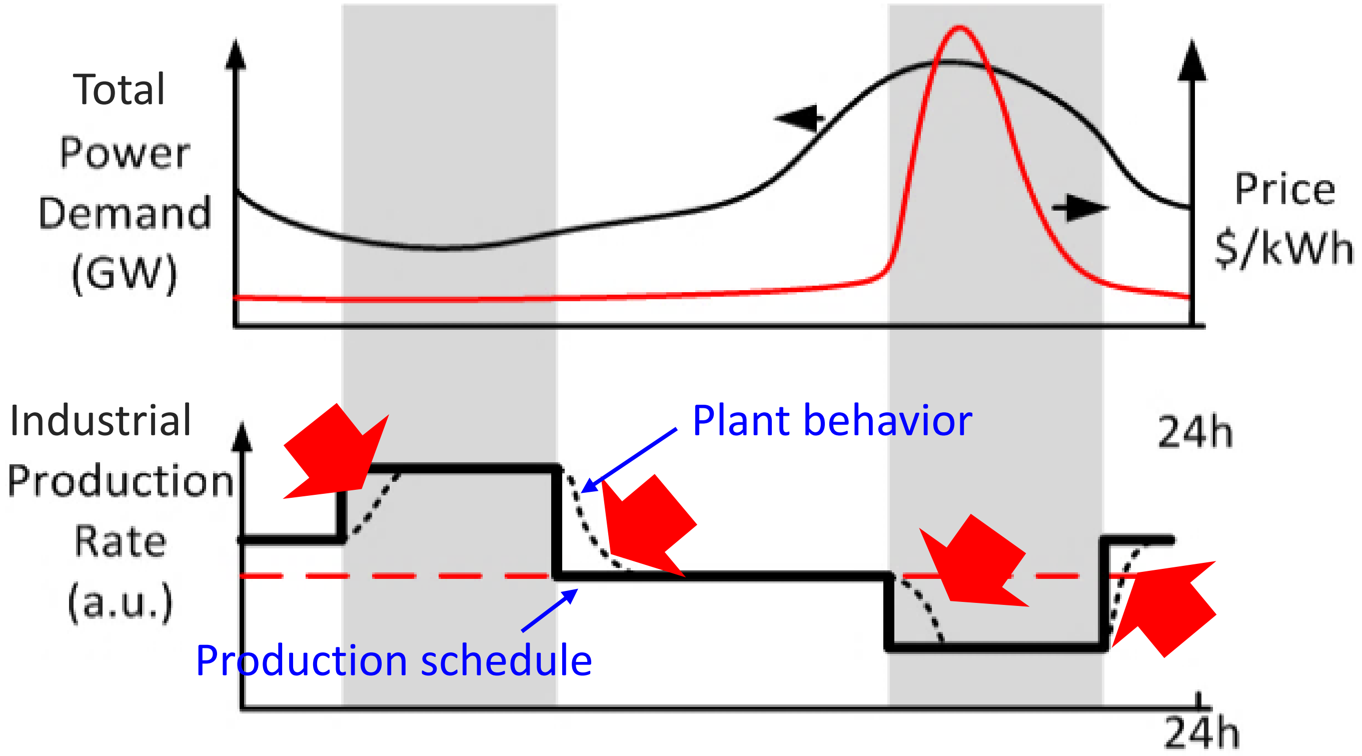

Requirements:
1. Account for plant dynamics
   a) Fast calculations(<1 hour)
2. MILP formulation
   a) Communicate model to power grid
   b) Favored in scheduling problems
   c) Powerful commercial solvers available

- **Paired events:** overproduce during low demand/emissions times and store extra product to use during peak hours when production is lower
  - Frequent schedule changes, account for process dynamics (same time scale as scheduling decisions)
  - Assumptions: excess capacity, product storage, fast transitions are possible

CAISO. (2017). California Independent System Operator. Retrieved from http://www.caiso.com/Pages/default.aspx

Requirements for integrating scheduling and control

- Fast and frequent changes in scheduling targets required to maximize profit
  - Scheduling slot length comparable to process time constants
- Combine longer (scheduling) time horizon with shorter (control) execution time
  - Nonlinear, stiff and high dimensional

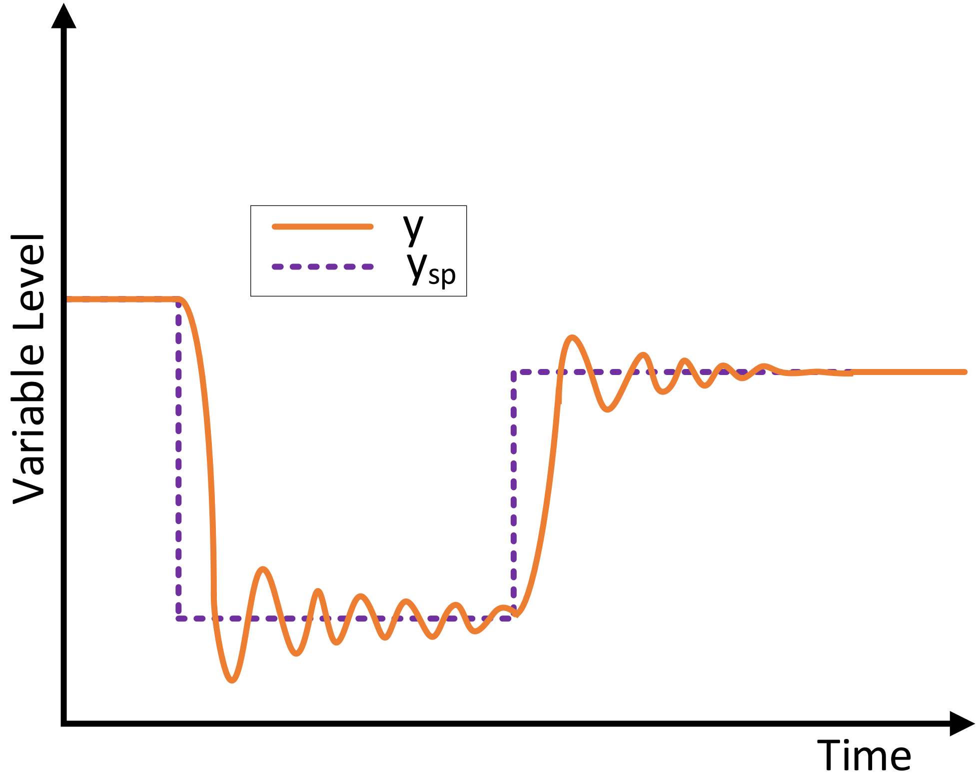

Baldea, M., & Harjunkoski, I. (2014). Integrated production scheduling and process control: A systematic review. *Computers & Chemical Engineering*, *71*, 377–390. https://doi.org/10.1016/j.compchemeng.2014.09.002

Multiple time grids for process representation

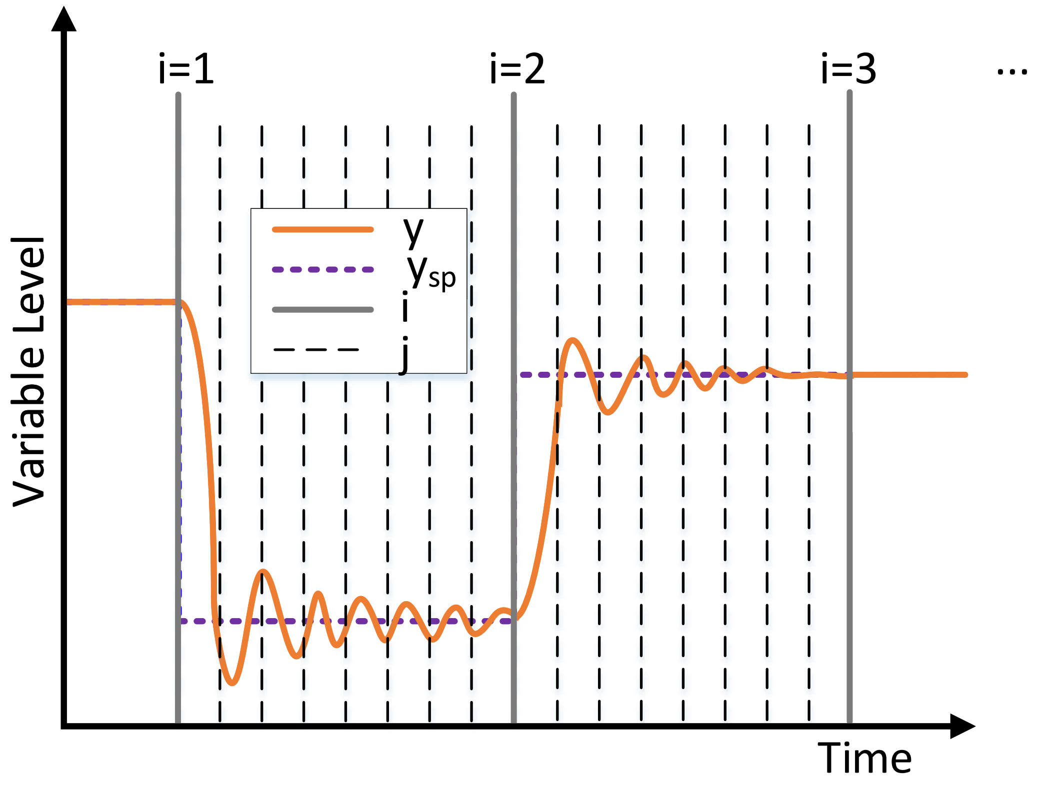

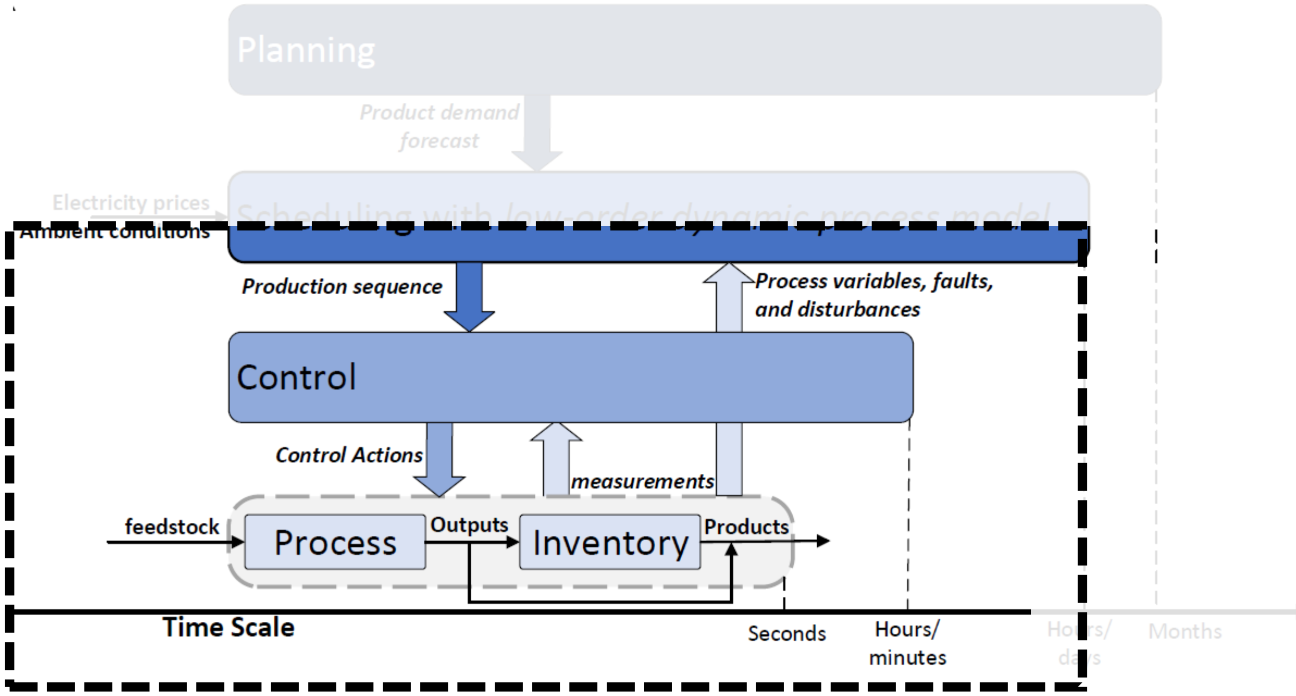

y_{sp} is supplied by the scheduling layer, and y is how the process reacts to y_{sp}

Scale-bridging models

Bridge disparate time scales between scheduling and process dynamics/control

- Low-order
- Utilize input/output (closed-loop) operating data
- Only capture scheduling-relevant variables

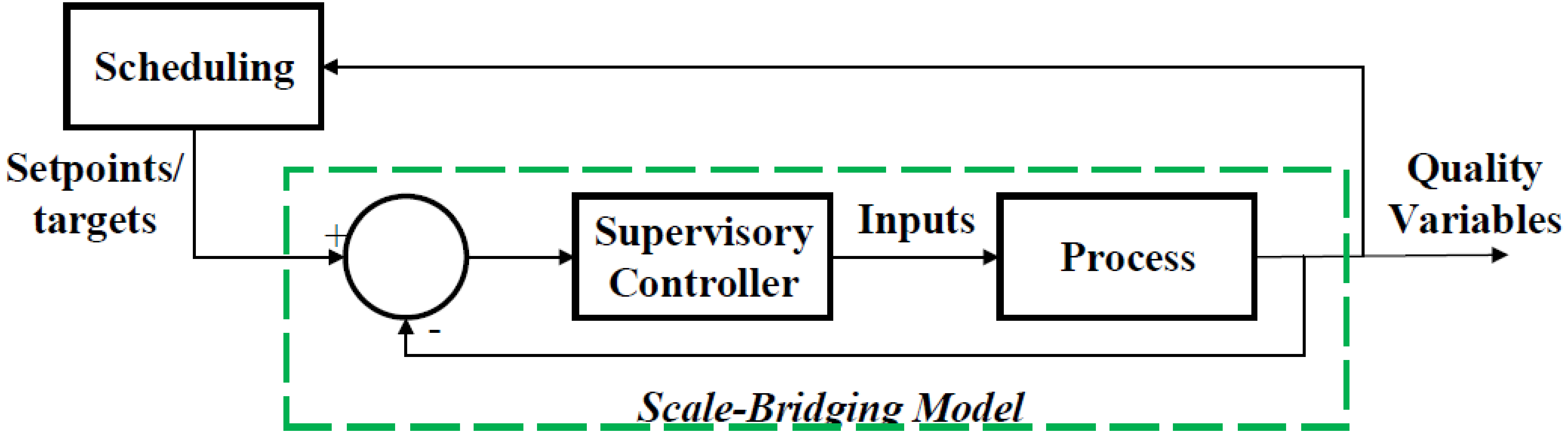

Du, J., Park, J., Harjunkoski, I., & Baldea, M. (2015). A time scale-bridging approach for integrating production scheduling and process control. *Computers & Chemical Engineering*, *79*, 59–69. https://doi.org/10.1016/j.compchemeng.2015.04.026

Removal of complicating constraints and parallel computing

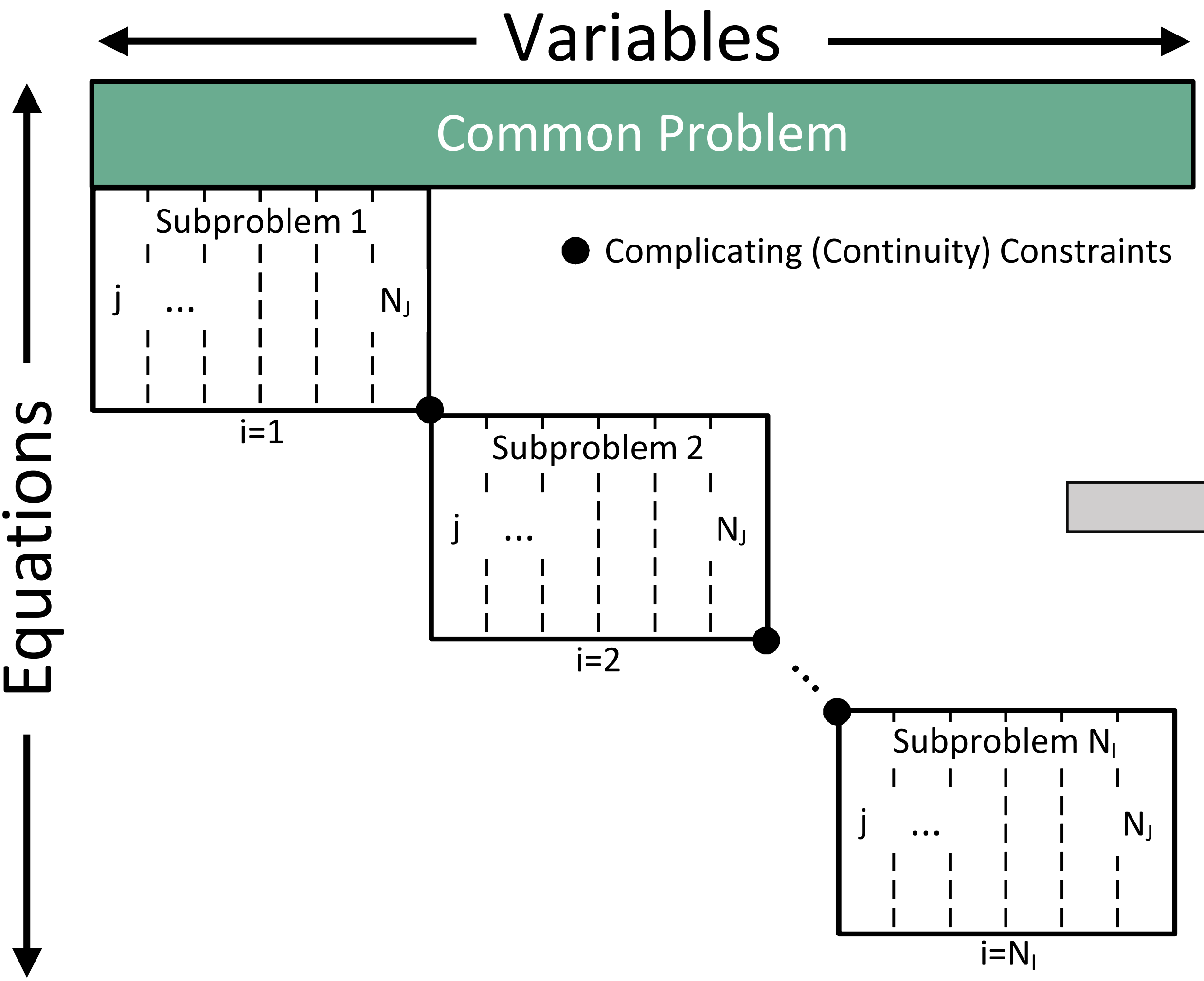

Now each subproblem can be solved independently

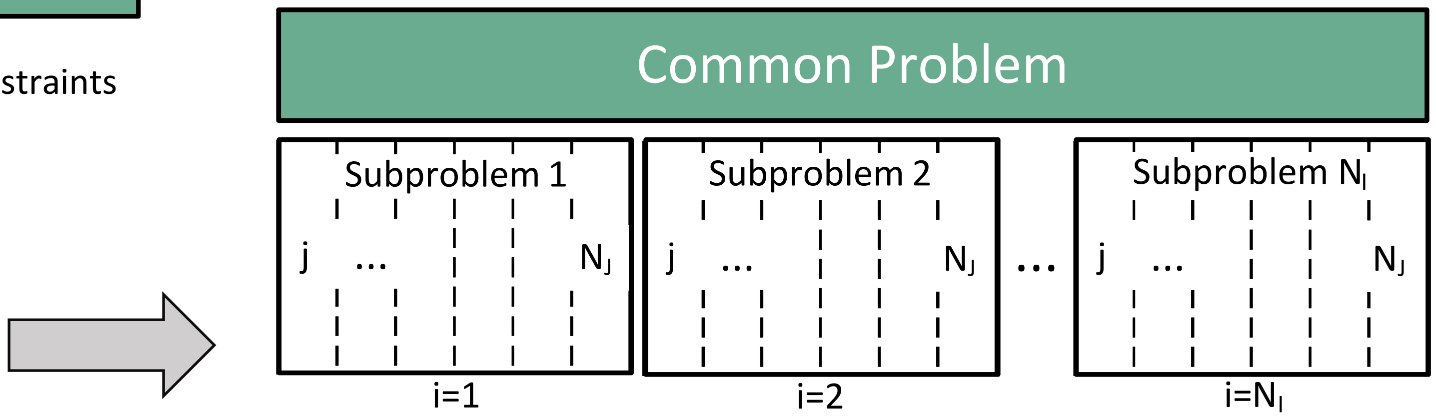

Difference between linking constraints are added to the objective

Kelley, M. T., Pattison, R. C., Baldick, R. & Baldea, M. An efficient MILP framework for integrating nonlinear process dynamics and control in optimal production scheduling calculations. *Comput. Chem. Eng.* 110, 35–52 (2018).

Lagrangian Relaxation

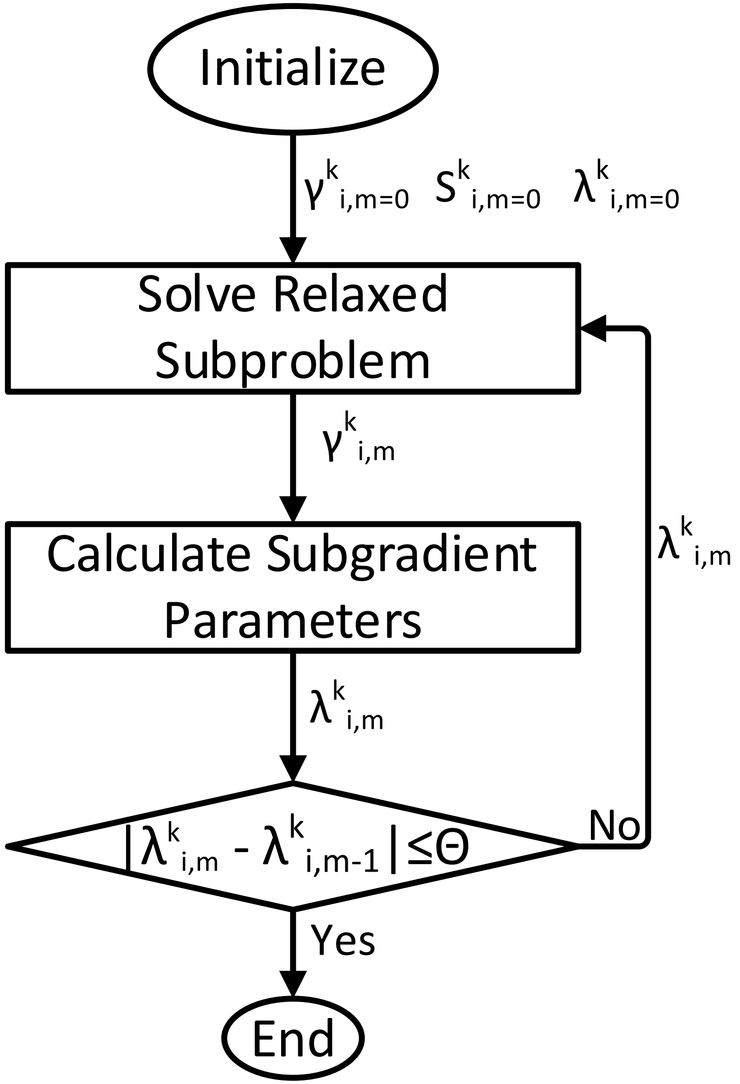

Guignard, M. Lagrangean relaxation. *Top* **11**, 151–200 (2003).

$$\gamma_i = \sqrt{\left(x^k_{i-1,N_j} - x^k_{i,j=1}\right)^2 + \epsilon} \quad \forall i > 1, k = 1 \ldots n$$

$$S_{i,m} = \frac{\theta_m (L_m - J_m)}{\varepsilon + \left\|\gamma^k_{i,m}\right\|_2}$$

$$\lambda_i = \max\left(0, \lambda^k_{i,m-1} S^k_{i,m} \gamma^k_{i,m}\right)$$

$$\left|\lambda^k_{\mathrm{i,m-1}} - \lambda^k_{\mathrm{im}}\right| \leq \Theta$$

Theorem in literature proves that **PI** is equivalent to **PII** in linear problems so long as a solution to **PI** exists

PII

$$\max L_m = J_m - \sum_{k=1}^{n} \sum_{i=2}^{N_I} \lambda^k_{im} \gamma^k_{im}$$

s.t.
Scale bridging models
Initial Conditions
Process/safety constraints
Quality constraints

Kelley, M. T., Pattison, R. C., Baldick, R. & Baldea, M. An efficient MILP framework for integrating nonlinear process dynamics and control in optimal production scheduling calculations. *Comput. Chem. Eng.* 110, 35–52 (2018).

“Small-Scale” Case study: Cryogenic Air Separation

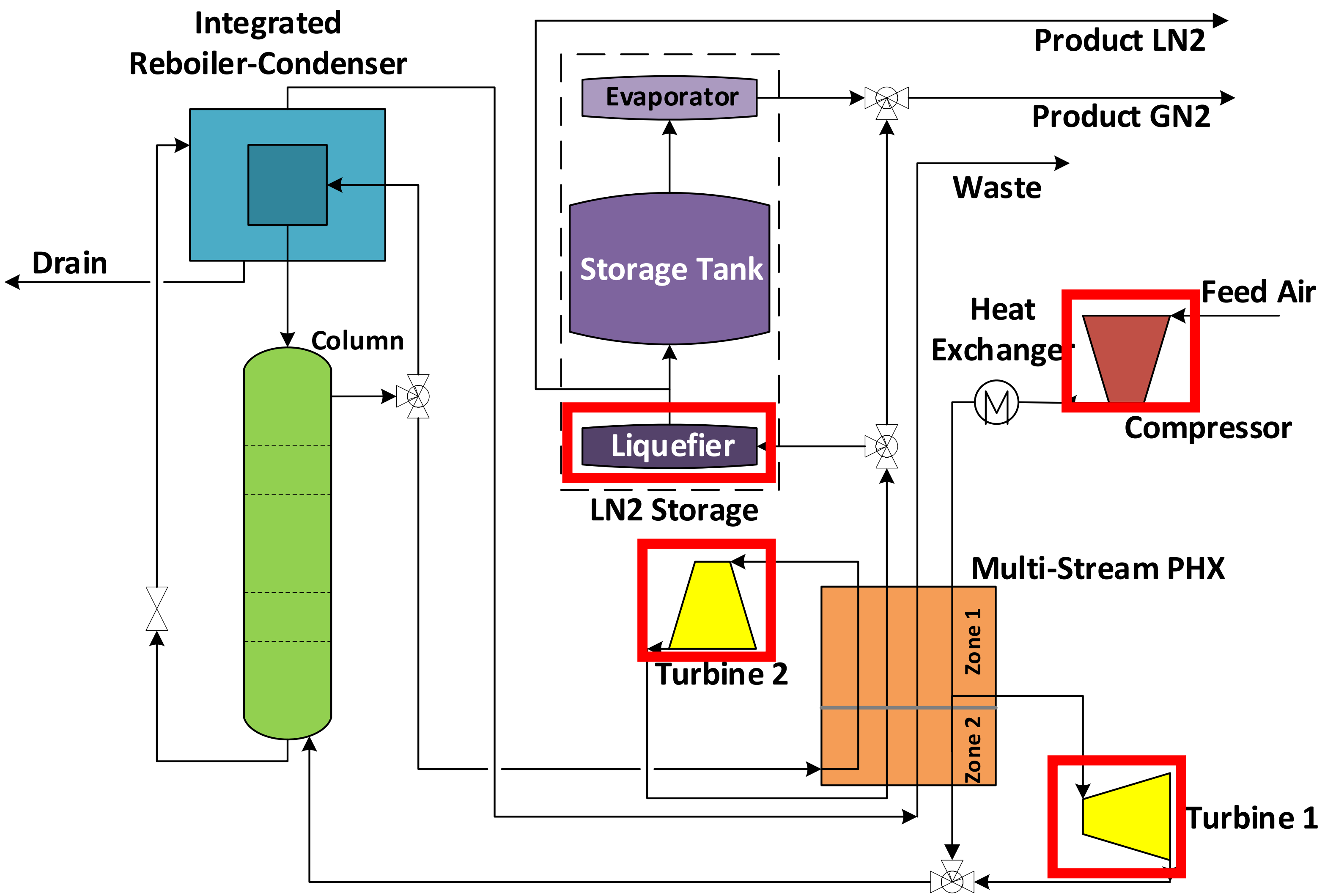

Industrial gas sector accounted for 2.62% of industrial electricity consumption in 2014

Products: LN_2, GN_2

Vary the inlet feed flowrate to modulate production levels

Longer time horizon=more savings

US EIA. (2017). *Manufacturing Energy Consumption Survey 2014*. Washington, D.C.

Summary of Small-Scale Case Study Results

Problem	Model	Predicted Cost ($)	Cost ($)	Savings (%)	CPU	Constraint Violations?
P1	Full-Order	--	1,012.56	1.22	94.62h	N
P2	Nonlinear SBM	1,014.81	1,014.68	1.01	5.10h	N
P3	Discrete SBM	1,013.31	1,013.64	1.12	11.7min	N
P4	Discrete SBM+LR	1,013.31	1,013.64	1.12	7.12min	N
Constant Prod. Rate*	--	--	1,025.09	--	--	--

*Reference problem

Same solution

Solution time improvement

P3:
Continuous Variables: 85,131
Integer Variables: 1,512
P4:
Continuous Variables: 90,325
Integer Variables: 1,512

Kelley, M. T., Pattison, R. C., Baldick, R. & Baldea, M. An MILP framework for optimizing demand response operation of air separation units. *Appl. Energy* 222, 951–966 (2018).

Power Requirements

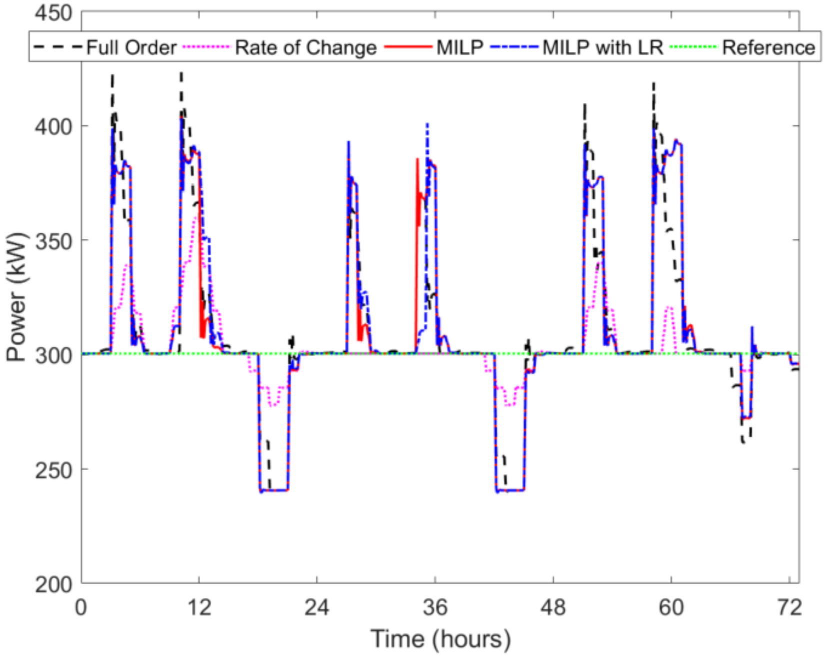

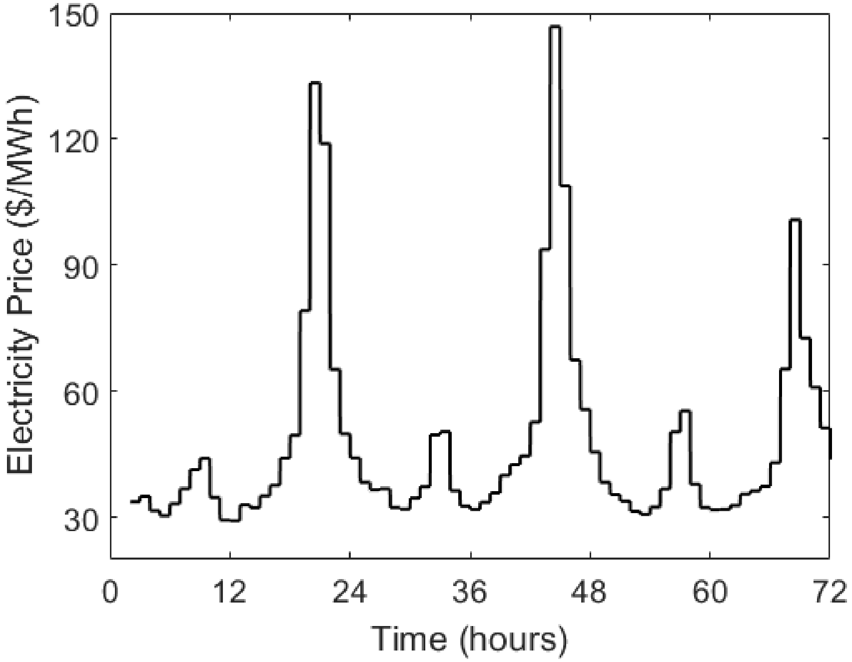

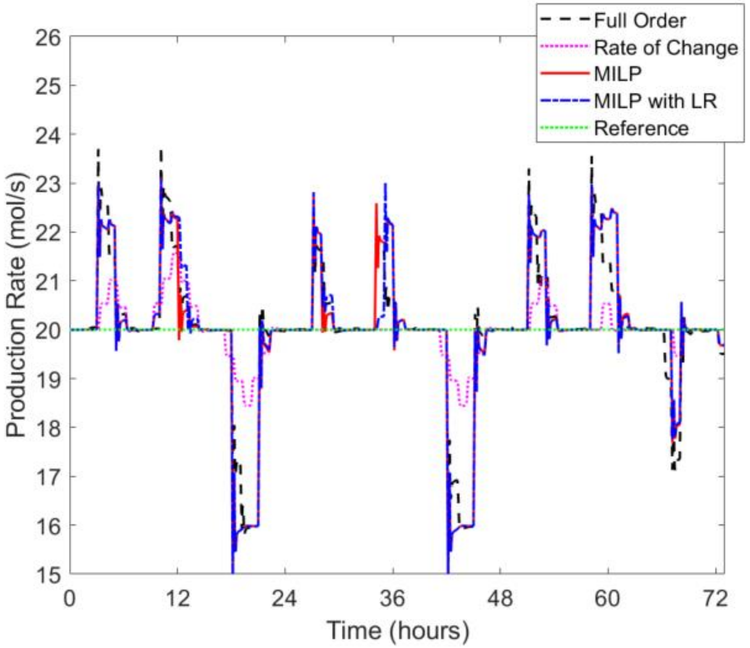

Increases overall energy use (+0.64 MWh, +2.97%)

N_2 liquefaction for storage

Decreases **peak** demand (-0.061MW, -20.00%)

Specific Power Consumption: 0.15 MWh/ton N_2

Future work: Network of ASUs operating together to meet localized demand

Kelley, M. T., Pattison, R. C., Baldick, R. & Baldea, M. An MILP framework for optimizing demand response operation of air separation units. *Appl. Energy* 222, 951–966 (2018).

Large-Scale Case study: industrial-scale demand response

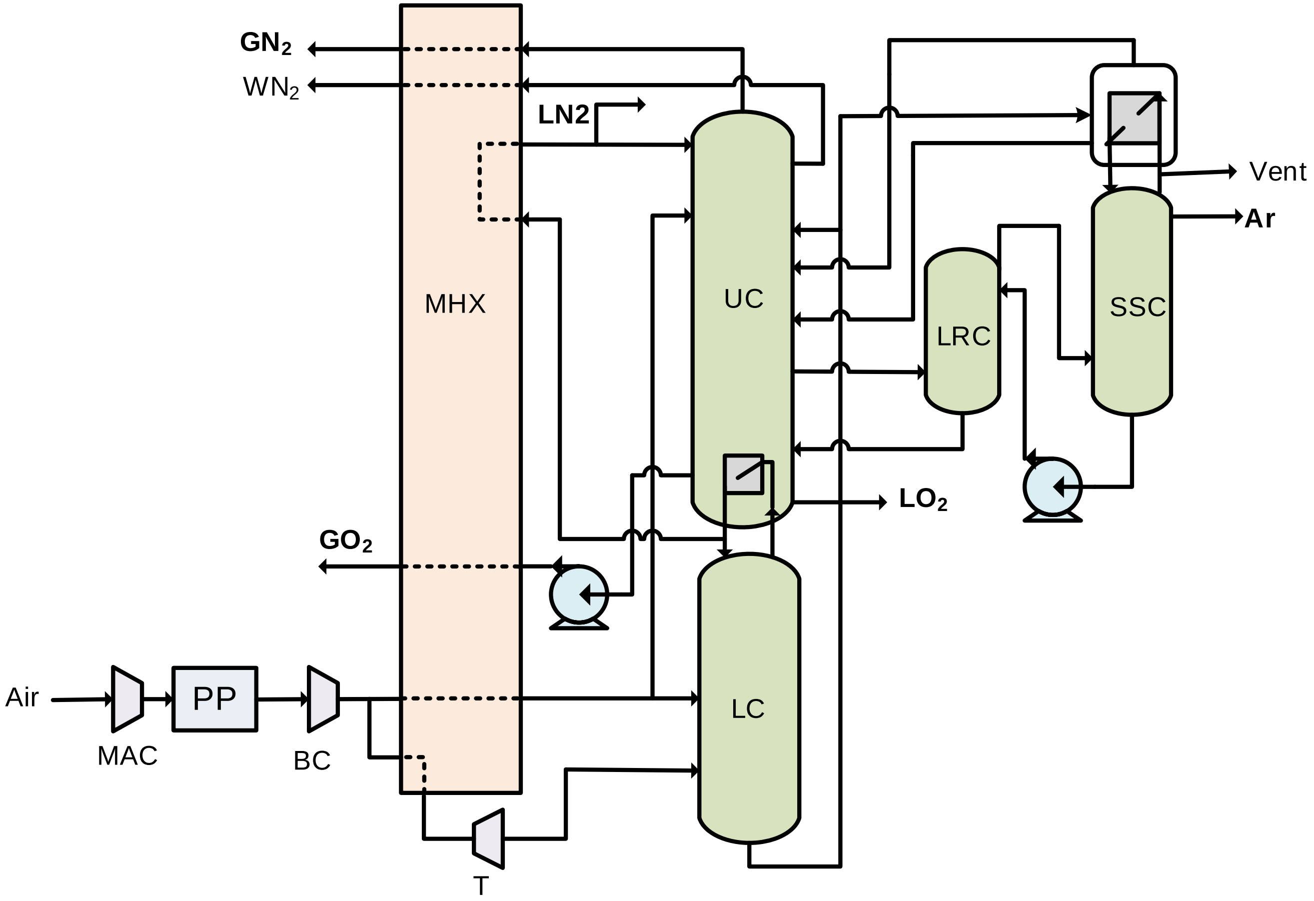

Industrial ASU producing LO2, GO2, LN2, GN2, and Ar

Fit linear ARX models to historical data from 1 year of operation

Model Structure: ARX

$$y(t) + a_1 y(t-1) + \cdots + a_{na} y(t-n_a) = b_1 u(t-n_k) + \cdots + b_{nb} u(t-n_b-n_k+1) + e(t)$$

n_a: number of poles
n_b: number of zeros
n_k: dead time

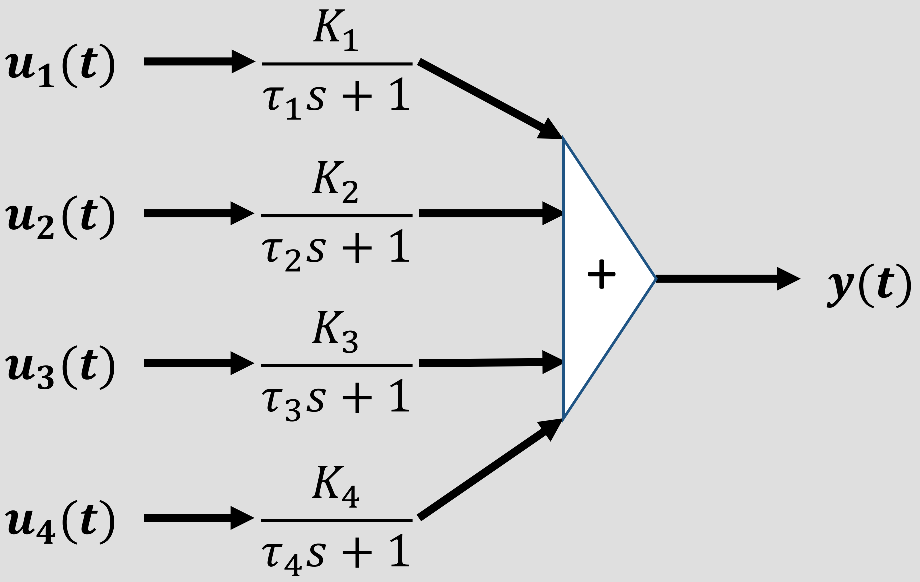

DR Scheduling problem structure: ARX models

$$y(t) + a_1 y(t-1) + \cdots + a_{na} y(t-n_a) = b_1 u(t-n_k) + \cdots + b_{nb} u(t-n_b-n_k+1) + e(t)$$

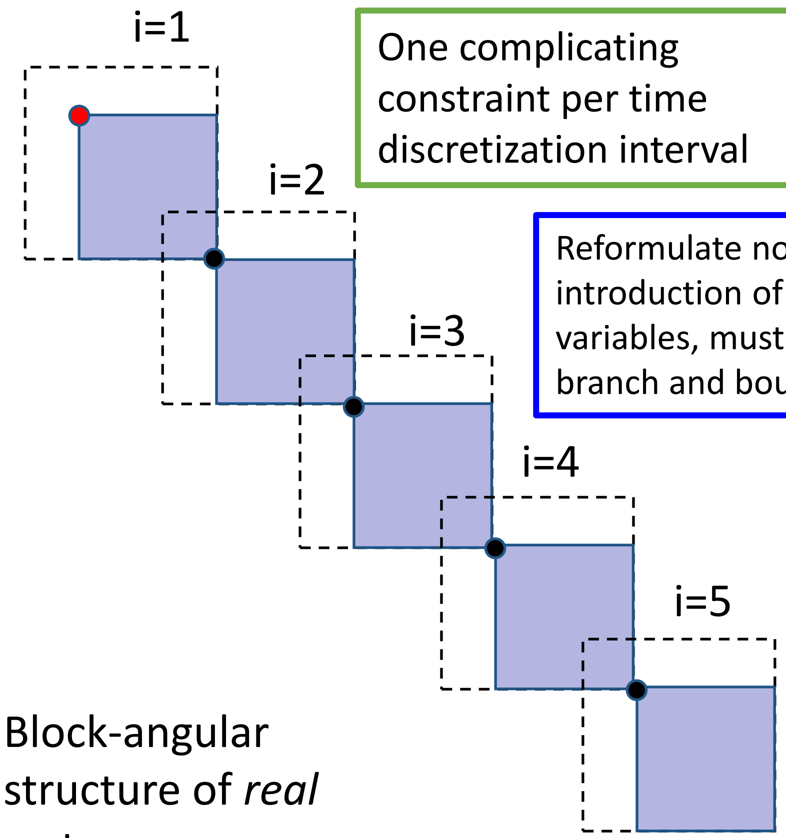

One complicating constraint per time discretization interval

Reformulate nonlinearity: introduction of integer variables, must solve using branch and bound algorithm

Block-angular structure of *real* system

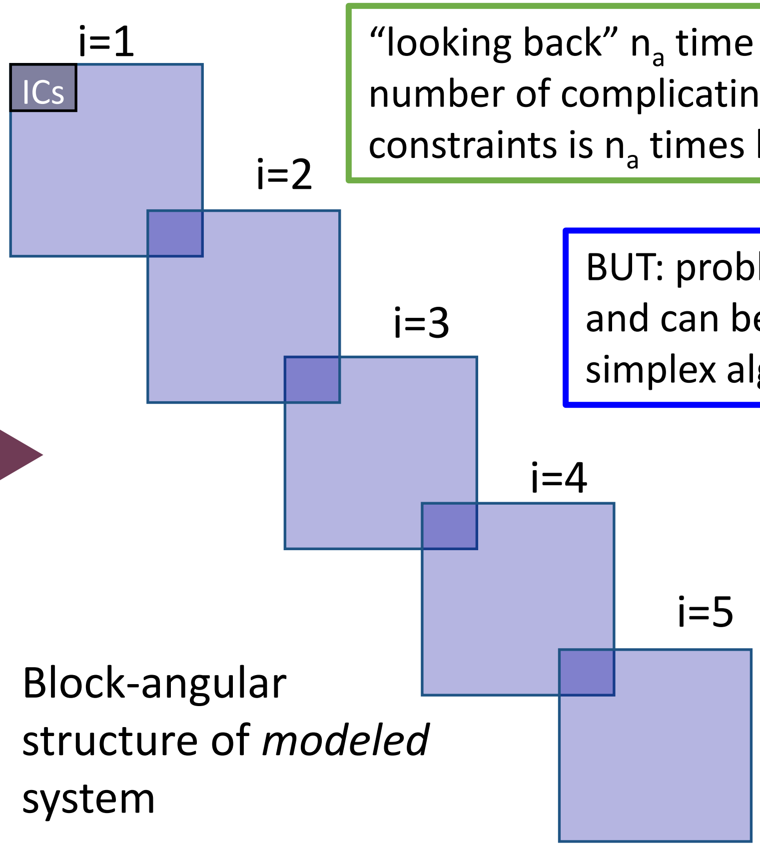

“looking back” n_a time steps: number of complicating constraints is n_a times higher

BUT: problem is an LP and can be solved with simplex algorithm

Block-angular structure of *modeled* system

Modeling measurement error

Key challenge: data-driven models inherit any measurement errors and/or biases from plant sensors

- These errors will then propagate to optimal setpoints provided by the DR problem—solutions will not be physically meaningful (e.g. mass balances won't close)

Solution: compute relevant errors from given data and model these errors using ARX models—capture both error magnitude and dynamics

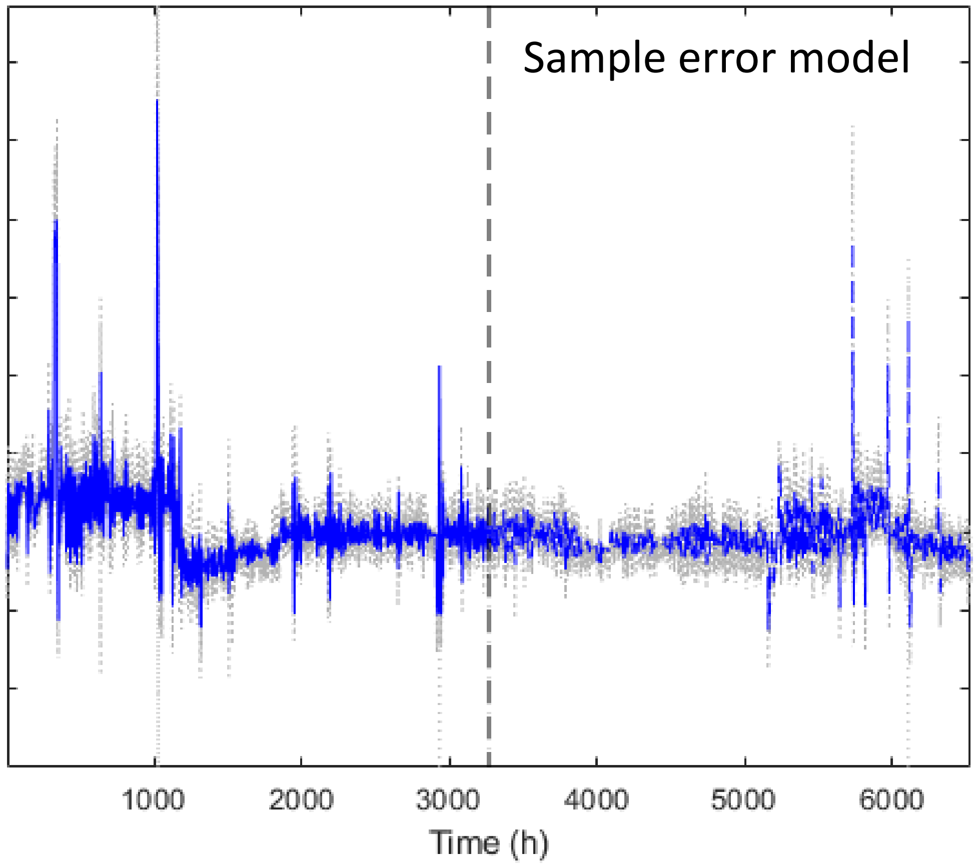

Morgan T. Kelley, Calvin Tsay, Yanan Cao, Yajun Wang, Jesus Flores-Cerrillo, Michael Baldea, A data-driven linear formulation of the optimal demand response scheduling problem for an industrial air separation unit, Chemical Engineering Science, Volume 252, 2022, 117468, ISSN 0009-2509, https://doi.org/10.1016/j.ces.2022.117468.

Large-Scale: ARX model fits

Variable	Input	n_a	n_b	NMSE (training)	NMSE (test)
P_1	PC_1, PC_2, T	2	2	7.8561e-09	8.2419e-09
P_2	PC_1, PC_2, T	2	2	1.8987e-09	1.6896e-09
P_3	PC_1, PC_2, T	2	2	2.2687e-08	2.4331e-08
F_{GN2}	$f(\bar{F}_{air})$	3	3	7.8075e-08	5.9252e-08
F_{LN2}	$\bar{F}_{LN2}$	3	3	4.2225e-10	3.5797e-10
F_{GO2}	$\bar{F}_{GO2}$	3	3	4.988e-10	4.551e-10
F_{LO2}	$f(\bar{F}_{air}, \bar{F}_{GO2})$	1	1	1.1259e-07	1.7783e-07
F_{Ar}	$\bar{F}_{Ar}$	3	3	4.0058e-09	1.8106e-09
F_{Air}	$\bar{F}_{air}$	3	1	1.1312e-10	6.6157e-11
C_F	$\bar{F}_{air}$	3	3	1.0325e-09	9.2544e-10

NMSE values are all very small
Process knowledge was used to select model inputs

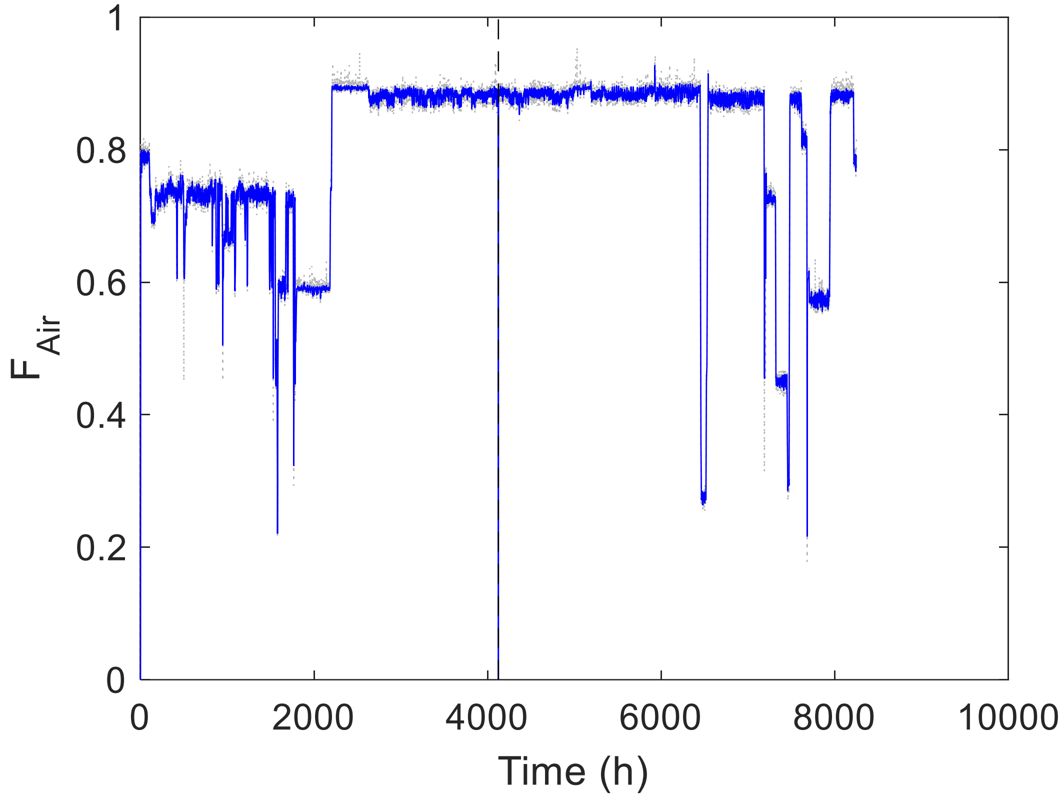

ARX model of the inlet air flow
Data is scaled between upper and lower bounds

Morgan T. Kelley, Calvin Tsay, Yanan Cao, Yajun Wang, Jesus Flores-Cerrillo, Michael Baldea, A data-driven linear formulation of the optimal demand response scheduling problem for an industrial air separation unit, Chemical Engineering Science, Volume 252, 2022, 117468, ISSN 0009-2509, https://doi.org/10.1016/j.ces.2022.117468.

Optimal Schedule

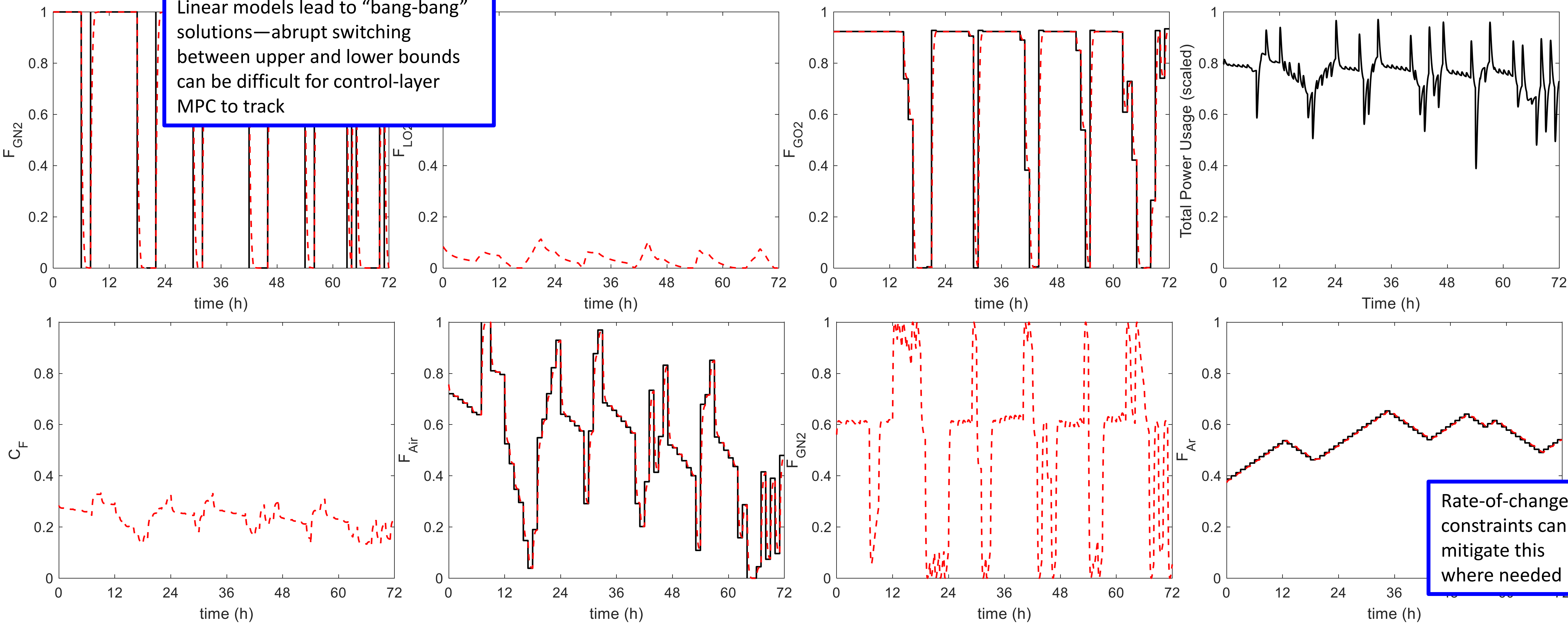

Linear models lead to “bang-bang” solutions—abrupt switching between upper and lower bounds can be difficult for control-layer MPC to track

Rate-of-change constraints can mitigate this where needed

Cost savings: 8.91% (compared to no DR)

Computation time: 1.97 mins

Morgan T. Kelley, Calvin Tsay, Yanan Cao, Yajun Wang, Jesus Flores-Cerrillo, Michael Baldea, A data-driven linear formulation of the optimal demand response scheduling problem for an industrial air separation unit, Chemical Engineering Science, Volume 252, 2022, 117468, ISSN 0009-2509, https://doi.org/10.1016/j.ces.2022.117468.

In Practice: Transfer learning of model parameters

Future work: Adaptation of current models to new plants

Parameter Updates

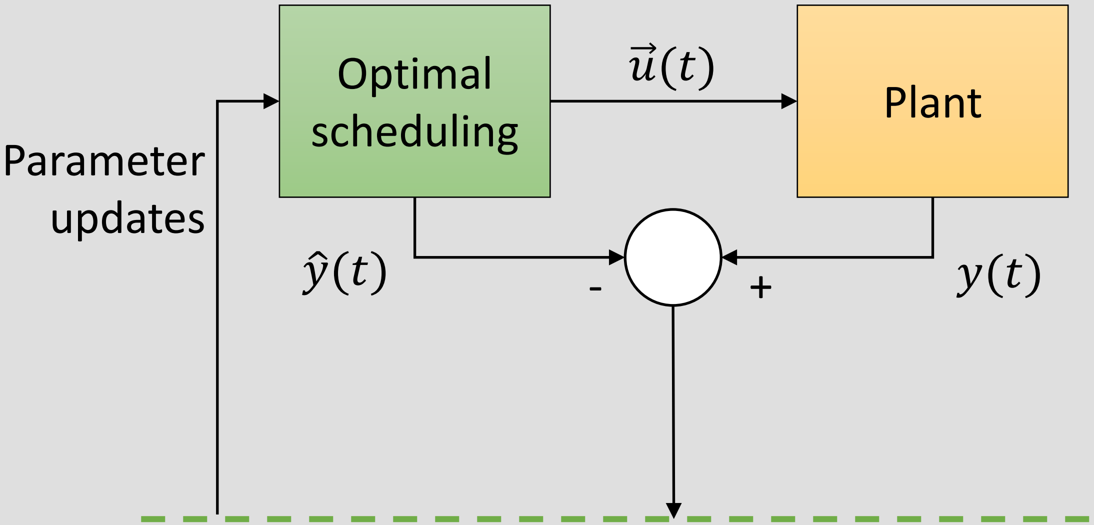

Kalman Filter

$$\hat{\theta}(t) = \hat{\theta}(t-1) + K(t)\big(y(t) - \hat{y}(t)\big)$$

$$\hat{y}(t) = \psi^T \hat{\theta}(t-1)$$

$$K(t) = Q(t)\psi(t)$$

$$Q(t) = \frac{P(t-1)}{R_2 + \psi^T(t)P(t-1)\psi(t)}$$

$$P(t) = P(t-1) + R_1 - \frac{P(t-1)\psi(t)\psi^T(t)P(t-1)}{R_2 + \psi^T(t)P(t-1)\psi(t)}$$

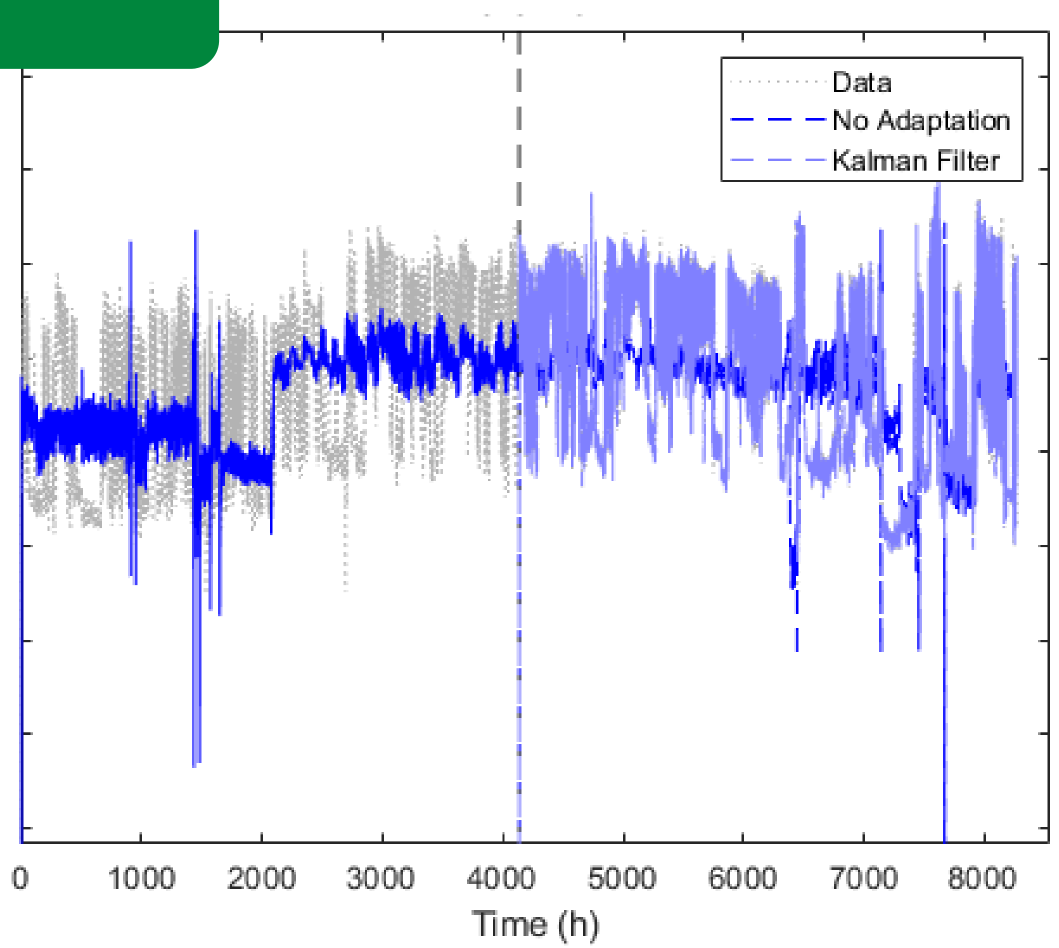

Preliminary work demonstrating efficacy of Kalman filters has been done on current plant data

Additional Study: Grid-Based Emissions

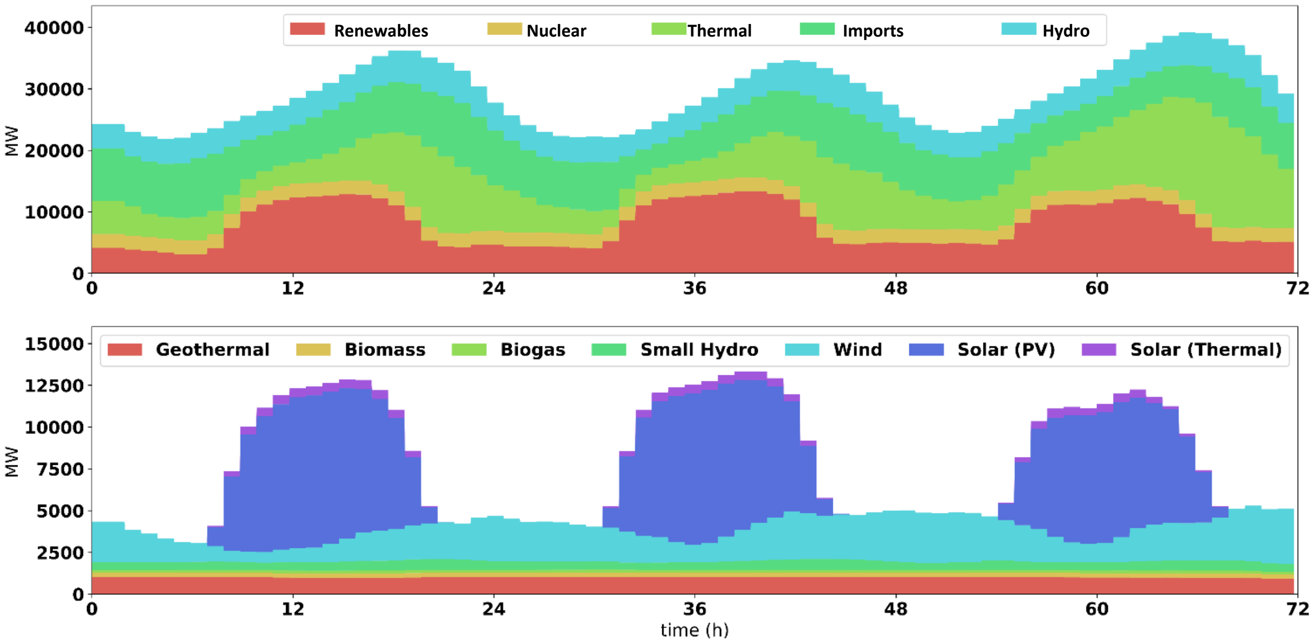

Generation over time in MW for each electricity source (top) and breakdown of renewables contribution (bottom) for July 3-5 2017 in California, as supplied by CAISO

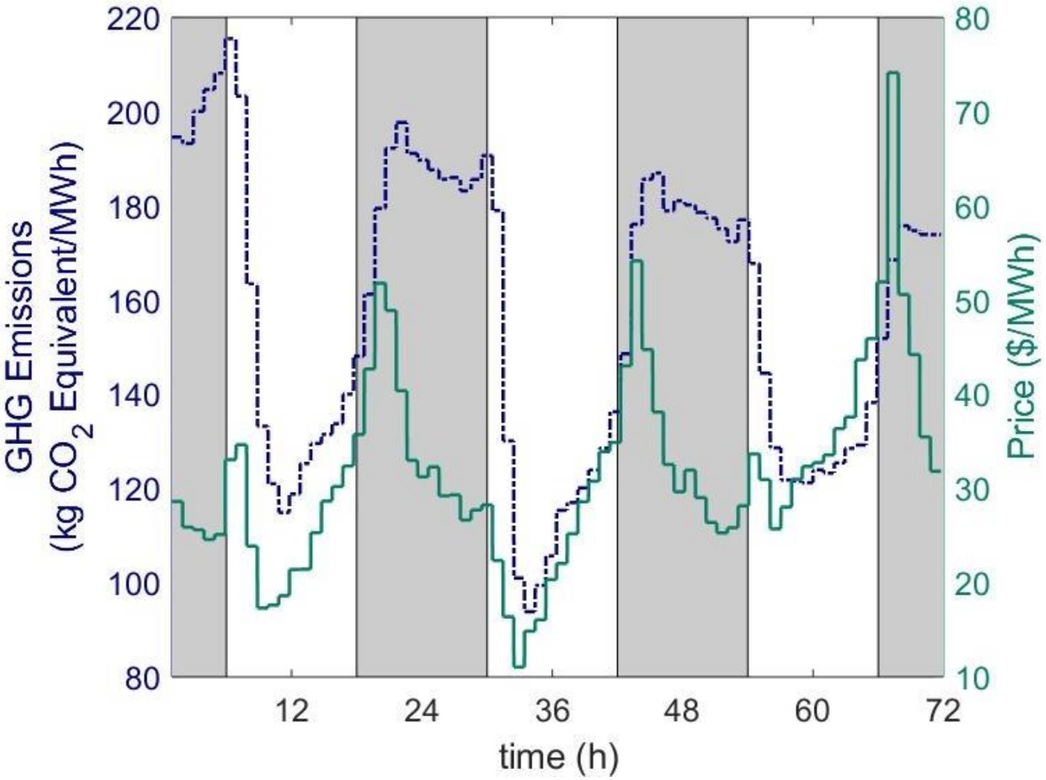

Calculated combined emissions factors for July 3-5 2017 from data supplied by CAISO [2]

U.S. electricity generation by source, amount, and share of total in 2017. (2018). Retrieved from https://www.eia.gov/tools/faqs/faq.php?id=427&t=3
Daily Renewables Output Data. (2017). Folsom, CA. Retrieved from http://www.caiso.com/market/Pages/ReportsBulletins/RenewablesReporting.aspx

Grid-side Emissions Reduction

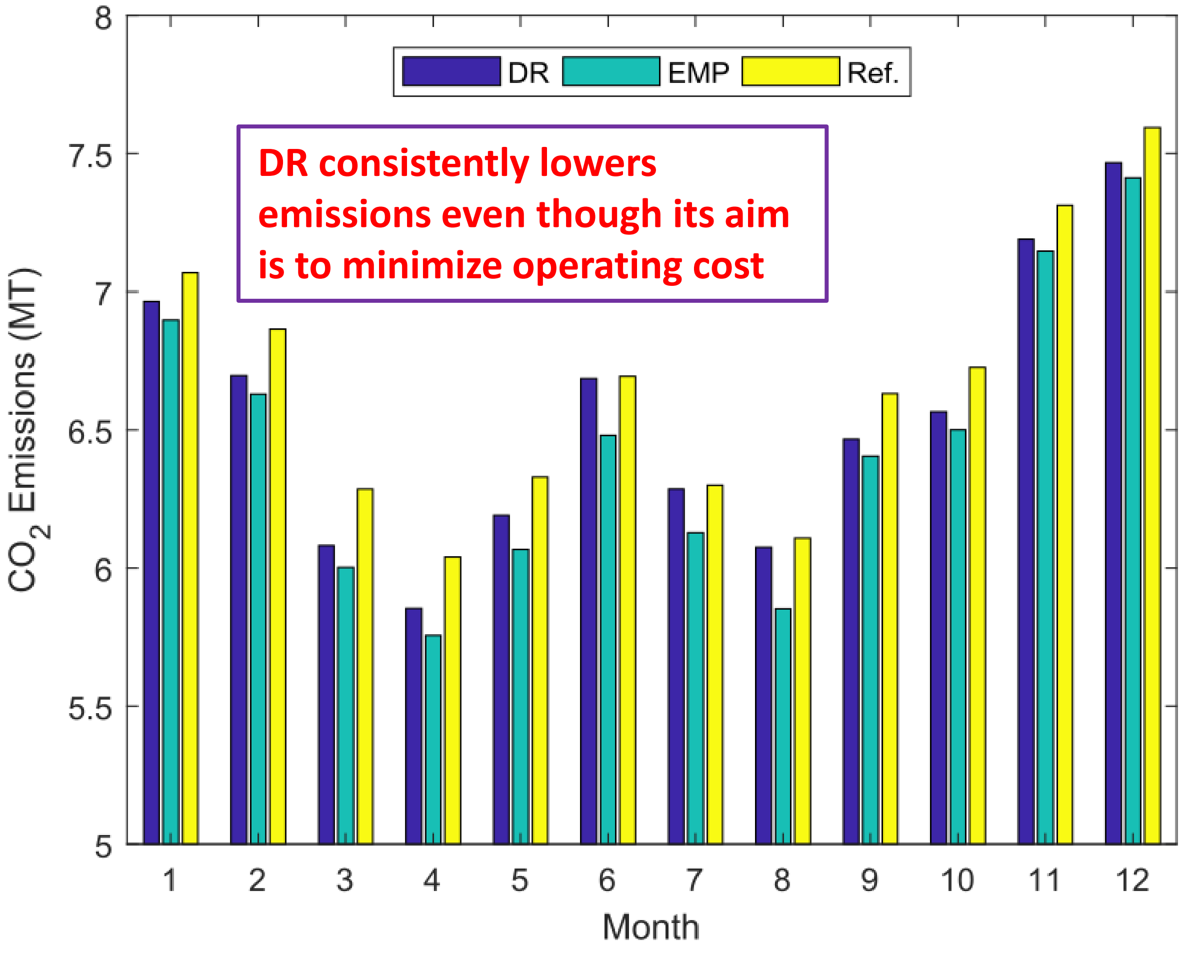

EMP emissions reduction: 2.3-4.9%
DR emissions reduction: 0.13-3.36%

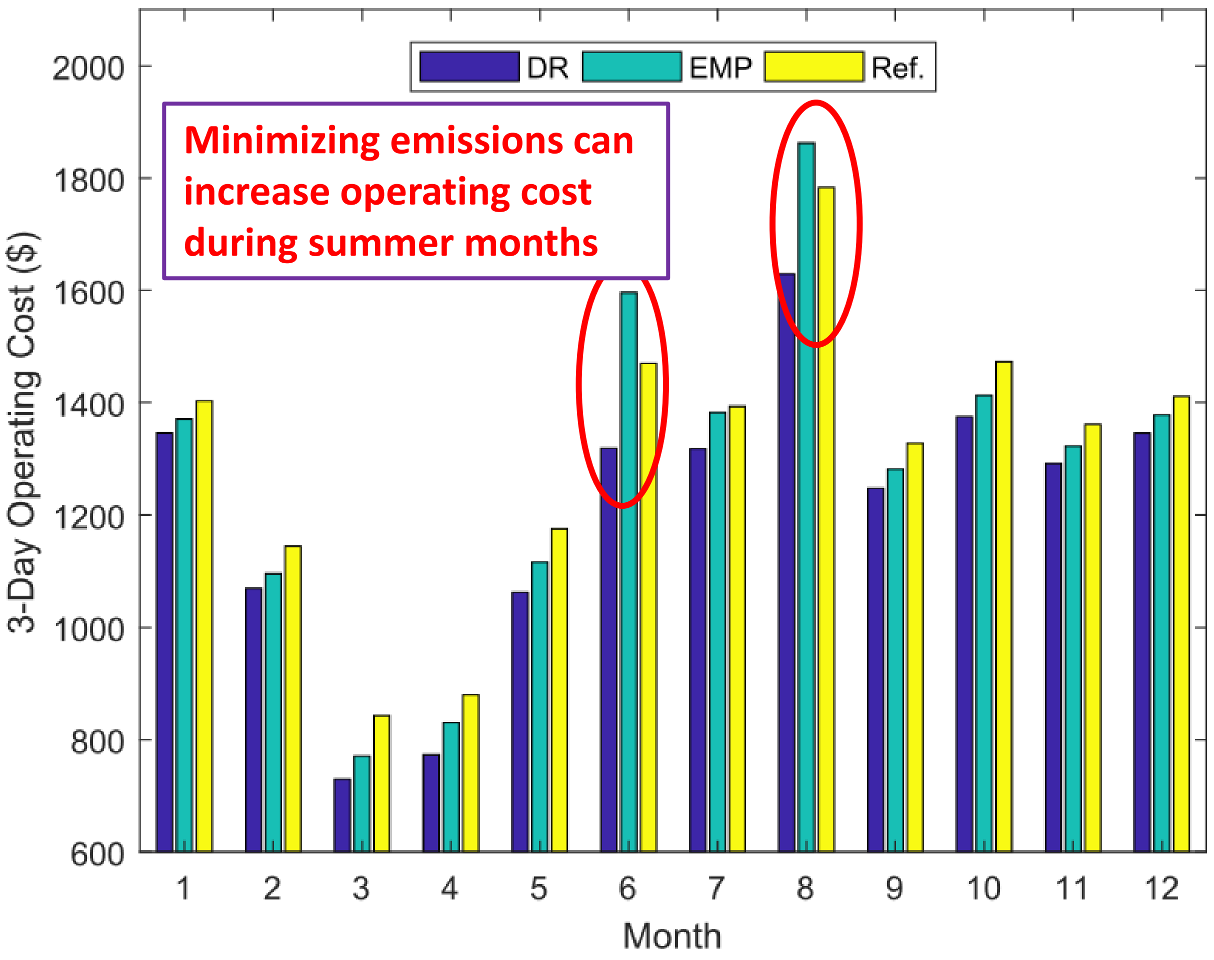

DR cost reduction: 4.3-15.5%
EMP cost reduction: -7.9 to 9.3%

EMP: Emissions Minimizing Production

Kelley, M. T., Baldick, R. & Baldea, M. Demand Response Operation of Electricity-Intensive Chemical Processes for Reduced Greenhouse Gas Emissions: Application to an Air Separation Unit. *ACS Sustain. Chem. Eng.* 7, 1909–1922 (2019).

Conclusions and Future Outlook

- DR has huge potential for mitigating grid instability and reducing emissions while saving companies electricity costs
- Involves little to no capital expenditure—primarily changes in operating habits
- Advances in computer technology, models, and algorithms enable efficient solution of large-scale DR problems

Future/Concurrent Work:

Applications outside of industrial plants:

- Time-of-use electricity pricing for residential and commercial entities
- Demand Response has potential to play a roll in remote computing tasks
  - Can schedule run time (and location) of large problems with flexible load (e.g., credit card transactions, large research compute tasks) based on grid conditions in different places

Acknowledgements

- Baldea and Edgar research groups
- DOE CSGF Family
- Funding support from:
  - Department of Energy Computational Science Graduate Research Fellowship (DOE CSGF) award DE-FG02-97ER25308
  - US Department of Energy under award DE-OE0000841
  - National Science Foundation (NSF) through the CAREER Award 1454433 and Award CBET-1512379

Dynamic Modeling and Optimal Scheduling of Chemical Processes Participating in Fast-Changing Electricity Markets: A Data-Driven Approach

Morgan Kelley
2022 Howes Scholar

Publications

1. **Kelley, M. T.,** Pattison, R. C., Baldick, R. & Baldea, M. An efficient MILP framework for integrating nonlinear process dynamics and control in optimal production scheduling calculations. *Comput. Chem. Eng.* 110, 35–52 (2018).
2. **Kelley, M. T.,** Pattison, R. C., Baldick, R. & Baldea, M. An MILP framework for optimizing demand response operation of air separation units. *Appl. Energy* 222, 951–966 (2018).
3. **Kelley, M. T.,** Baldick, R. & Baldea, M. Demand Response Operation of Electricity-Intensive Chemical Processes for Reduced Greenhouse Gas Emissions: Application to an Air Separation Unit. *ACS Sustain. Chem. Eng.* 7, 1909–1922 (2019).
4. **Kelley, M. T.,** Baldick, R. & Baldea, M. An empirical study of moving horizon closed-loop demand response scheduling. *J. Process Control* 92, 137–148 (2020).
5. **Kelley, M. T.,** Baldick, R. & Baldea, M. *A Discrete Multiple Shooting Formulation for Efficient Dynamic Optimization*. *Computer Aided Chemical Engineering* 48, (Elsevier Masson SAS, 2020).
6. Simkoff, J. M., Lejarza, F., **Kelley, M. T.,** Tsay, C. & Baldea, M. Process Control and Energy Efficiency. *Annu. Rev. Chem. Biomol. Eng.* 11, 423–445 (2020).
7. **Kelley, M. T.,** Baldick, R. & Baldea, M. A direct transcription-based multiple shooting formulation for dynamic optimization. *Comput. Chem. Eng.* 140, 106846 (2020).
8. **Kelley, M. T.,** Baldick, R. & Baldea, M. Demand response scheduling under uncertainty: Chance-constrained framework and application to an air separation unit. *AIChE J.* 66, (2020).
9. **Kelley, M. T.,** Tsay, C. & Baldea, M. A data-driven linear formulation of the optimal demand response scheduling problem for an industrial air separation unit. *Chem. Eng. Sci. Submitted*. (2021).
10. **Kelley, M. T.,** Do, T. T. & Baldea, M. Evaluating the Demand Response Potential of Ammonia Plants. *AIChE Journal, In revision*. (2021).

Representation of Dynamics

Finite Step Response (FSR) Models:

- Data-driven non-parametric models used for unknown model order and time delay
- Can be reduced to reflect setpoint, u, that only changes once per scheduling time slot, i

$$w_{ij} = w_{i-1,j} + S_j(u_i - u_{i-1})$$

Hammerstein-Wiener (HW) Models

- Linear State-space block
- Static input/output nonlinearities: piece-wise linear (PWL)
  - Linearized using Special Ordered Sets of Type II (SOS2)

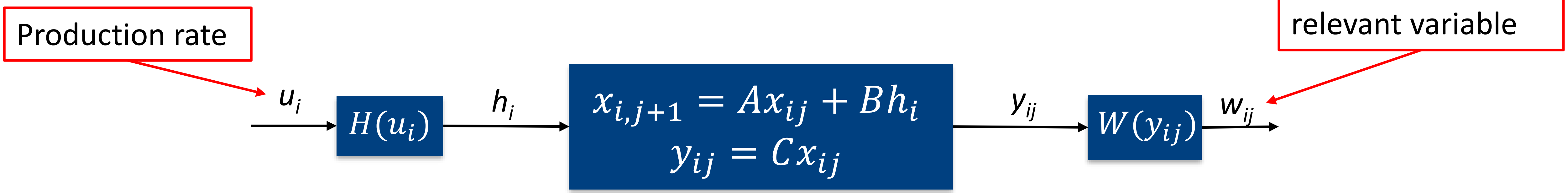

Billings, S. A. (2013). *Nonlinear system identification : NARMAX methods in the time, frequency, and spatio-temporal domains*. Chichester, West Sussex: John Wiley & Sons.

MATLAB. (2016). MATLAB 2016a. Natick, MA, USA: The Mathworks, Inc.

M. T. Kelley, R. C. Pattison, R. Baldick, and M. Baldea, "An MILP framework for optimizing demand response operation of air separation units," *Appl. Energy*, vol. 222, pp. 951–966, Jul. 2018.

Ogunnaike, B. & Harmon Ray, W. *Process Dynamics, Modeling, and Control*. (Oxford University Press, 1994).

Static blocks: Linearize nonlinearities

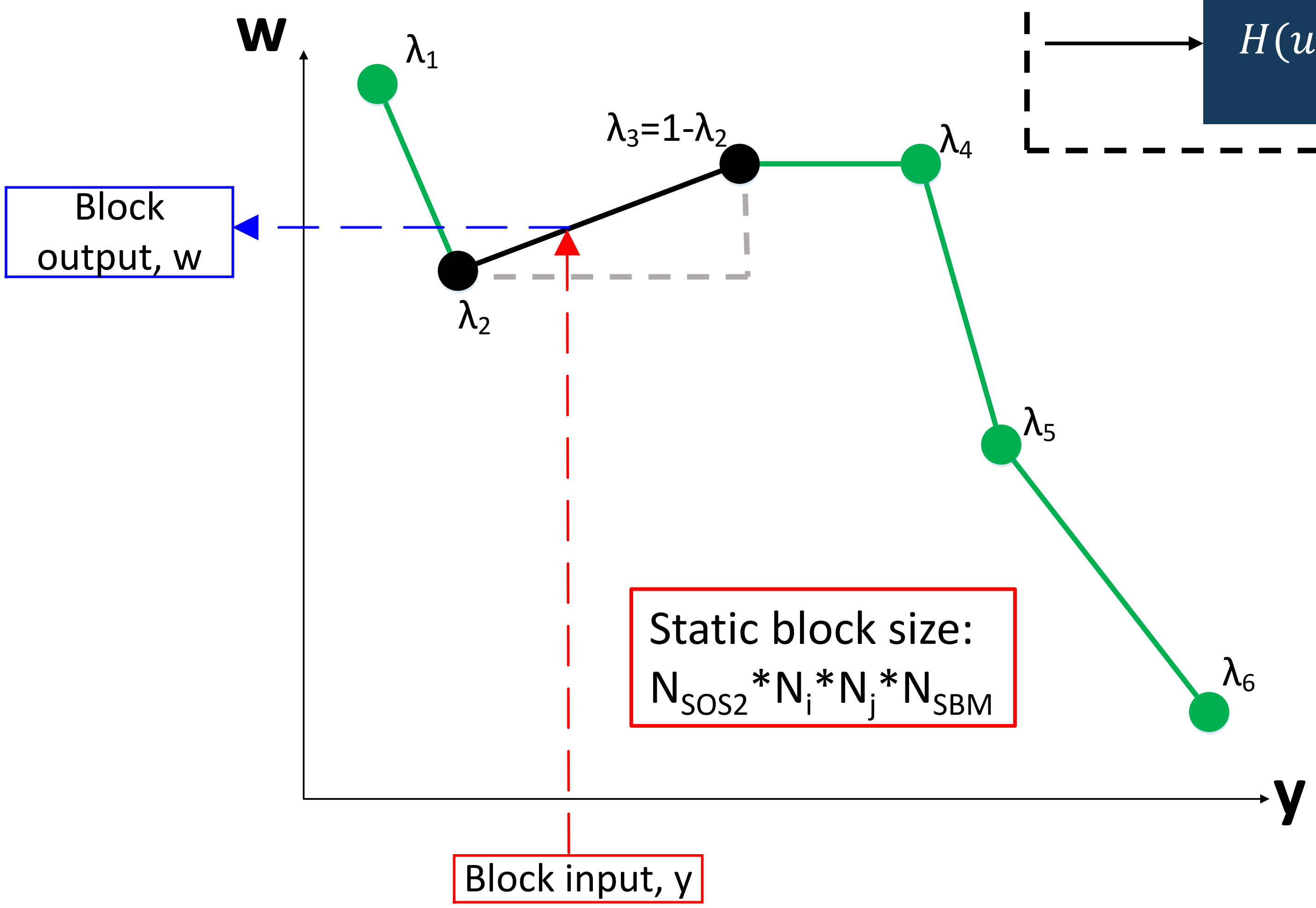

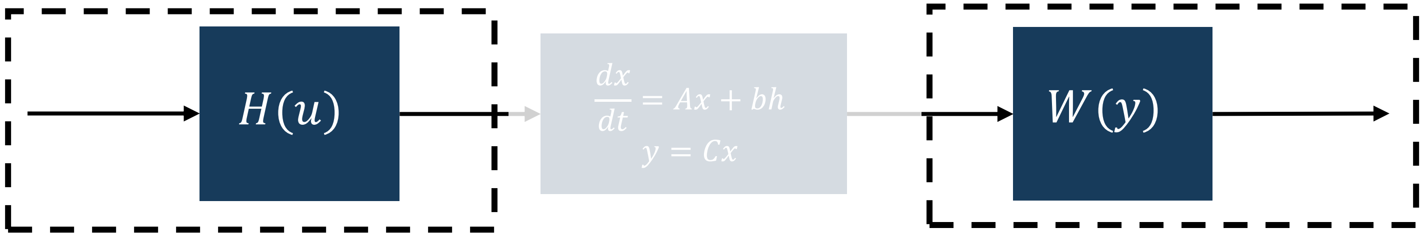

Special Ordered Sets of type 2 (SOS2)

- Benefits:
  - *Most* linear optimization solvers have architecture in place to solve SOS2 variables directly
  - Result in *exact* linearization—no loss of information
- Drawbacks:
  - Introduces multiple integer variables at each time point
    - Exponential increases in solution time with each integer variable added

Linear Reformulations of HW Models (I)

Option 1: Special Ordered Sets of Type 1 (SOS1)

- *Exact* linearization of PWC functions
- Applicable when set-points take *discrete values (e.g., multi-product plant)*

$$\sum_k \kappa_{ik}^H = 1$$

$$u_i = \sum_k \kappa_{ik}^H bp_k$$

$$h_i = \sum_k \kappa_{ik}^H pw_k$$

$$\kappa_{ik}^H = \{0, 1\}$$

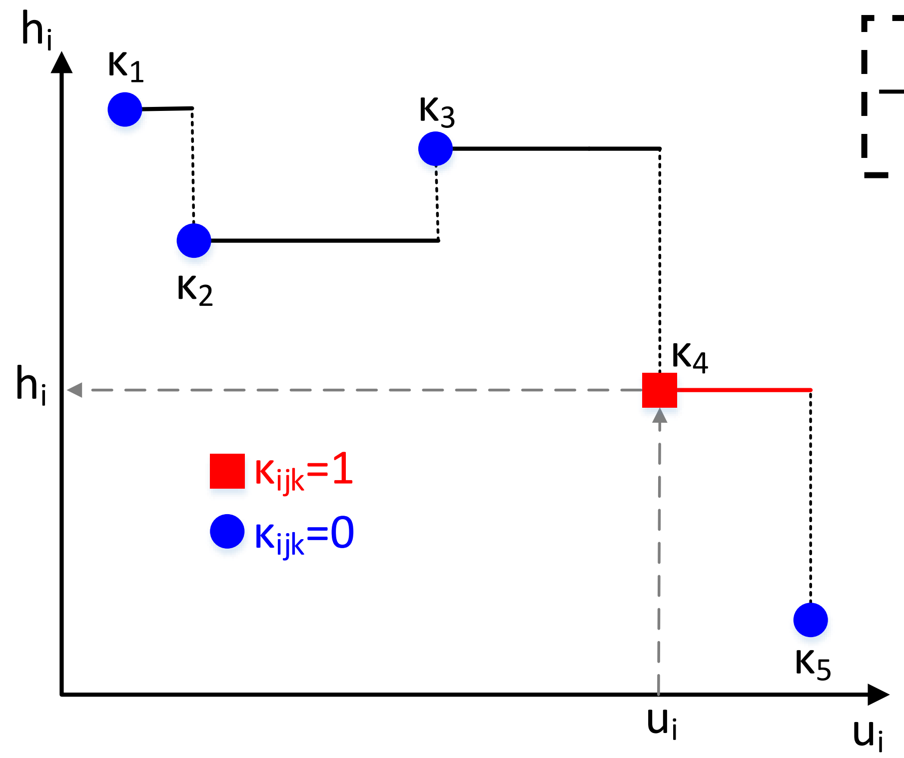

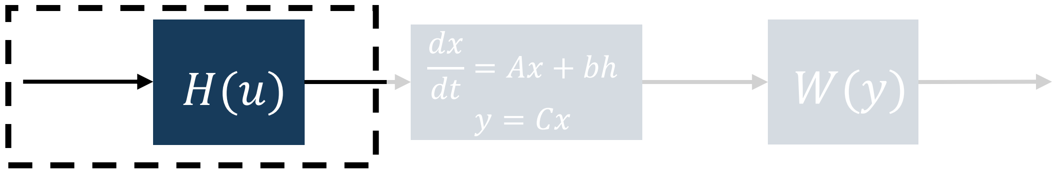

Beale, E., & Tomlin, J. (1970). Special Facilities in a General Mathematical Programming System for Nonconvex Problems Using Ordered Sets of Variables. In *Proceedings of the 5th International Conference on Operational Research*. London.

Linear Reformulations of HW Models (II)

Option 2: Special Ordered Sets of Type 2 (SOS2)

- *Exact* linearization of PWL functions
- Applicable when set-points are *continuous*
- Some solvers have built-in support for SOS2 variables

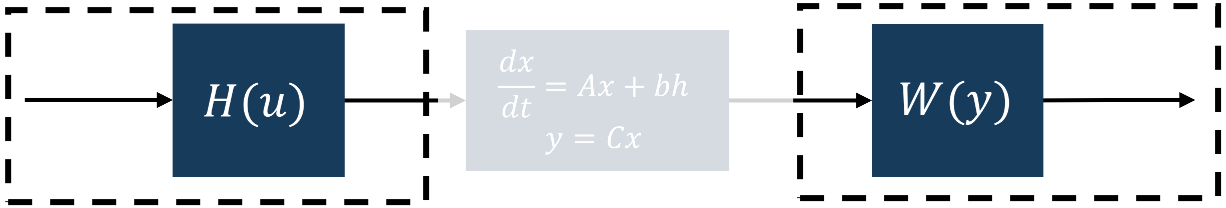

$$y_{ij} = \sum_k [\lambda^W_{ijk} bp^W_{ijk}] \qquad \sum_k \lambda^W_{ijk} = 1$$

$$w_{ij} = \sum_k [\lambda^W_{ijk} pw^W_{ijk}] \qquad \lambda^W_{ijk} \le b^W_{ijk}$$

$$\sum_k b^W_{ijk} = 2$$

$$b^W_{ijk} + b^W_{ijk'} \le 1 \ \forall k' > k+1$$

$$b^W_{ik} \in \{0,1\}$$

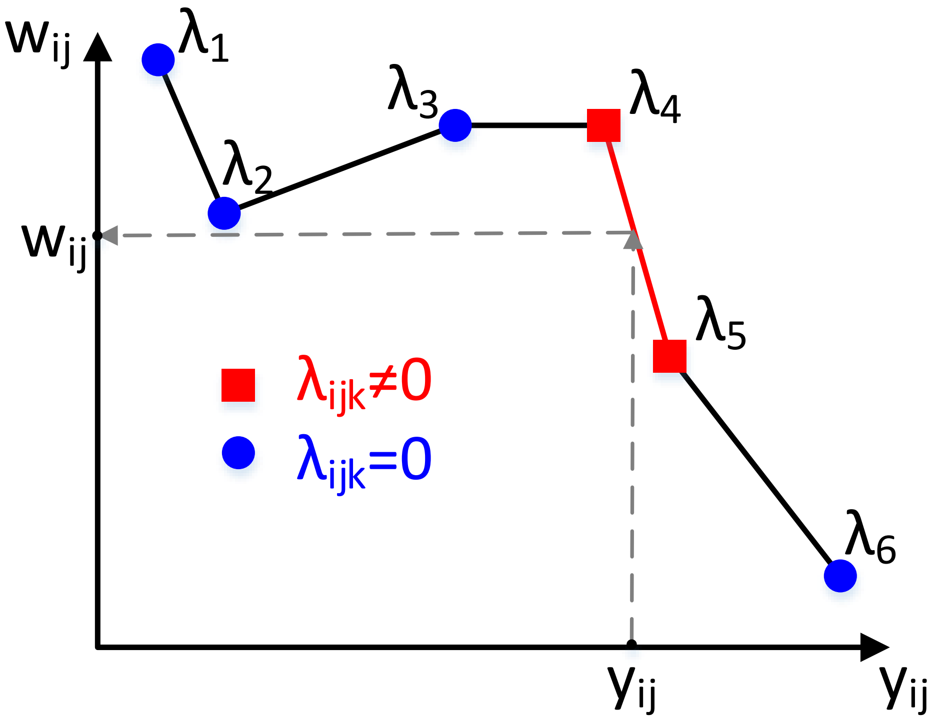

IBM. (2017). CPLEX 12.7. Armonk, NY: IBM.
BDMLP Solver. (2017). In *GAMS User Guide* (24.7). Washington, DC
XPRESS Solver Engine. (2017). Incline Village, NV: FrontlineSolvers..

Linear Reformulations of HW Models (III)

Option 3: Big-M

- Linearize PWL functions
- General formulation for handling if-then structures—computationally more costly

$$w_{ij} = PW^W_{ij,k=0} + \sum_k [(PW^W_{ijk} - PW^W_{i,j,k-1}) z^W_{ijk}] = PW^W_{ij,k=0} + \sum_k \boxed{A^W_{ijk} z^W_{ijk}} = PW^W_{ij,k=0} + \sum_k \boxed{B^W_{ijk}}$$

$$B^W_{ijk} \geq A^W_{ijk} - M^W (1 - z^W_{ijk})$$
$$B^W_{ijk} \leq A^W_{ijk} + M^W (1 - z^W_{ijk})$$
$$B^W_{ijk} \geq -M^W z^W_{ijk}$$
$$B^W_{ijk} \leq M^W z^W_{ijk}$$

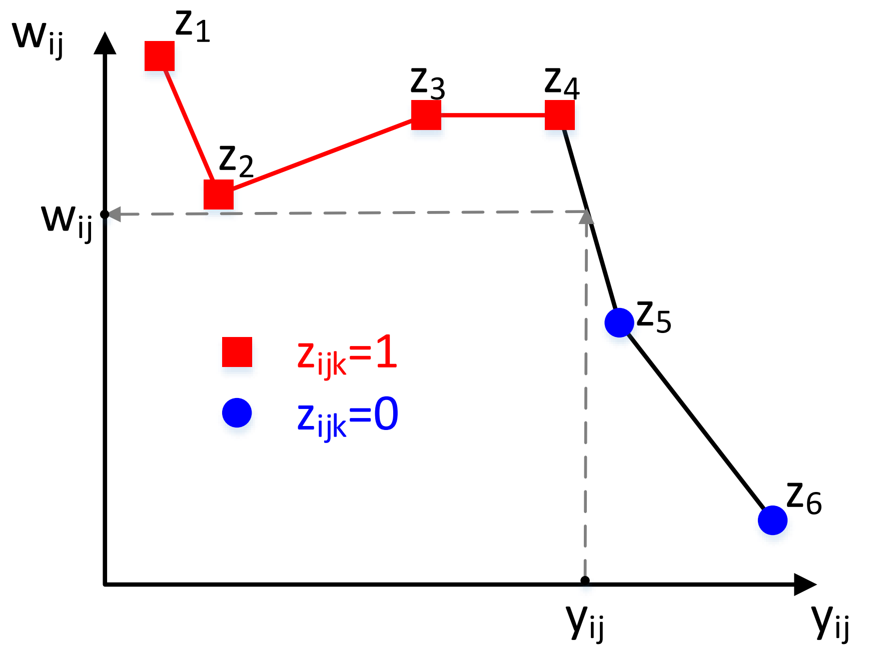

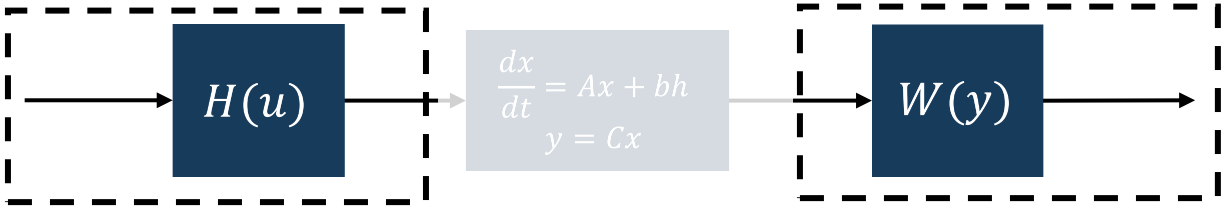

Linear Reformulation Options: Summary

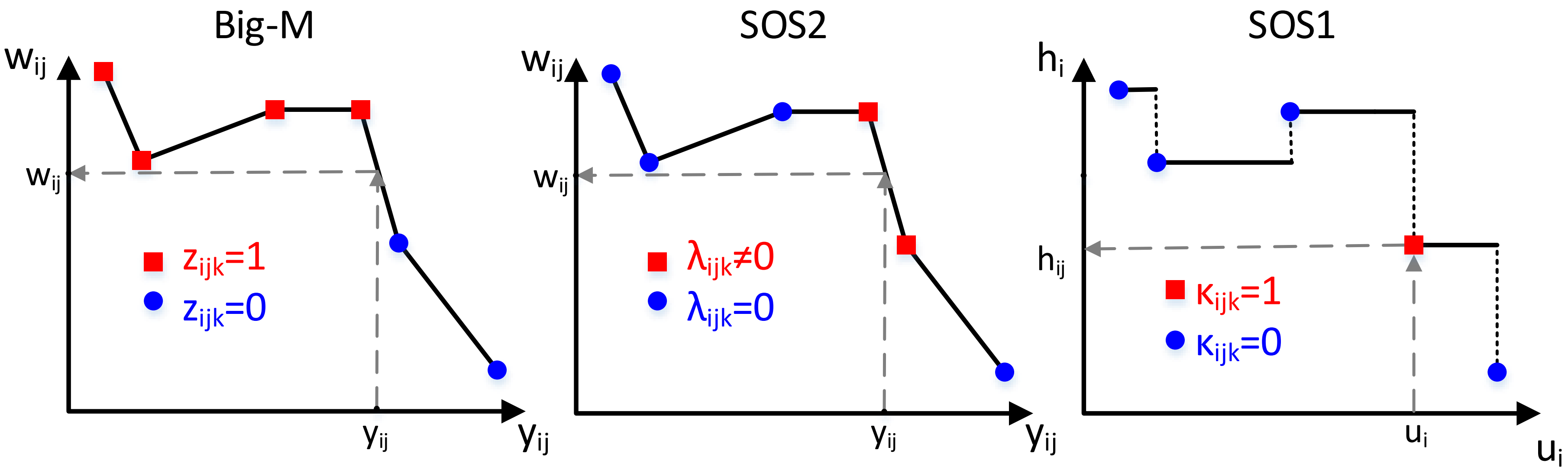

Method	Discrete Variables	Equations
Big-M	$3(N_I N_K)(N_J+1)$	$7(N_I N_K)(N_J+1)$
Explicit SOS2	$3(N_I N_K)(N_J+1)$	$5(N_I N_K)(N_J+1)$
Implicit SOS2	$1(N_I N_K)(N_J+1)$	$2(N_I N_K)(N_J+1)$
SOS1	$1(N_I N_K)(N_J+1)$	$2(N_I N_K)(N_J+1)$

- For solvers that support SOS2, this is the most efficient modeling option
- **SOS1: best suited for input nonlinearity (Hammerstein block)** with discrete set-points
- **SOS2: best suited for output nonlinearity (Wiener block)**, deal with continuous output of state-space block

Special Case: Breakpoint Elimination

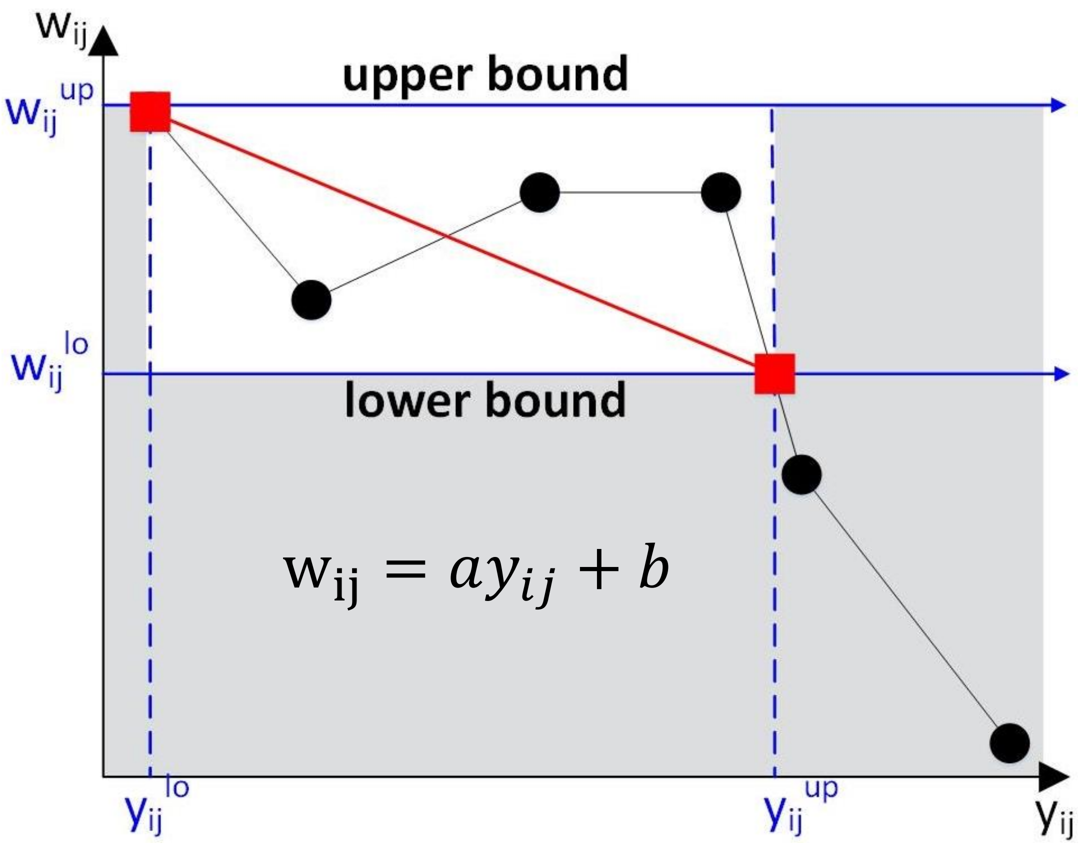

For variables *not* in the objective function:

- *Output* nonlinearity can be estimated by endpoints at the upper and lower bounds
  - Variable stays between bounds
  - Becomes linear function—breakpoint elimination

Can further simplify by bounding y and leaving W block out:
$y_{ij}^{lo} \leq y_{ij} \leq y_{ij}^{up}$

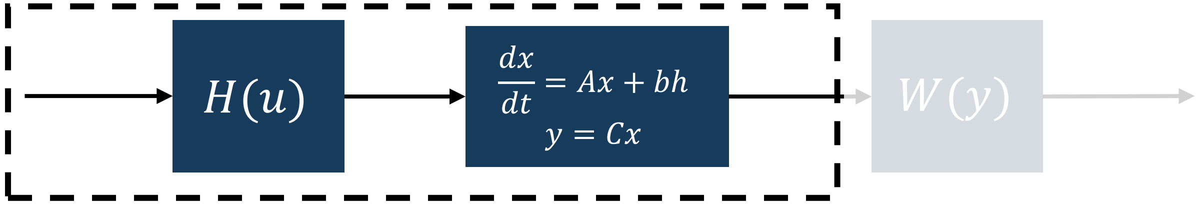

MMA free-radical polymerization results

Problem	Model description	CPU (s)	Obj ($)	T_C (h)
P1	Full-Order model	91.13	55,407	47.45
P2	I/O linearizing controller-based	6.13	56,188	46.72
P3	HW+LR	18.96	56,006	47.89
P4	HW	23.08	56,006	47.89
P5	HW+FSR+LR	3.19	56,289	48.18

Same solution

Significant improvement in computation time

Optimality gap: 0.00%

Optimal schedule: A→B→C→D

64 bit Windows system Intel Core i7-2600 CPU at 3.40 GHz and 16 GB RAM

Solved in GAMS/CPLEX

GAMS. (2016). General Algebraic Modeling System (GAMS). Release 24.7.4. Washington, D.C.: GAMS Development Corporation.

Kelley, M. T., Pattison, R. C., Baldick, R. & Baldea, M. An efficient MILP framework for integrating nonlinear process dynamics and control in optimal production scheduling calculations. *Comput. Chem. Eng.* 110, 35–52 (2018).

Dynamic block: Discrete state space representation

- Discretization:

$$h_i = H(u_i)$$
$$\vec{x}_{i,j+1} = A\vec{x}_{ij} + Bh_i$$
$$y_{ij} = C\vec{x}_{ij}$$
$$w_{ij} = W\left(y_{ij}\right)$$

- Requires state continuity constraint between scheduling time slots:

$$x_{i,j=1} = x_{i-1,j=N_j}$$

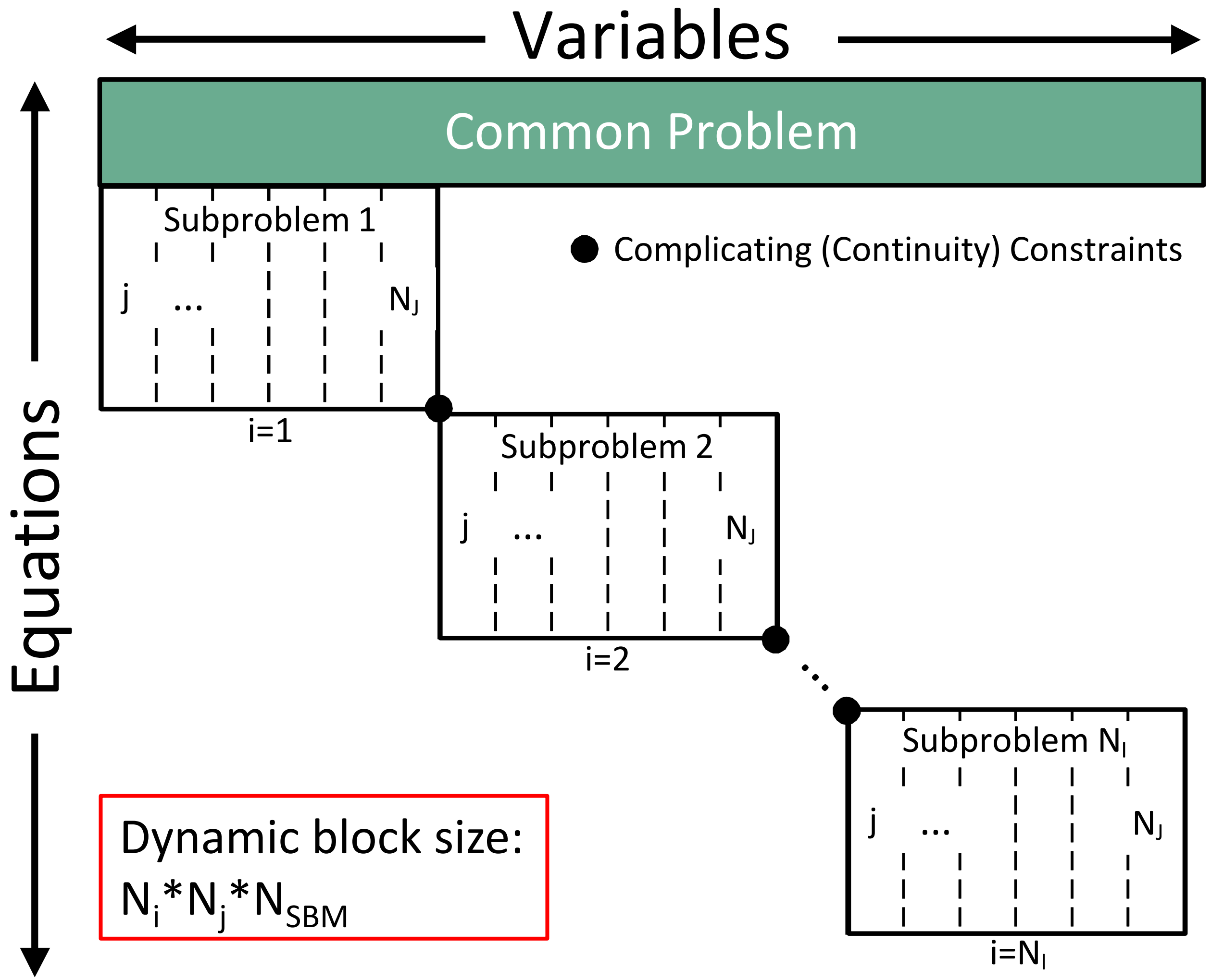

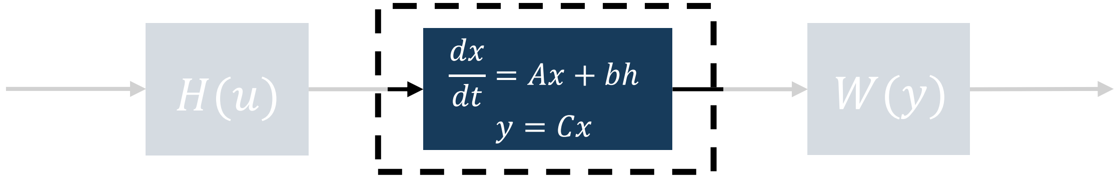

Kelley, M. T., Pattison, R. C., Baldick, R. & Baldea, M. An efficient MILP framework for integrating nonlinear process dynamics and control in optimal production scheduling calculations. *Comput. Chem. Eng.* 110, 35–52 (2018).

Base problem: PI

PI
max J
s.t.
Scale bridging models (HW/FSR)
Initial Conditions
Continuity Constraints
Process/safety constraints
Quality constraints

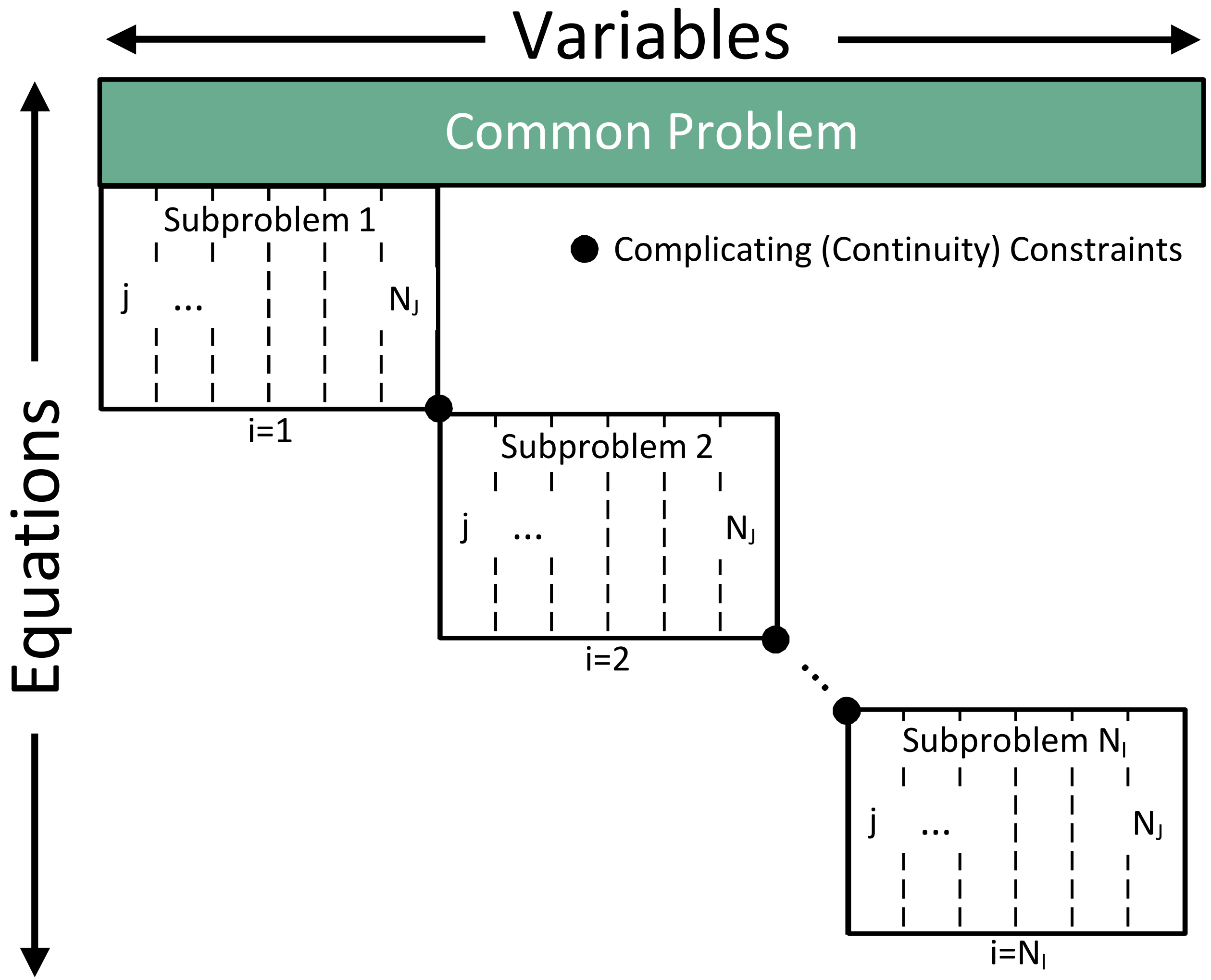

Kelley, M. T., Pattison, R. C., Baldick, R. & Baldea, M. An efficient MILP framework for integrating nonlinear process dynamics and control in optimal production scheduling calculations. *Comput. Chem. Eng.* 110, 35–52 (2018).

Batch reactor

Desired product: C
Undesired product: D
Reactor temperature is controlled via the cooling water flow rate (F_{cw})

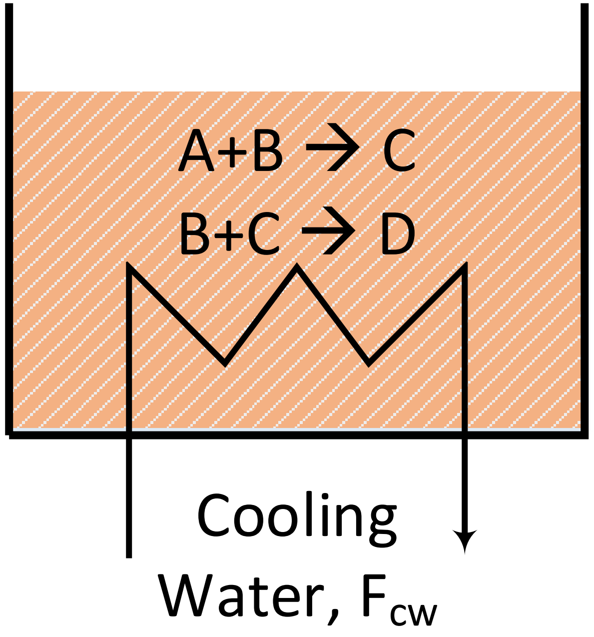

$$\max_{F_{cw_i}} J = 2N_{C,t_f} - U_{t_f}$$

s.t. Full-order process model
Process/quality constraints
Initial conditions

N_{C,t_f}: Moles of product C at the end of the horizon
U_{t_f}: Total amount of cooling water used during synthesis

Kelley, M. T., Baldick, R. & Baldea, M. A direct transcription-based multiple shooting formulation for dynamic optimization. *Comput. Chem. Eng.* 140, 106846 (2020).

Case Study: MMA free-radical polymerization

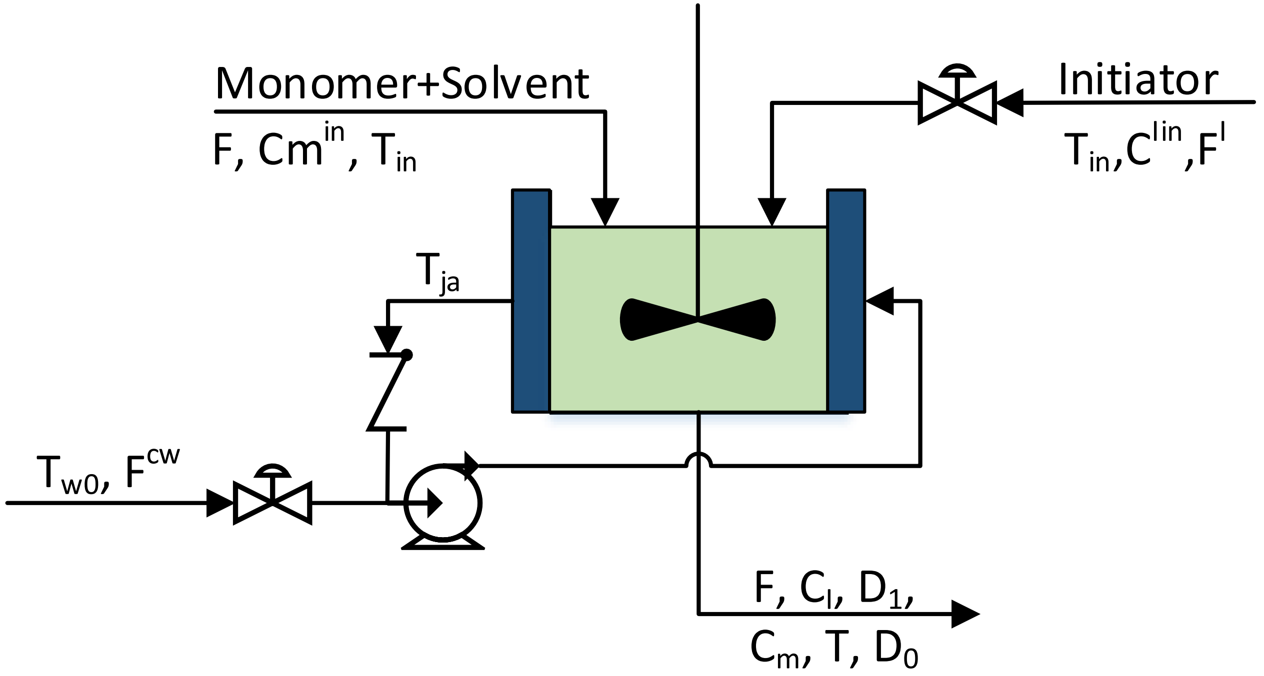

$$\max P = \sum_g R_g - c_g^{st}$$

s.t.
Process dynamics (HW/FSR models)
Initial Conditions
Process, safety, and quality constraints

- Continuous process
- Four product grades: g={A,B,C,D}
    - Defined by set-points: $u = \left\{\bar{\mu} = \frac{D_1}{Do}, \bar{T}\right\}$
- Scheduling-Relevant variables: $w_{ij} = \{F^{cw}, F^{I}, \mu, T\}$

Daoutidis, P., Soroush, M., & Kravaris, C. (1990). Feedforward/feedback control of multivariable nonlinear processes. *AIChE Journal*, *36*(10), 1471–1484. https://doi.org/10.1002/aic.690361003

Kelley, M. T., Pattison, R. C., Baldick, R. & Baldea, M. An efficient MILP framework for integrating nonlinear process dynamics and control in optimal production scheduling calculations. *Comput. Chem. Eng.* 110, 35–52 (2018).

Batch reactor results

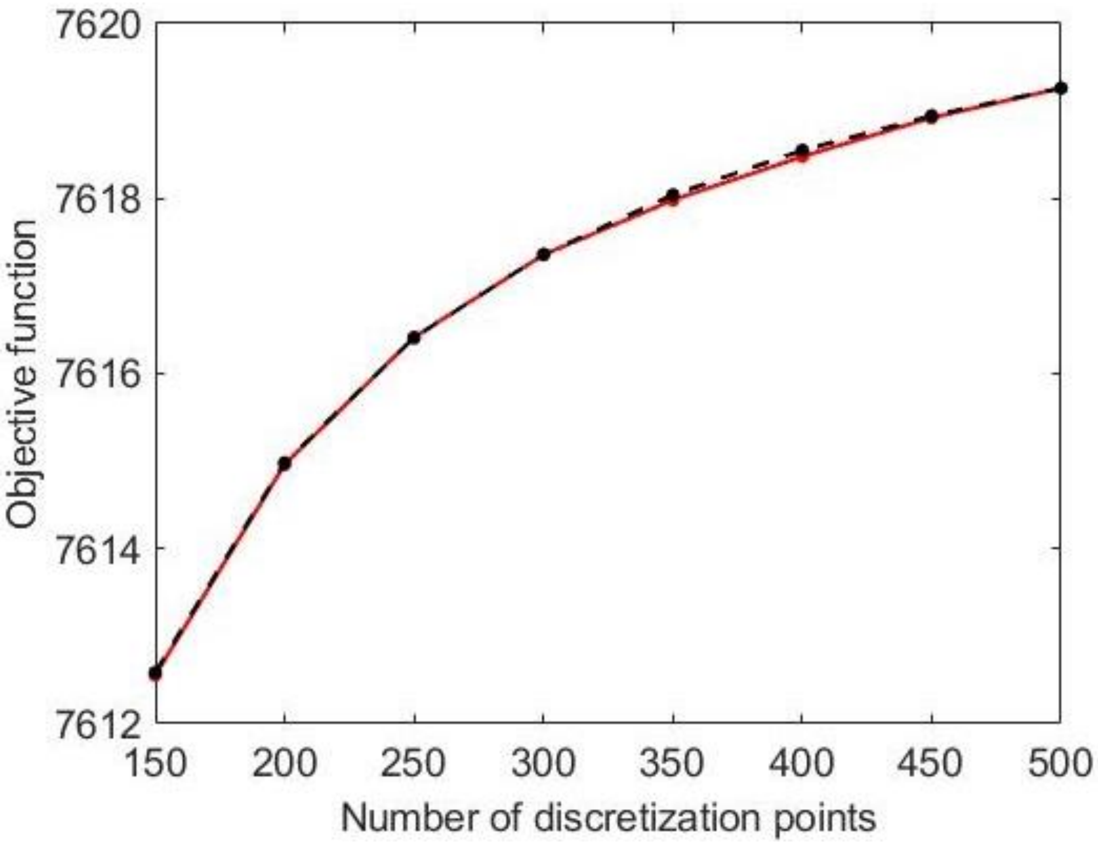

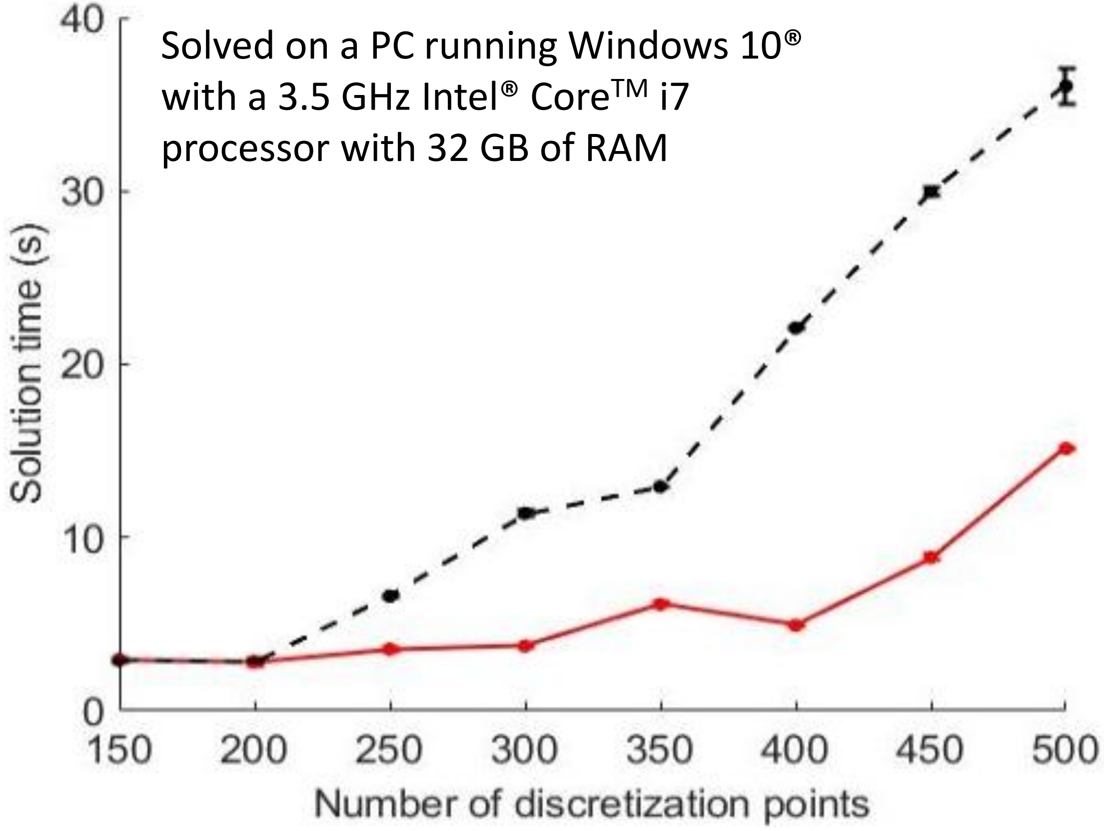

No LR: **Black** dash

LR: **Red** solid

Kelley, M. T., Baldick, R. & Baldea, M. A direct transcription-based multiple shooting formulation for dynamic optimization. *Comput. Chem. Eng.* 140, 106846 (2020).

Batch reactor results

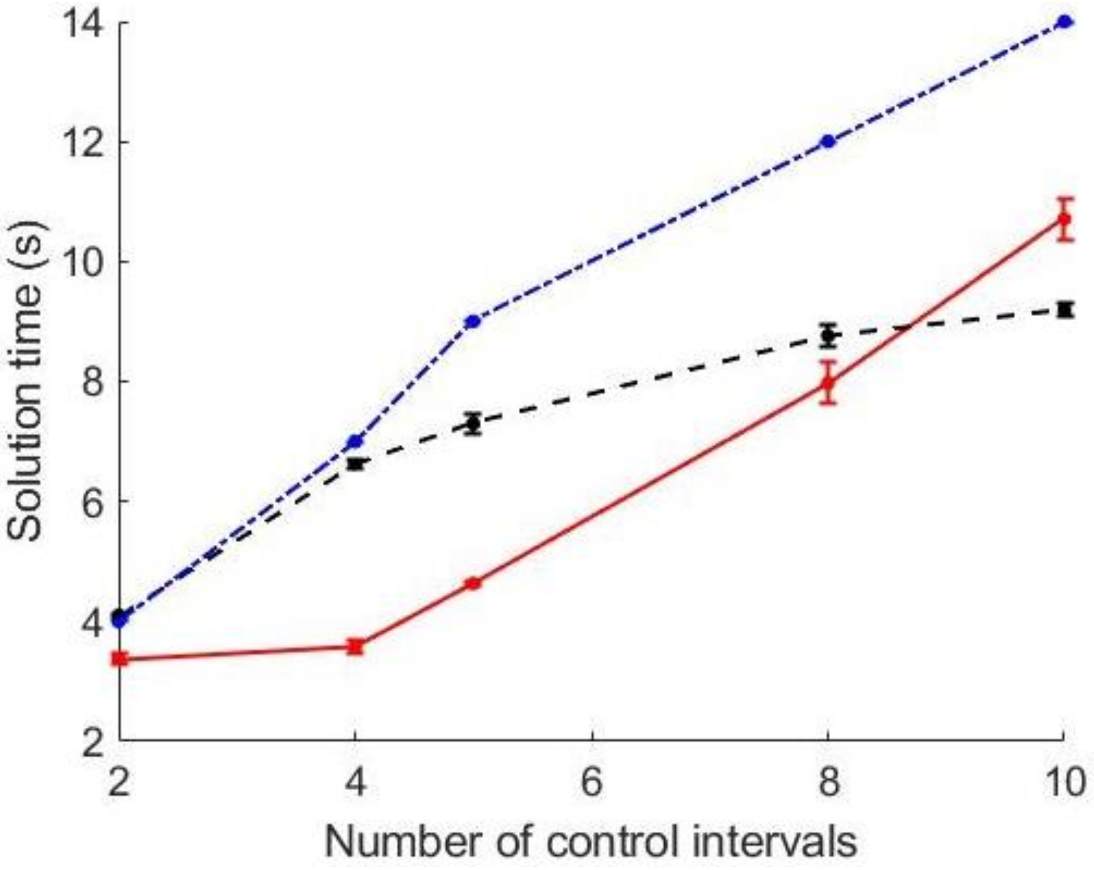

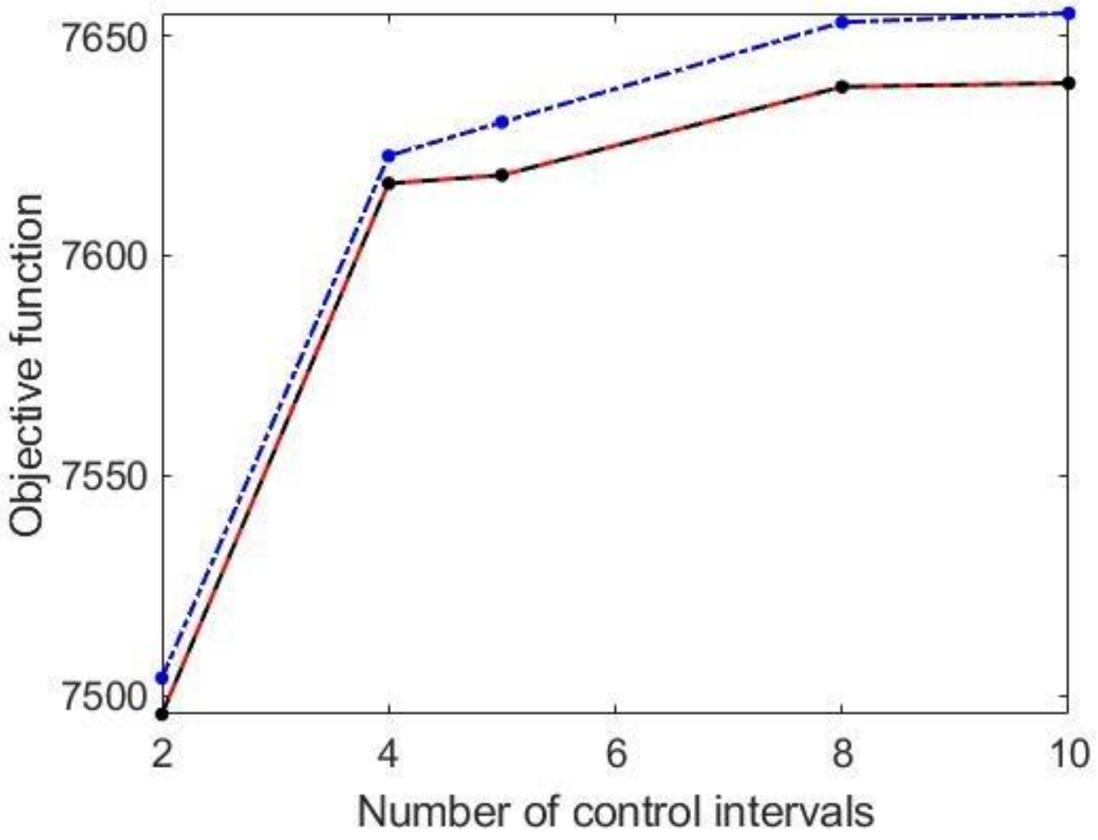

Sequential NLP solution: **Blue** dash-dot
No LR: **Black** dash
LR: **Red** solid

Kelley, M. T., Baldick, R. & Baldea, M. A direct transcription-based multiple shooting formulation for dynamic optimization. *Comput. Chem. Eng.* 140, 106846 (2020).

Storage System and Power Consumption Models

Demand Constraint:

$$F_{i,j}^{p} - D_{i,r} \geq f_{s_{i,j}}^{in} - f_{s_{i,j}}^{out}$$

Storage system:

$$s_{i,j+1} = \left(f_{s_{i,j}}^{in} - f_{s_{i,j}}^{out}\right)\Delta j + s_{i,j}$$

$$f_{s_{i,1}}^{in} = f_{s_{i-1,N_j}}^{in}$$

$$f_{s_{i,1}}^{out} = f_{s_{i-1,N_j}}^{out}$$

$$s_{i,1} = s_{i-1,N_j}$$

$$s_{N_i,N_j} \geq s_{1,1}$$

Power consumption:

$$\Phi_{i,j} = \mathcal{W}_{i,j}^{C} + \mathcal{W}_{i,j}^{t_1} + \mathcal{W}_{i,j}^{t_2} + \mathcal{W}_{i,j}^{\ell}$$

$$\mathcal{W}_{i,j}^{C} = \Omega_C F_{i,j}^{f} \qquad \mathcal{W}_{i,j}^{t_1} = \Omega_{t_1} F_{i,j}^{f} \qquad \mathcal{W}_{i,j}^{t_2} = \Omega_{t_2} F_{i,j}^{p} \qquad \mathcal{W}_{i,j}^{\ell} = \Omega_{\ell} f_{s_{i,j}}^{in}$$

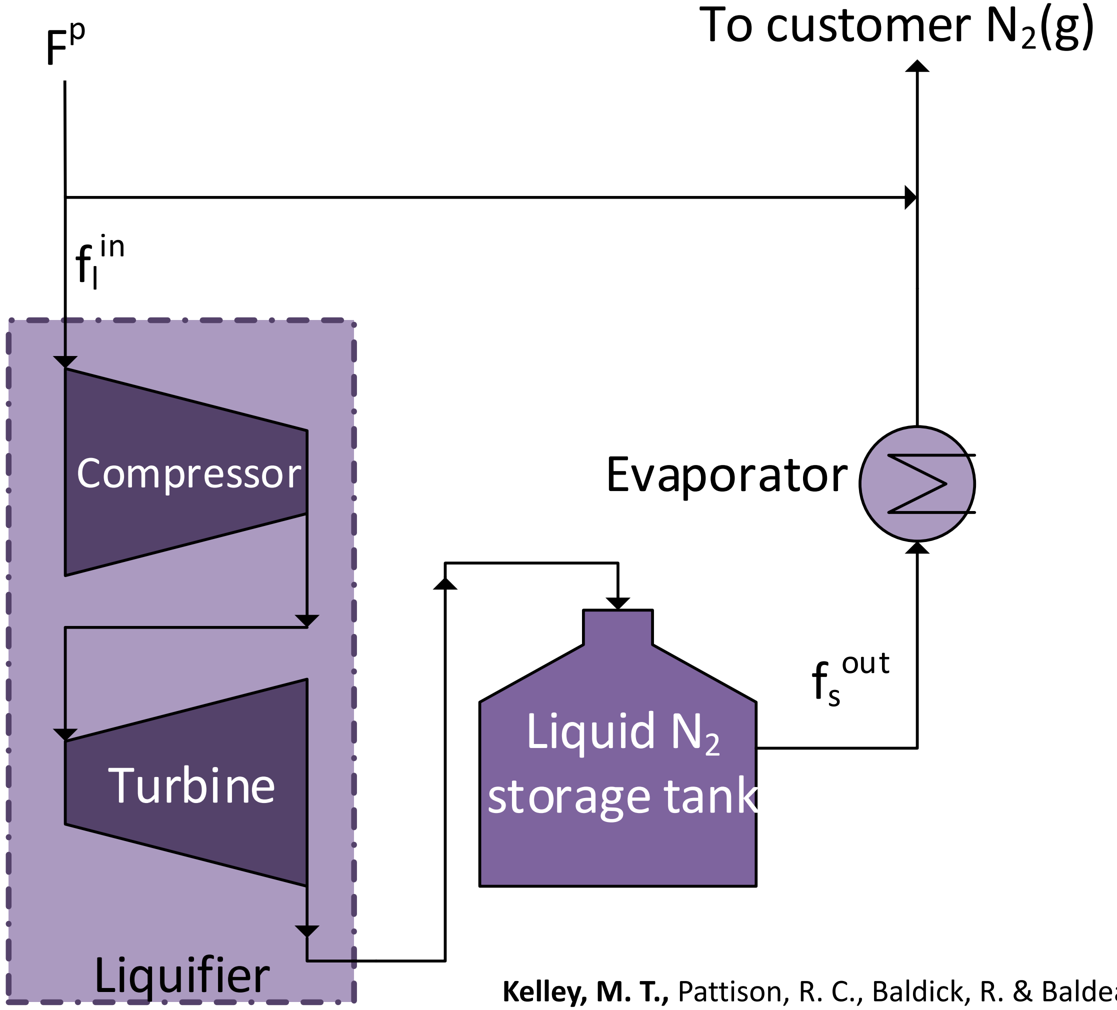

Kelley, M. T., Pattison, R. C., Baldick, R. & Baldea, M. An MILP framework for optimizing demand response operation of air separation units. *Appl. Energy* 222, 951–966 (2018).

Representing Uncertainty: Chance Constraints

- Confidence level of the optimization problem solution is increased by restricting the feasibility region
  - Confidence/robustness level is defined using desired probability of meeting the uncertain constraint(s)

$$\begin{aligned} &\min_{x} f(x,\xi) \\ &\text{s.t. } g(x) = 0 \\ &h(x,\xi) \geq 0 \\ &\xi \in \mathbb{R}^p \end{aligned}$$

Original problem, ξ is uncertain parameter

$$\begin{aligned} &\min_{\mathrm{x}} f(x,\xi) \\ &\text{s.t. } g(x) = 0 \\ &\mathbb{P}[h(x,\xi) \geq 0] \geq \alpha \\ &\xi \in \mathbb{R}^p \end{aligned}$$

Chance-constraint representation

Chance-constraints in DR scheduling problems

Uncertain electricity prices

$$\min C = \sum_i \sum_j P_i \Phi_{i,j}$$

s.t. $C + (1 - z_r^P)M \geq \sum_i \sum_j P_{i,r} \Phi_{i,j}$

$$\sum_r z_r^P \pi_r \geq \alpha$$

$\pi_r = \Pr[P_{i,r}]$

$0 < \alpha \leq 1$

$P_i \sim \mathcal{N}_{mvn}(\mu_i, \Sigma_\mathrm{i})$

Process model (HW/FSR)

Process constraints

Quality constraints

Initial conditions

Continuity conditions

Demand constraints (D_i=20 mol/s)

Uncertain product demand

$$\min C = \sum_i \sum_j P_i \Phi_{i,j}$$

s.t. $F_{i,j}^p - D_{i,r} \geq f_{s_{i,j}}^{in} - f_{s_{i,j}}^{out} - M(1 - z_r^D)$

$$\sum_r z_r^D \geq \alpha N_R^D$$

$0 \leq \alpha \leq 1$

$D_i \sim \mathcal{U}[16,23]\ t_{start} \sim \mathcal{U}[0,72]$

Process model (HW/FSR)

Process constraints

Quality constraints

Initial conditions

Continuity conditions

Kelley, M. T., Baldick, R. & Baldea, M. Demand response scheduling under uncertainty: Chance-constrained framework and application to an air separation unit. *AIChE J.* 66, (2020).

Problem comparison

	Operating Cost ($)	% increase	α* (%)	Solution time (min)	CPLEX optimality gap (%)
Reference	1023.50	--	--	--	--
Deterministic	1014.48	--	--	1.88 ± 0.020	0.17
Price Uncertainty	1020.39	0.58	95.1	7.39 ± 0.024	0.29
Demand Uncertainty	1163.67	14.7	95	2.06 ± 0.020	0.22
P&D Uncertainty	1172.69	15.6	95.1, 95	7.56 ± 0.032	0.29

Solved on a 64-bit Windows system with Intel Core-7-2600 CPU at 3.40 GHz with 16 Gb RAM using GAMS 25.1.3 /CPLEX 12.8.0

Summary:

Solution times are well-within the one hour time limit
The objective value increases (solution becomes more conservative) as the degree of uncertainty increases

- Effect of uncertain demand is strong

Key point:

The proposed method accounts for *errors* that arise in predictions of uncertain parameters—its applicability is independent of the methods chosen to predict electricity prices and demand

Kelley, M. T., Baldick, R. & Baldea, M. Demand response scheduling under uncertainty: Chance-constrained framework and application to an air separation unit. *AIChE J.* 66, (2020).

Optimal schedule of **Deterministic** vs **P&D Uncertainty**

Reference: 21.60 MWh
Deterministic: 22.29 MWh
P&D Uncertainty: 25.25 MWh

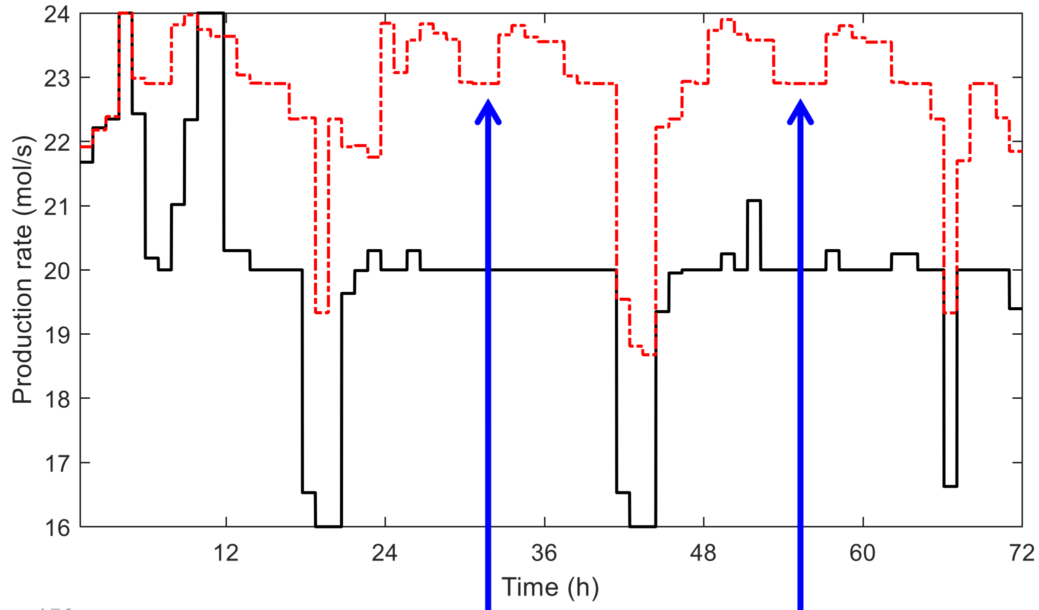

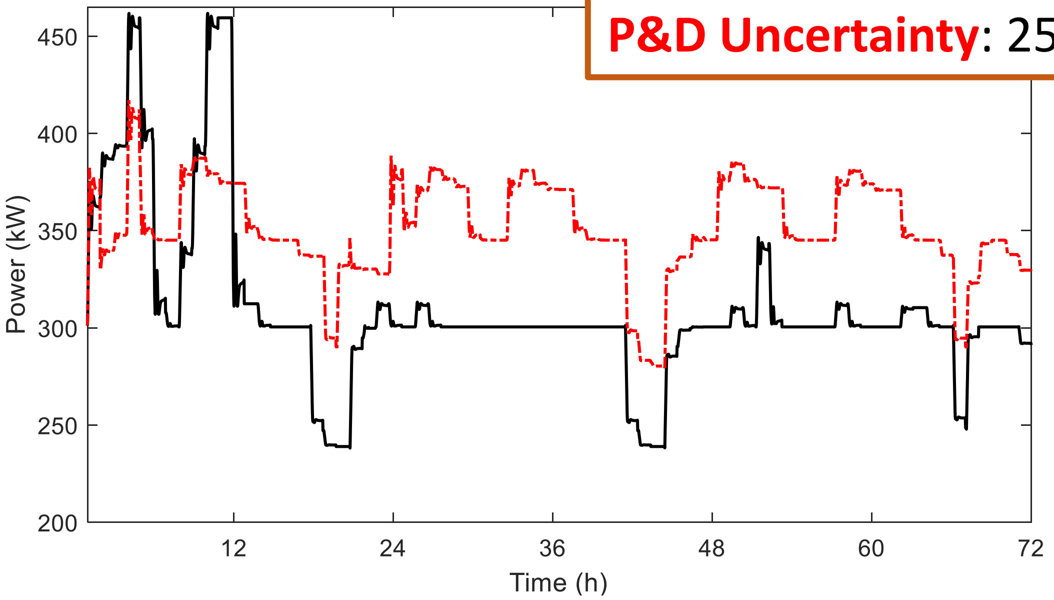

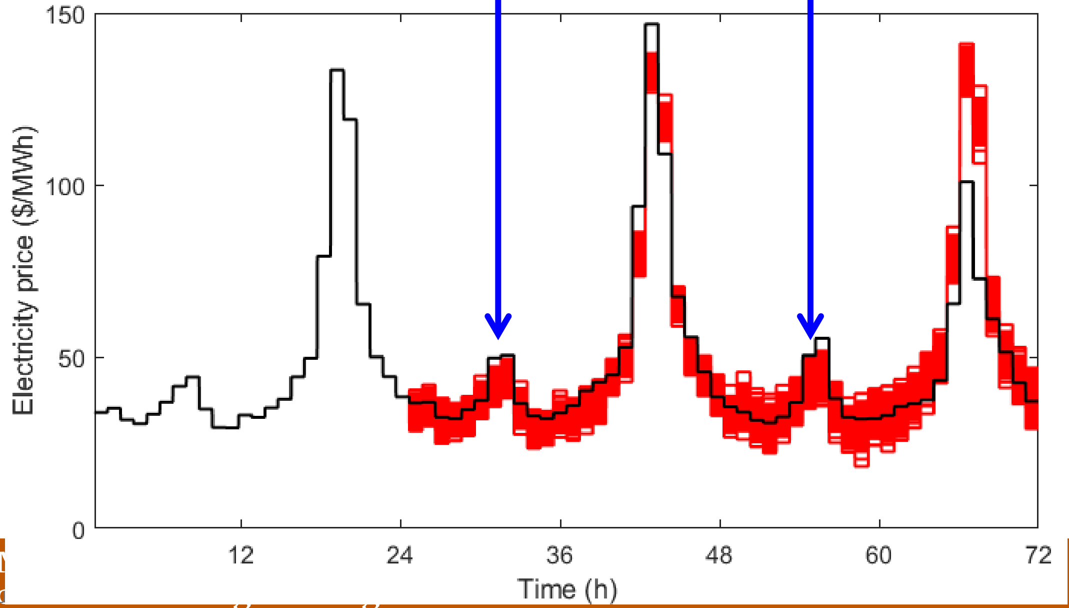

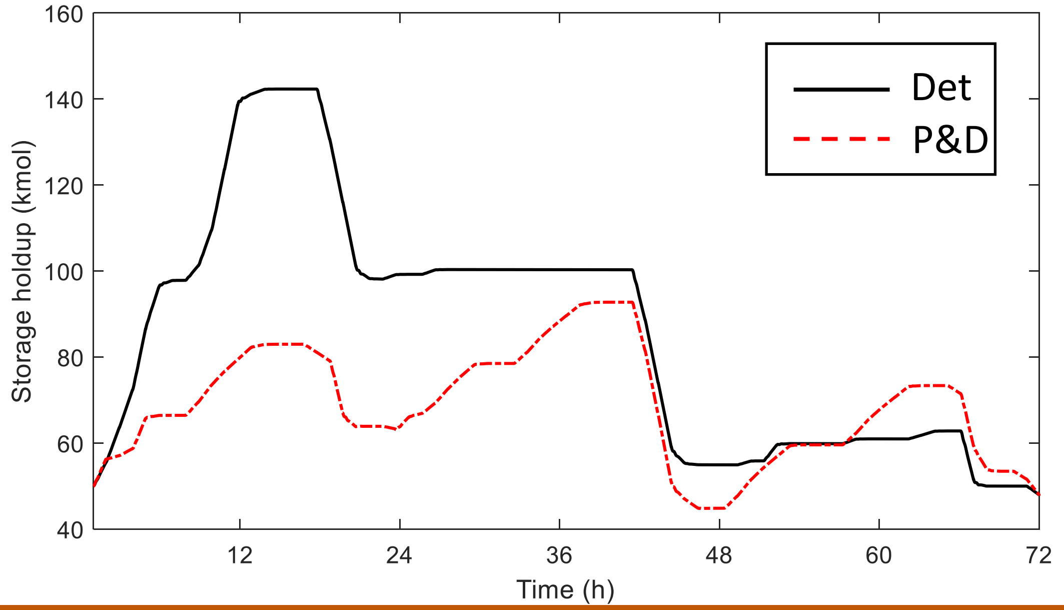

Kelley, M. T., Baldick, R. & Baldea, M. Demand response scheduling under uncertainty: Chance-constrained framework and application to an air separation unit. *AIChE J.* 66, (2020).

Moving Horizon Scheduling

Example: Scheduling of two days at a time, for a total time horizon of 4 days

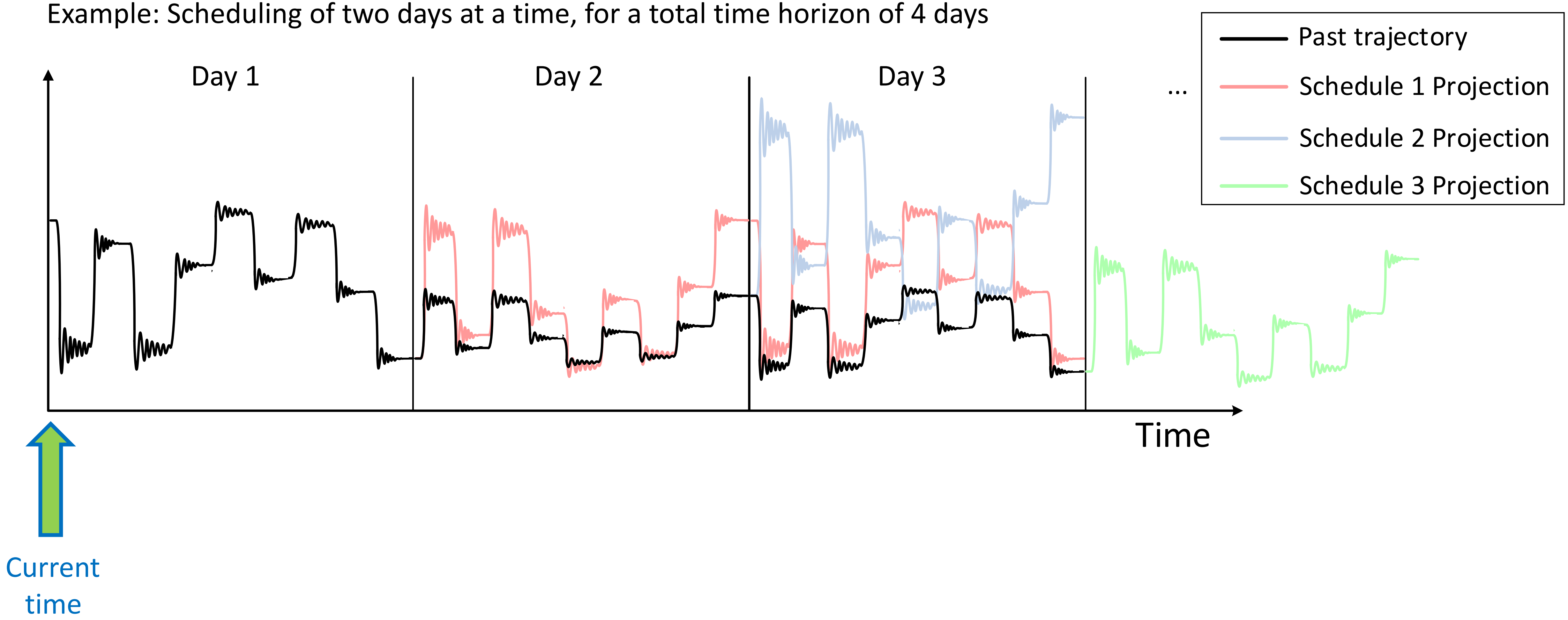

New information available

New information available

New information available

Periodic pricing updates

Scheduling Window | Unscheduled Day | Day in the past

PP1 Ideal

Reschedule 1	Day 1	Day 2	Day 3	Day 4	Day 5	Day 6

PP2 Realistic

Reschedule 1	Day 1	Day 1	Day 1			
Reschedule 2	Day 1	Day 2	Day 2	Day 2		
Reschedule 3	Day 1	Day 2	Day 3	Day 3	Day 3	
Reschedule 4	Day 1	Day 2	Day 3	Day 4	Day 4	Day 4

Key findings:

1. When accurate price predictions are known, scheduling methods are comparable
2. When forecasts are inaccurate, losses in savings are evident

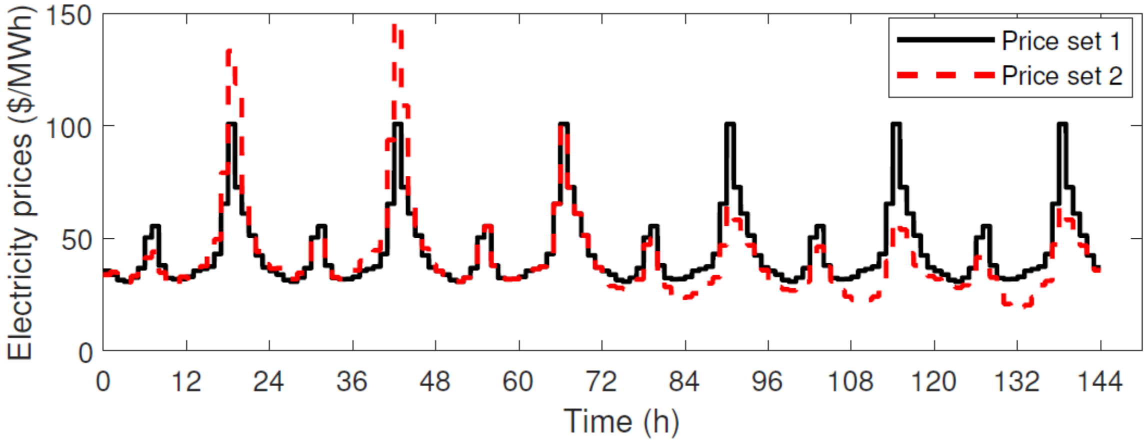

Price set 1: Truly periodic—comparison of scheduling methods without price effects

Price set 2: Historical values from CAISO

Kelley, M. T., Baldick, R. & Baldea, M. An empirical study of moving horizon closed-loop demand response scheduling. *J. Process Control* 92, 137–148 (2020).

CAISO. (2017). *California Independent System Operator*. http://www.caiso.com/Pages/default.aspx

Demand disturbances

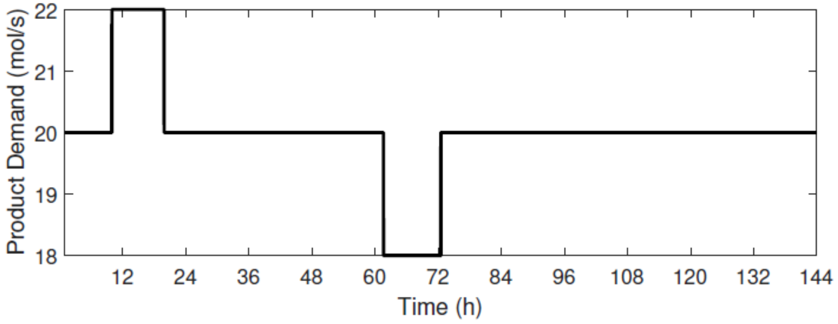

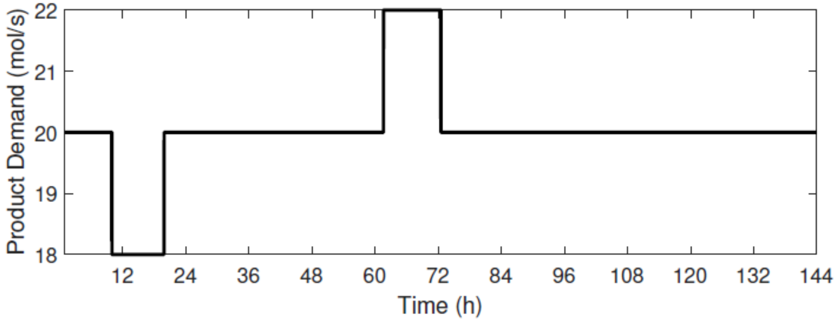

Key findings:
PD4 left room for constraint violations (particularly with a step down towards the end) due to storage depletion

PD5 was far and away a more conservative solution, but mitigated infeasibilities

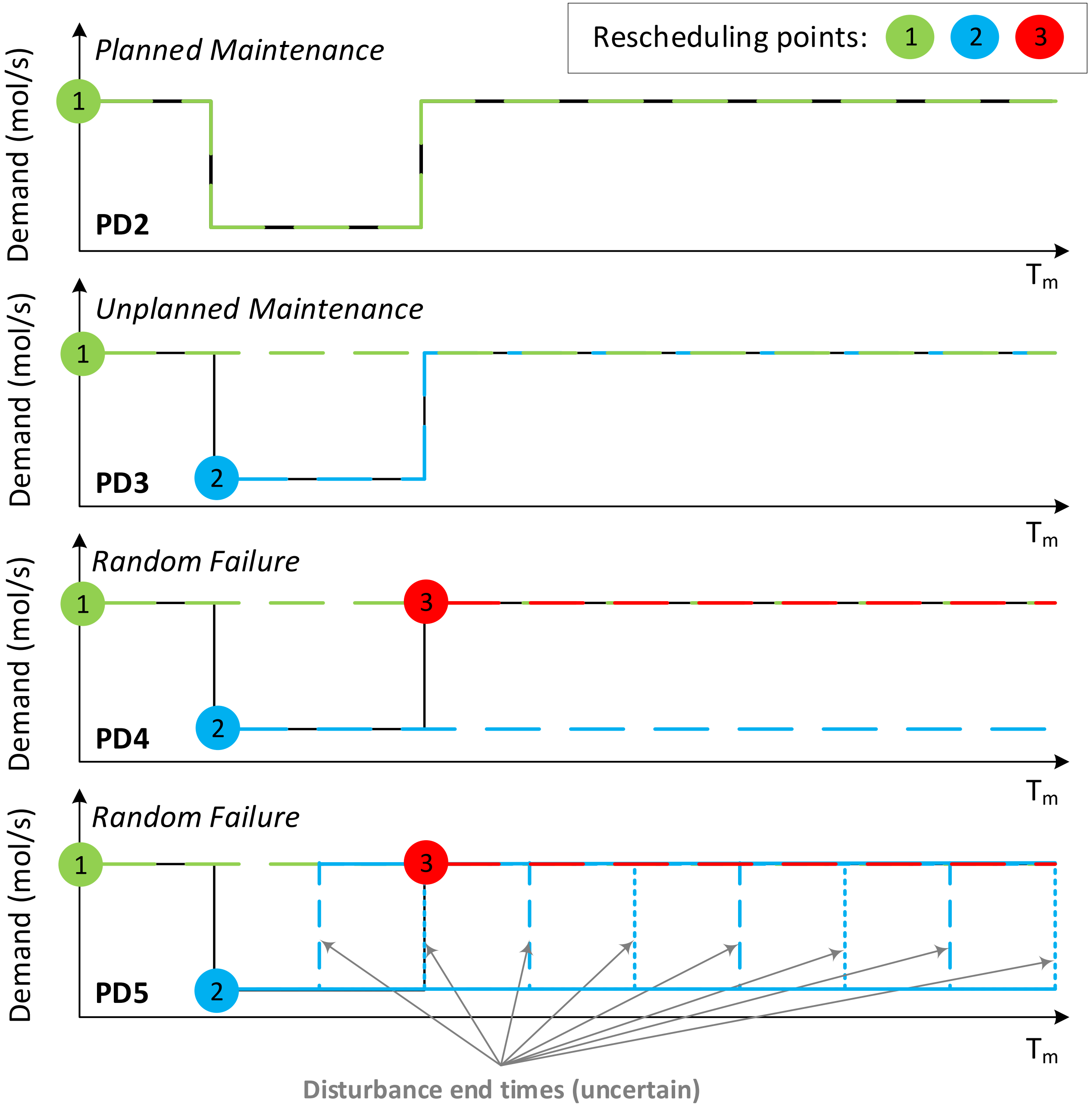

Kelley, M. T., Baldick, R. & Baldea, M. An empirical study of moving horizon closed-loop demand response scheduling. *J. Process Control* 92, 137–148 (2020).

Moving horizon vs chance-constraints

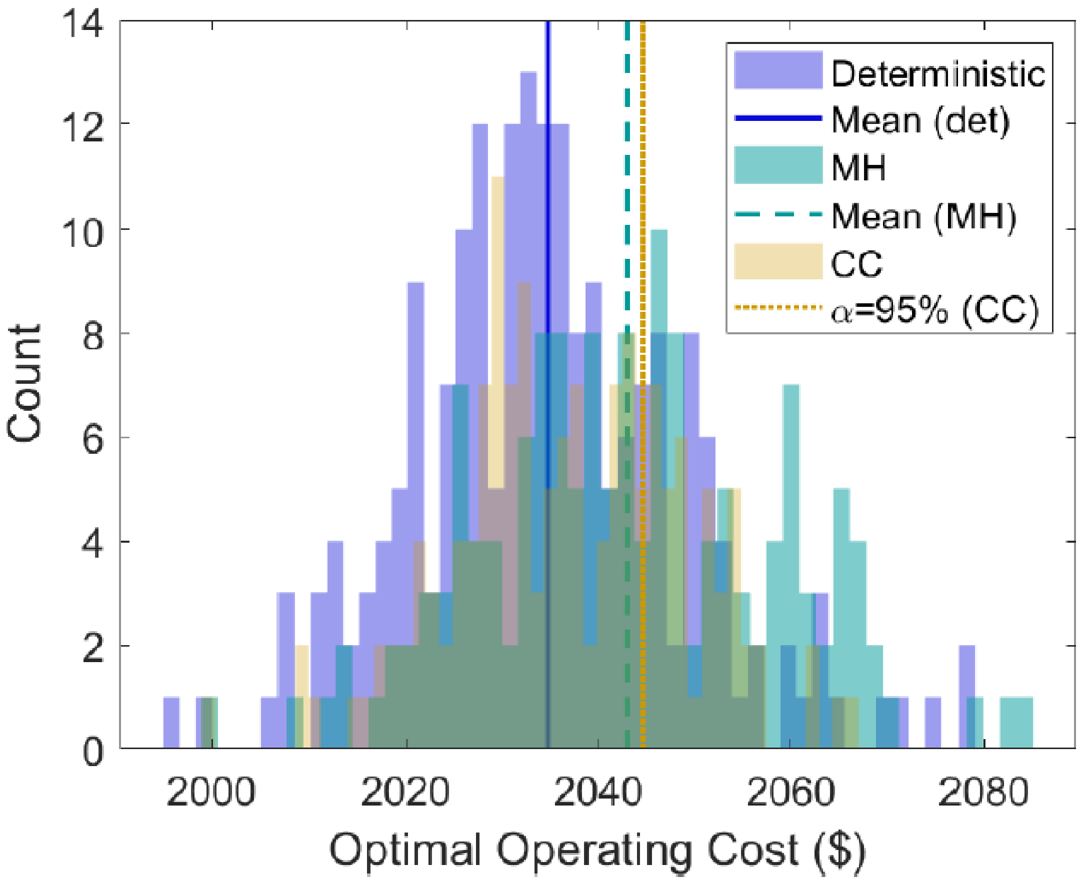

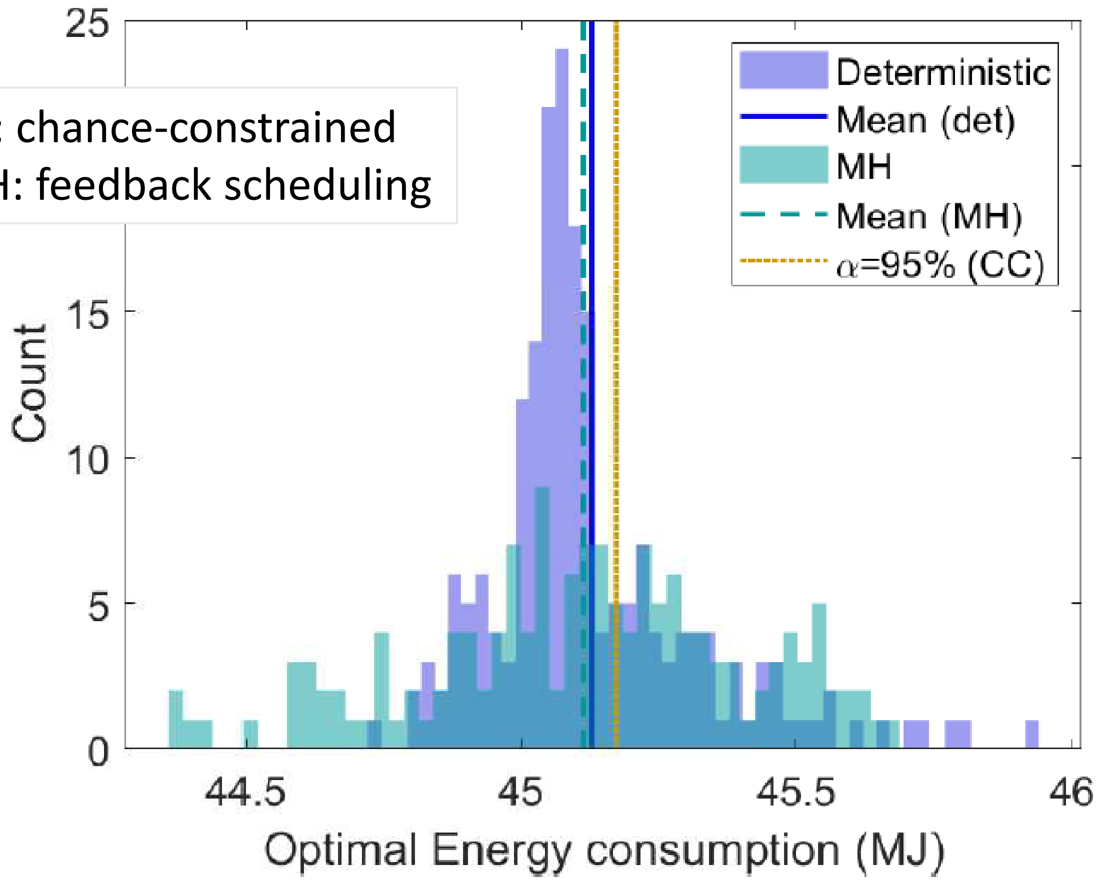

CC: chance-constrained
MH: feedback scheduling

MH and CC methods are comparable, with the MH method allowing more room for correction at rescheduling points

Future work: Extension of feedback vs. uncertainty quantification methods to supply chain planning

Summary: Large-scale application to an air separation unit

- DR scheduling of an ASU using SBMs and LR
  - Found a reduction in operating cost of 1.1%
  - Future work: Network of ASUs operating to meet localized demand
- Two computationally efficient methods of capturing uncertainties
  - Chance-constraints
  - Moving-horizon scheduling
- Future work: Extension of feedback vs. uncertainty quantification methods to supply chain planning
- Publications:

Kelley, M. T., Pattison, R. C., Baldick, R. & Baldea, M. An MILP framework for optimizing demand response operation of air separation units. *Appl. Energy* 222, 951–966 (2018).

Kelley, M. T., Baldick, R. & Baldea, M. An empirical study of moving horizon closed-loop demand response scheduling. *J. Process Control* 92, 137–148 (2020).

Kelley, M. T., Baldick, R. & Baldea, M. Demand response scheduling under uncertainty: Chance-constrained framework and application to an air separation unit. *AIChE J.* 66, (2020).

EMP overview

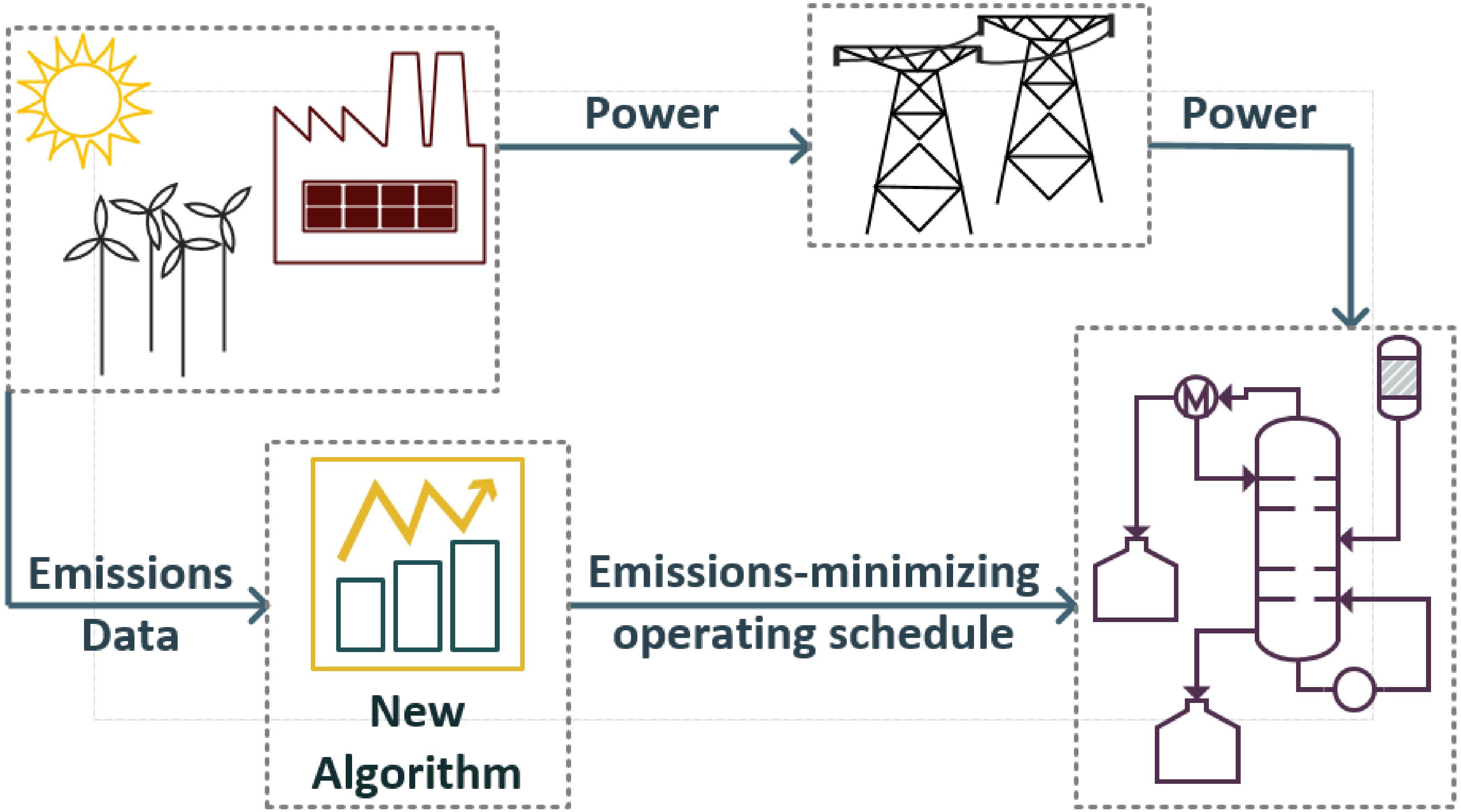

Emissions Factor

Combined hourly emissions factor for each source:

Source	kg CO_2/MWh[4]
Biomass	366.66*
Biogas	177.66
Thermal	181.04
Imports	428

*Average of biomass emissions factors

Renewables	Non-renewables
Geothermal	Thermal (natural gas)
Biomass	Nuclear
Biogas	Imports (petroleum, coal, etc.)
Small# hydropower	Large hydropower
Wind	
PV-Solar	
Solar Thermal	

#<30 MW generation capacity

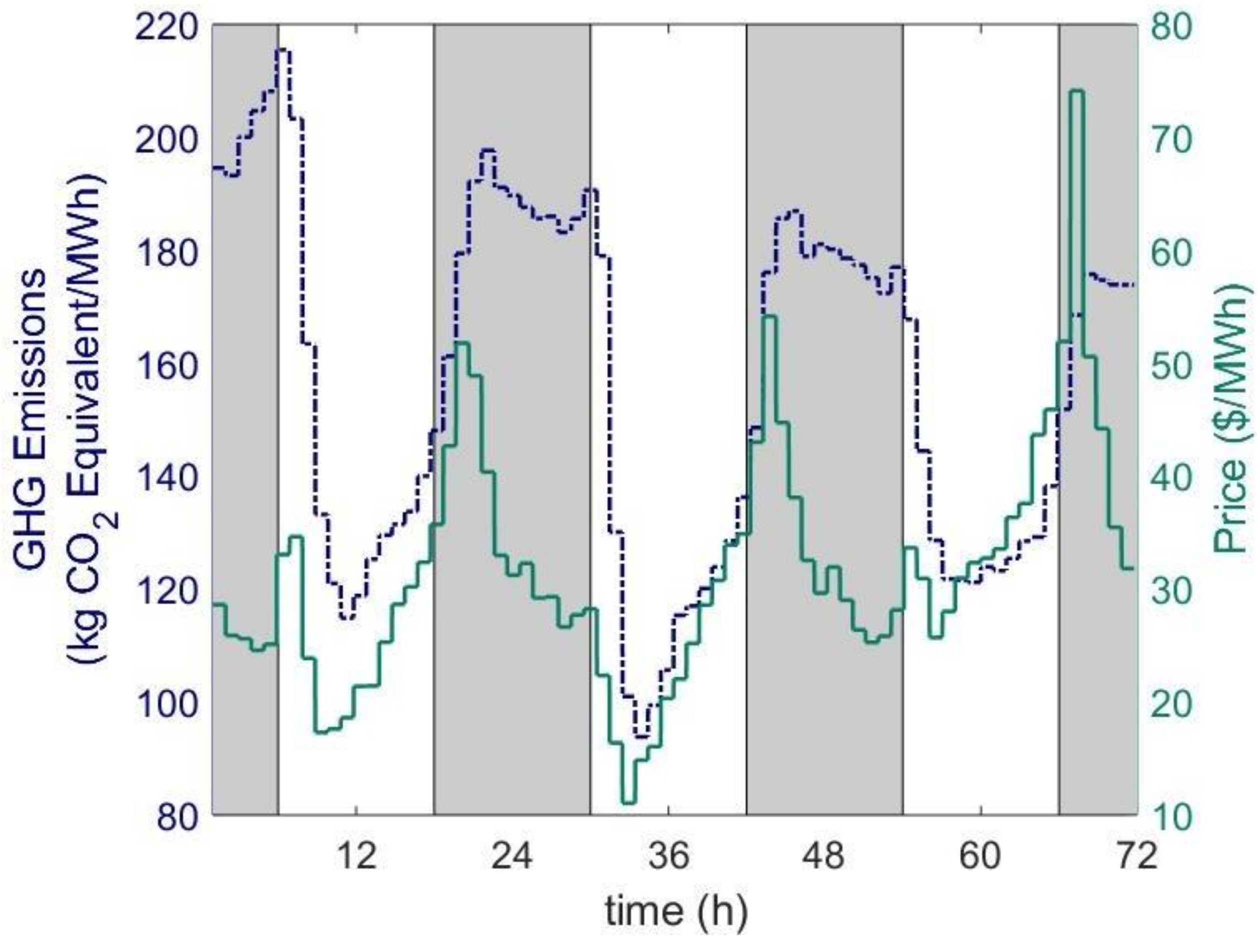

Calculated combined emissions factors for July 3-5 2017 from data supplied by CAISO [2]

[4] *Emission Factors for Greenhouse Gas Inventories*. EPA (2014).

DR scheduling of an ammonia plant

Linear dynamic models

More accurately represent systems than steady-state models

- Account for differing time-scales/time delays within the plant

Power consuming units

- Compressors drive power consumption within the process
- Can modulate their power usage by changing variables in the process such as flowrates and reactor splits

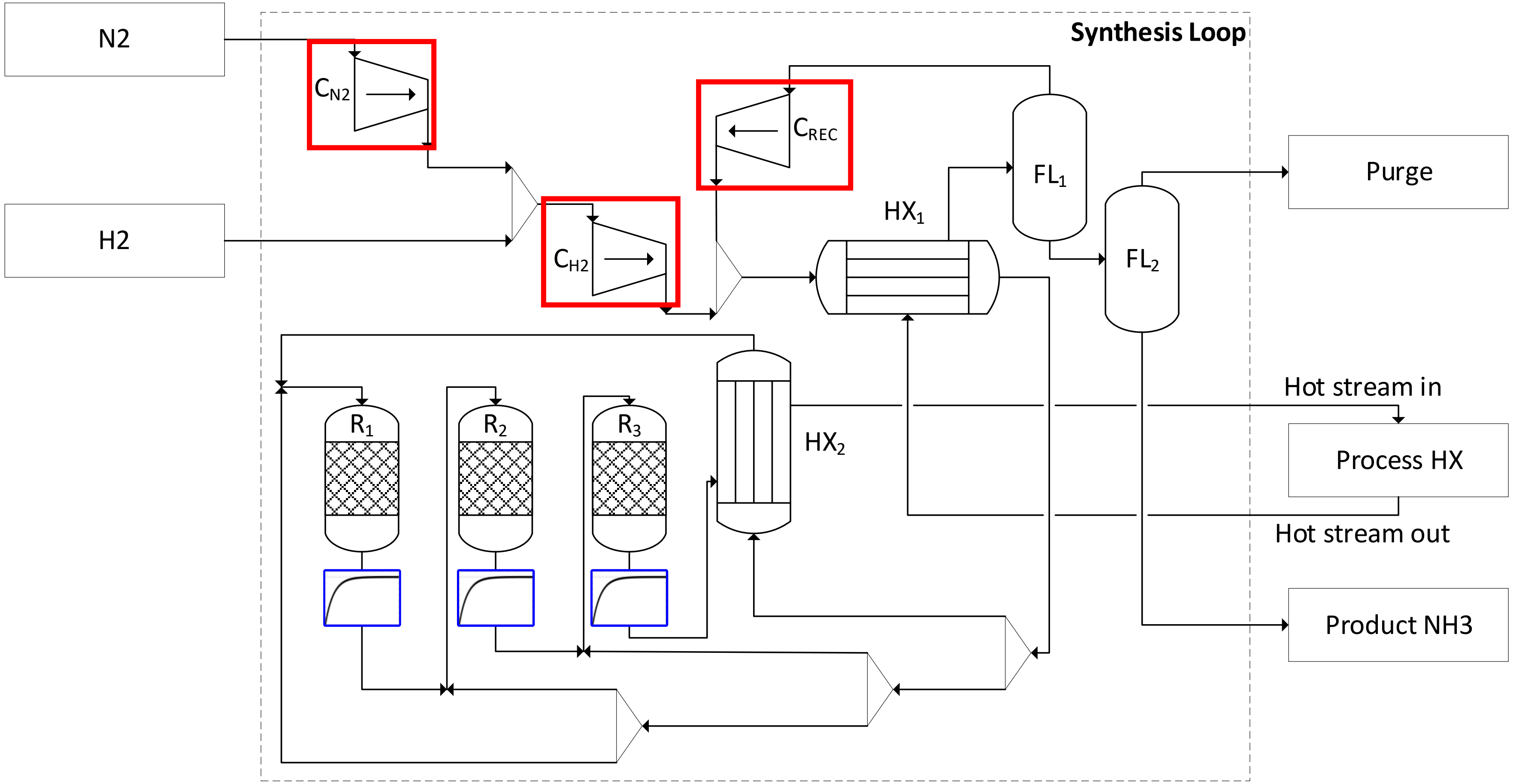

Compared to a process operating at steady-state:

- 1.5% reduction in operating cost a
- 7.74% decrease in peak power consumption

Future work:

1. Verify this heuristic approach to modeling dynamics via plant data
2. Ammonia synthesis loop as part of a larger system (including an ASU) for DR

Kelley, M. T., Do, T. T. & Baldea, M. Evaluating the Demand Response Potential of Ammonia Plants. *AIChE Journal, In revision*. (2021).

Summary: Extensions of DR scheduling work

- Adapted DR scheduling framework to grid-side emissions minimizing production (EMP)
- Identified linear ARX models for representing a 3-product ASU based on a year's worth of plant data, demonstrating savings of 8.9%

  Future work: Adaptation of current models to new plants

- Demonstrated applicability of ammonia synthesis loop for DR operation with savings of 1.5%
  - Future work: (1) Verify this heuristic approach to modeling dynamics via plant data, and (2) Ammonia synthesis loop as part of a larger system (including an ASU) for DR

Publications:

Kelley, M. T., Baldick, R. & Baldea, M. Demand Response Operation of Electricity-Intensive Chemical Processes for Reduced Greenhouse Gas Emissions: Application to an Air Separation Unit. *ACS Sustain. Chem. Eng.* 7, 1909–1922 (2019).

Kelley, M. T., Tsay, C. & Baldea, M. A data-driven linear formulation of the optimal demand response scheduling problem for an industrial air separation unit. *Chem. Eng. Sci. Submitted.* (2021).

Kelley, M. T., Do, T. T. & Baldea, M. Evaluating the Demand Response Potential of Ammonia Plants. *AIChE Journal, In revision.* (2021).

Lagrangean Relaxation

Theorem 1. If $\mathbf{PI}$ is feasible and the equality constraints in $\mathbf{PII}$ are met, then the solution to $\mathbf{PII}$ is *optimal* for $\mathbf{PI}$

Proof: Assume a feasible solution exists to $\mathbf{PI}$ (i.e. state continuity constraints can be met, and the production schedule is *dynamically feasible*).

Then, when equality constraints $\gamma_i = \left| x_{i-1,N_J} - x_{i,1} \right| = 0$ are met, the objectives of $\mathbf{PI}$ and $\mathbf{PII}$ are the same, $\mathrm{L} = \mathrm{J}$, and the relaxed sub-problem $\mathbf{PII}$ is equivalent to the original problem $\mathbf{PI}$. □

PII

$$\max L_m = J_m - \sum_{k=1}^{n} \sum_{i=2}^{N_I} \lambda_{im}^k \gamma_{im}^k$$

s.t.

Linear surrogate models (HW/FSR)

Initial Conditions

Process/safety constraints

Quality constraints

[12] Guignard, M. (2003). Lagrangean relaxation. *Top*, *11*(2), 151–200. https://doi.org/10.1007/BF02579036

Slot-based Cyclical Scheduling

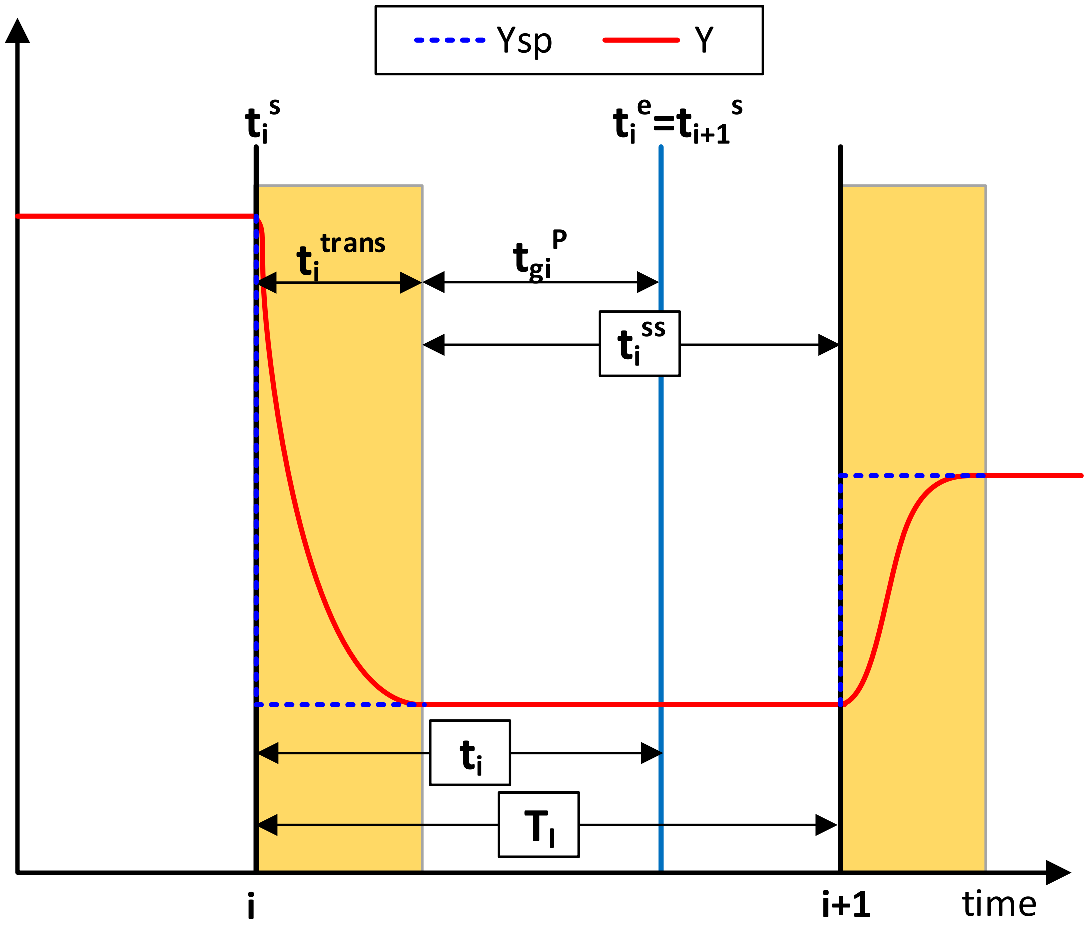

Product assignment to slots

$$\sum_g z_{gi} = 1 \ \forall i$$

$$\sum_i z_{gi} = 1 \ \forall g$$

Demand satisfaction

$$D_g \leq p_g \leq p_g^{max}$$

$$p_g \geq P_g t_g^P$$

Timing

$$t_{gi}^P = t_g^P z_{gi}$$

$$t_i^{trans} = T_I - t_i^{ss}$$

$$t_i^e = t_i^s + t_i^{trans} + \sum_g t_{gi}^P$$

Inventory Model

Cost of storage

$$c_g^{st} = C_g^{st} \sum_i t_{gi}^{st} p_{gi}$$

Revenue

$$R = \sum_g Pr_g p_g$$

Maximum storage holdup

$$0 \leq s_{gij} < s_g^{max}$$

Time spent in storage

$$t_{gi}^{st} = z_{gi}(t_C - t_i^e)$$

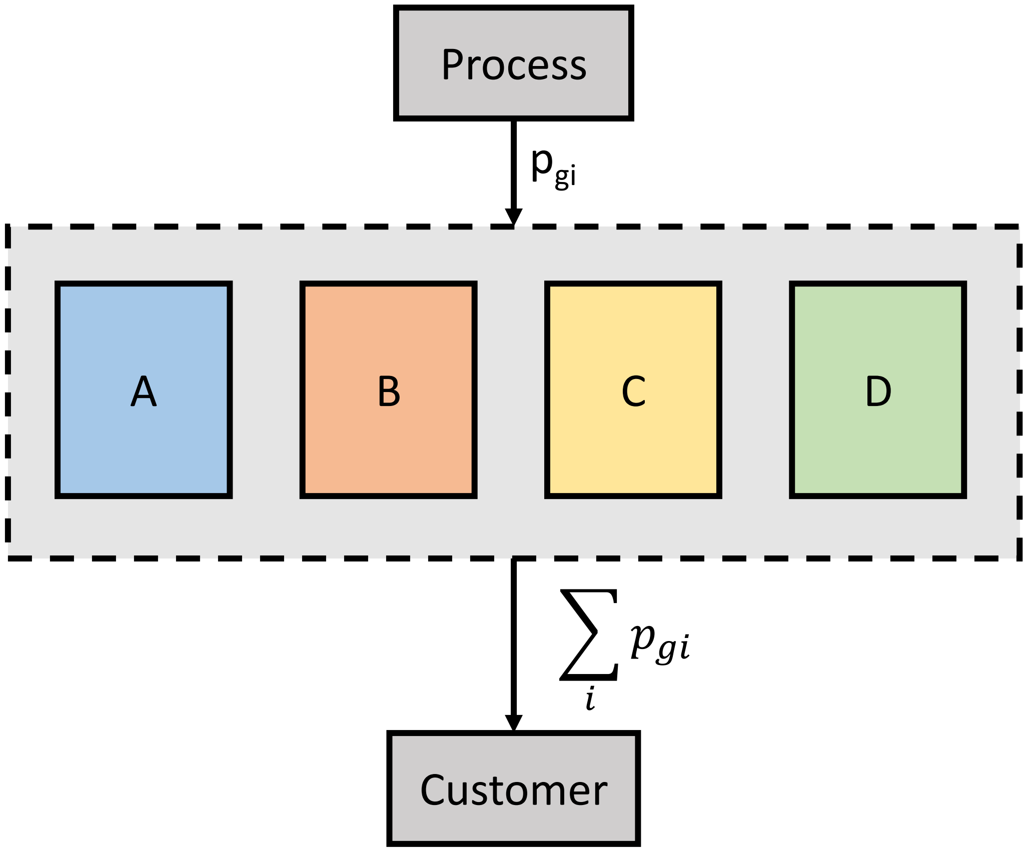

Process Dynamics: SBMs

- Scheduling-Relevant Variables: $w_{ij} = \{F^{cw}, F^{I}, \mu, T\}$
- Sampling times (mins): $T_J = \{5.96, 5.96, 2.68, 2.68\}$
- HW models:

Input	Output	H(u)	State-space Order	W(y)	Sample time (s)	%fit
$\bar{T}_i$	F^{cw}	4	2	10	5.96	99.79
$\bar{T}_i$	F^{I}	4	2	13	5.96	99.35
$\bar{T}_i$	T	1	2	0	2.68	99.93
$\bar{T}_i$	μ	4	2	0	2.69	99.89

- FSR models:

Input	Output	Sample time (s)	%fit
$\bar{T}_i$	F^{cw}	5.96	99.64
$\bar{T}_i$	F^{I}	5.96	99.99
$\bar{T}_i$	T	2.68	99.65
$\bar{T}_i$	μ	2.69	99.99

$$\%fit = \frac{100\left(\left|\sum w_{ij}^{ref} - \sum w_{ij}\right|\right)}{\sum w_{ij}^{ref}}$$

Solution methods

Sequential	Simultaneous	Multiple Shooting (MS)
Decision variables are discretized and optimized with an NLP solver	Discretize the entire problem space	Time horizon divided into smaller intervals with piecewise control vector (solved with Lagrangian relaxation)
$\max_{u} J = f\left(\boldsymbol{x}, \boldsymbol{y}, \boldsymbol{u}, t_f\right)$ $s.t. \frac{dx}{dt} = g(\boldsymbol{x}, \boldsymbol{y}, \boldsymbol{u})$ $\boldsymbol{x}(t_o) = \boldsymbol{x}_o$ $\boldsymbol{x}^L \leq \boldsymbol{x} \leq \boldsymbol{x}^U$ $\boldsymbol{y}^L \leq \boldsymbol{y} \leq \boldsymbol{y}^U$ $\boldsymbol{u}^L \leq \boldsymbol{u} \leq \boldsymbol{u}^U$	$\max_{\boldsymbol{u}_i} J = f\left(\boldsymbol{x}_{N_i,N_j}, \boldsymbol{y}_{N_i,N_j}, \boldsymbol{u}_{N_i}\right)$ $s.t. \quad \boldsymbol{x}_{i,j+1} = g\left(\boldsymbol{x}_{i,j+1}, \boldsymbol{y}_{i,j+1}, \boldsymbol{u}_i\right)\Delta \mathrm{j} + \mathbf{x}_{\mathrm{i,j}}$ $\boldsymbol{x}_{i-1,N_j} = \boldsymbol{x}_{i,j=1} \; \forall i > 1$ $\boldsymbol{x}(t_o) = \boldsymbol{x}_o$ $\boldsymbol{x}^L \leq \boldsymbol{x}_{i,j} \leq \boldsymbol{x}^U$ $\boldsymbol{y}^L \leq \boldsymbol{y}_{i,j} \leq \boldsymbol{y}^U$ $\boldsymbol{u}^L \leq \boldsymbol{u}_{i,j} \leq \boldsymbol{u}^U$	$\max_{\boldsymbol{u}_i} L = J - \sum_i \boldsymbol{\lambda}_i \boldsymbol{\gamma}_i$ $s.t. \quad \boldsymbol{x}_{i,j+1} = g\left(\boldsymbol{x}_{i,j+1}, \boldsymbol{y}_{i,j+1}, \boldsymbol{u}_i\right)\Delta \mathrm{j} + \mathbf{x}_{\mathrm{i,j}}$ $\boldsymbol{x}(t_o) = \boldsymbol{x}_o$ $\boldsymbol{x}^L \leq \boldsymbol{x}_{i,j} \leq \boldsymbol{x}^U$ $\boldsymbol{y}^L \leq \boldsymbol{y}_{i,j} \leq \boldsymbol{y}^U$ $\boldsymbol{u}^L \leq \boldsymbol{u}_{i,j} \leq \boldsymbol{u}^U$

ASU SBMs

HW models

Input	Output	Input Nonlinearity	Linear Dynamics	Output Nonlinearity		NMSE	
u	w	H(u) Breakpoints	State-space Order	W(y) Type	W(y) Breakpoints	Training	Validation
$\underline{F}^p$	I^P	4	4	PWL	6	0.82	0.52
$\underline{F}^p$	M^R	3	4	linear	--	0.78	0.75
$\underline{F}^p$	δ^f	5	5	quadratic	--	0.91	0.92
$\underline{F}^p$	P^d	2	8	quadratic	--	0.83	0.97
$\underline{F}^p$	ΔT	9	4	PWL	6	0.69	0.84

Variable	Sample Time (mins)	%Fit
I^P	6	99.85
M^R	0.5	99.93
dT	6	99.80
δ^f	10	99.63
P^d	10	99.97

Linearization is exact

FSR models

Variable	Sample Time (mins)	%Fit to full order model data
F^P	1	99.81
F^f	1	99.96

R. C. Pattison, C. R. Touretzky, T. Johansson, I. Harjunkoski, and M. Baldea, "Optimal Process Operations in Fast-Changing Electricity Markets: Framework for Scheduling with Low-Order Dynamic Models and an Air Separation Application," *Ind. Eng. Chem. Res.*, vol. 55, no. 16, pp. 4562–4584, Apr. 2016.

DR Optimal Scheduling with Nonlinear Models

Full-order first-principles model (P1)

$$\min_{y_p^{sp,n},\, \alpha^{sp,n}, y_{inv}^{sp,n}} J = \int_0^{T_m} \Phi\left(p, v_p, y_p, y_{inv}, \tilde{y}\right) dt$$

s.t.
Timing constraints
Process model (Full-order)
Inventory model
Product split
Product mixing
Initial Conditions
Process and Quality Constraints

Time horizon: 72 hours
Solution time: 94.62 hours
Optimal operating cost: $1,012.56
Cost savings (%): 1.22%

[4]

64 bit Windows system Intel Core i7-2600 CPU at 3.40 GHz and 16 GB RAM
Solved in gPROMS[5]

Reduced-order nonlinear HW models (P2)

$$\min_{F_p^{sp,n}} \phi = \int_0^{T_m} Price(t)\mathcal{P}(t)\, dt$$

s.t.
Timing constraints
Process model (HW)
Inventory model
Product split
Product mixing
Initial Conditions
Process and Quality Constraints

Time horizon: 72 hours
Solution time: 5.10 hours
Optimal operating cost: $1,014.81
Cost savings (%): 1.01%

[4]

64 bit Windows system Intel Core i7-2600 CPU at 3.40 GHz and 16 GB RAM
Solved in gPROMS[5]

[5] Process Systems Enterprise, “gPROMS Process Builder.”

DR Optimal Scheduling with Linear Models

MILP HW/FSR models (P3)

$\min_{u_i} J = \sum_i \sum_j Price_i \mathcal{P}_{ij}$ **(P3)**

s.t.

Timing constraints

Process model (HW/FSR)

Inventory model

Initial Conditions

Process and Quality Constraints

Continuity Constraints

Continuous Variables: 85,131

SOS2 Variables: 1,512

Time horizon: 72 hours

Solution time: 11.7 min

Optimal operating cost: $1,013.64

Cost savings: 1.12%

Optimality gap: 0.053%

MILP HW/FSR models with LR (P4)

$$\min_{u_i} L_m = \sum_i \sum_j Price_i \mathcal{P}_{ijm} + LD_{im}\gamma_{im}$$

s.t.

Timing constraints

Process model (HW/FSR)

Inventory model

Initial Conditions

Process and Quality Constraints

Continuous Variables: 90,325

SOS2 Variables: 1,512

Time horizon: 72 hours

Solution time: 7.12 mins

Optimal operating cost: $1,013.64

Cost savings: 1.12%

Optimality gap: 0.040%

Uncertain Electricity Prices

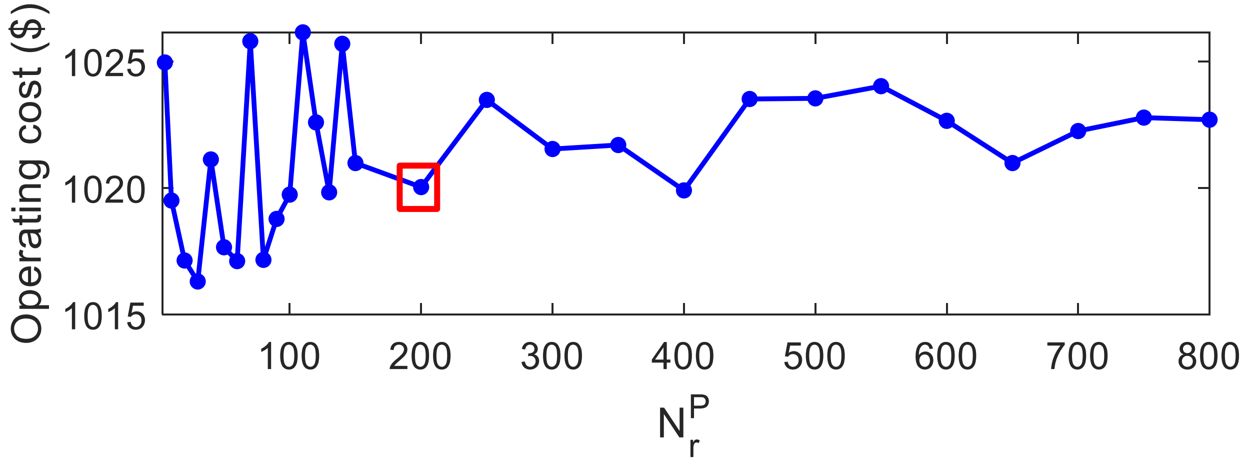

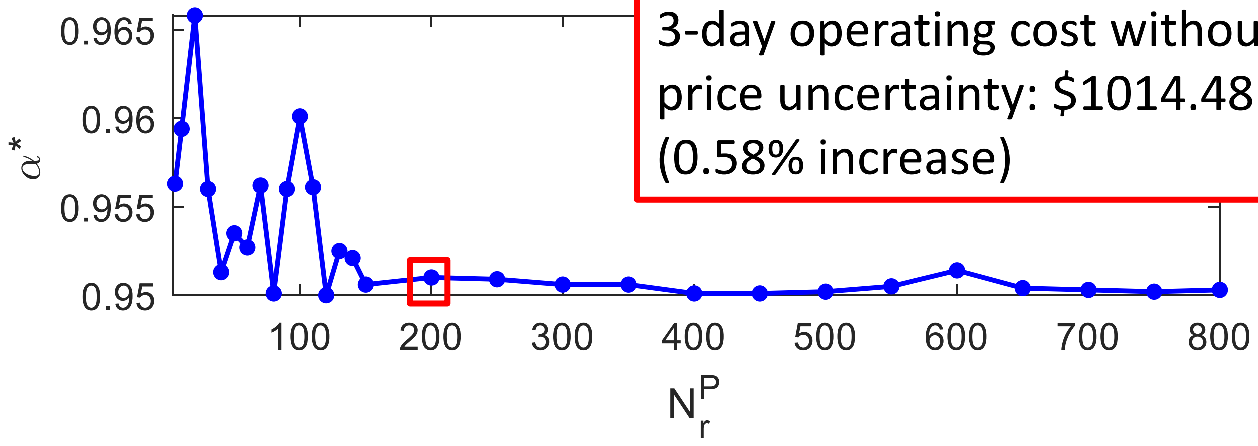

3-day operating cost without price uncertainty: $1014.48 (0.58% increase)

For $N_r^P = 200, \alpha = 0.95$
Optimal cost: $1020.39
Soln time: 7.39 ± 0.02 min

$$\min C = \sum_i \sum_j P_i \Phi_{i,j}$$

s.t. $C + (1 - z_r^P)M \geq \sum_i \sum_j P_{i,r} \Phi_{i,j}$

$$\sum_r z_r^P \pi_r \geq \alpha$$

$\pi_r = \Pr[P_{i,r}]$

$0 < \alpha \leq 1$

$P_i \sim \mathcal{N}_{mvn}(\mu_i, \Sigma_\mathrm{i})$

Process model (HW/FSR)

Process constraints

Quality constraints

Initial conditions

Continuity conditions

Demand constraints (D_i=20 mol/s)

Uncertain Product Demand

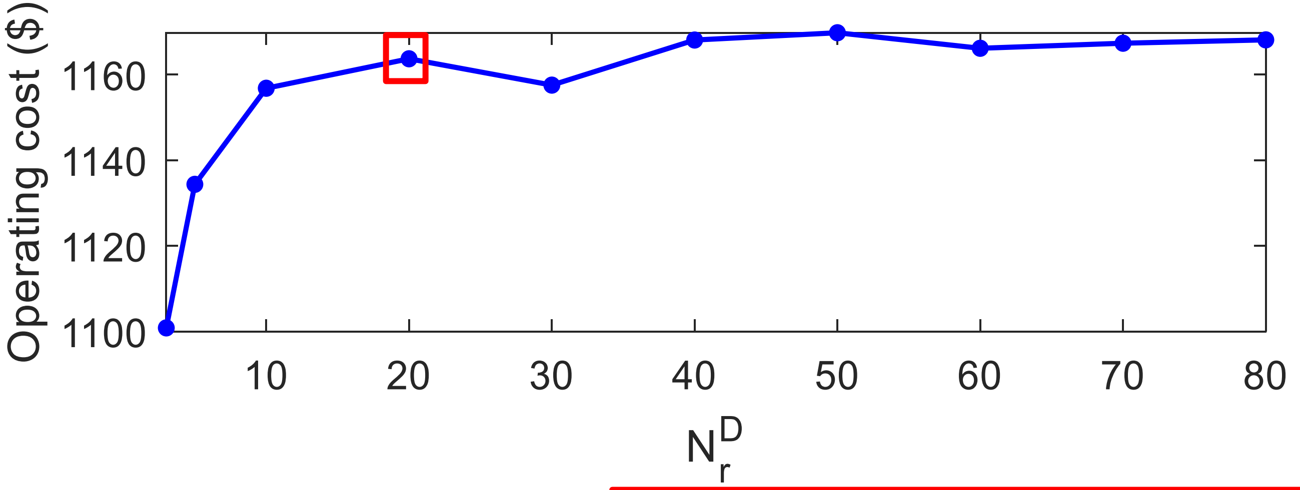

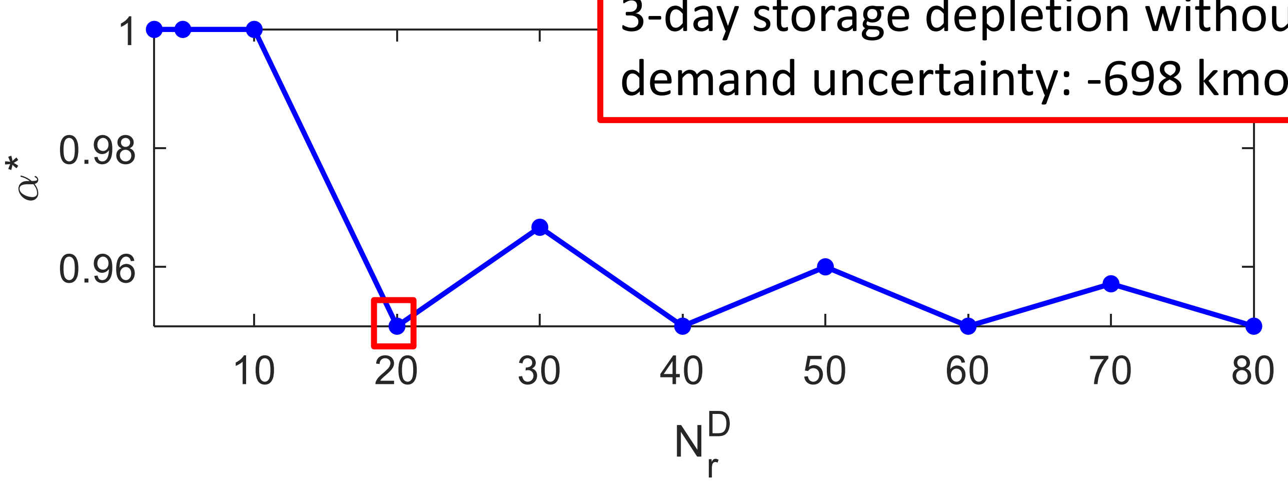

3-day storage depletion without demand uncertainty: -698 kmol

For $N_r^D = 20, \alpha = 0.95$
Optimal cost: \$1163.67 (+14.7%)
Soln time: 2.06 ± 0.02 min

$$\min C = \sum_i \sum_j P_i \Phi_{i,j}$$

s.t. $F_{i,j}^p - D_{i,r} \geq f_{s_{i,j}}^{in} - f_{s_{i,j}}^{out} - M(1 - z_r^D)$

$$\sum_r z_r^D \geq \alpha N_R^D$$

$$0 \leq \alpha \leq 1$$

$$D_i \sim \mathcal{U}[16,23] \; t_{start} \sim \mathcal{U}[0,72]$$

Process model (HW/FSR)

Process constraints

Quality constraints

Initial conditions

Continuity conditions

Uncertain Electricity Prices and Product Demand

$\min C$

s.t. $C + (1 - z_r^P)M \geq \sum_i \sum_j P_{i,r}\Phi_{i,j}$

$$\sum_r z_r^P \pi_r \geq \alpha$$

$\pi_r = \Pr\left[P_{i,r}\right]$

$F_{i,j}^p - D_{i,r} \geq f_{s_{i,j}}^{in} - f_{s_{i,j}}^{out} - M(1 - z_r^D)$

$$\sum_r z_r^D \geq \alpha N_R^D$$

$0 \leq \alpha \leq 1$

$D_i \sim \mathcal{U}[16,23]$

$P_i \sim \mathcal{N}_{mvn}(\mu_i, \Sigma_\mathrm{i})$

Process model (HW/FSR)

Process and quality constraints

Initial conditions

Continuity conditions

For $N_r^D = 20$, $\mathrm{N_r^P} = 200$, $\alpha = 0.95$

Optimal cost: \$1,172.69 (+15.6%)

Soln. time: 7.56 ± 0.03 min

Key point:

The proposed method accounts for *errors* that arise in predictions of uncertain parameters—its applicability is independent of the methods chosen to predict electricity prices and demand

ARX Models

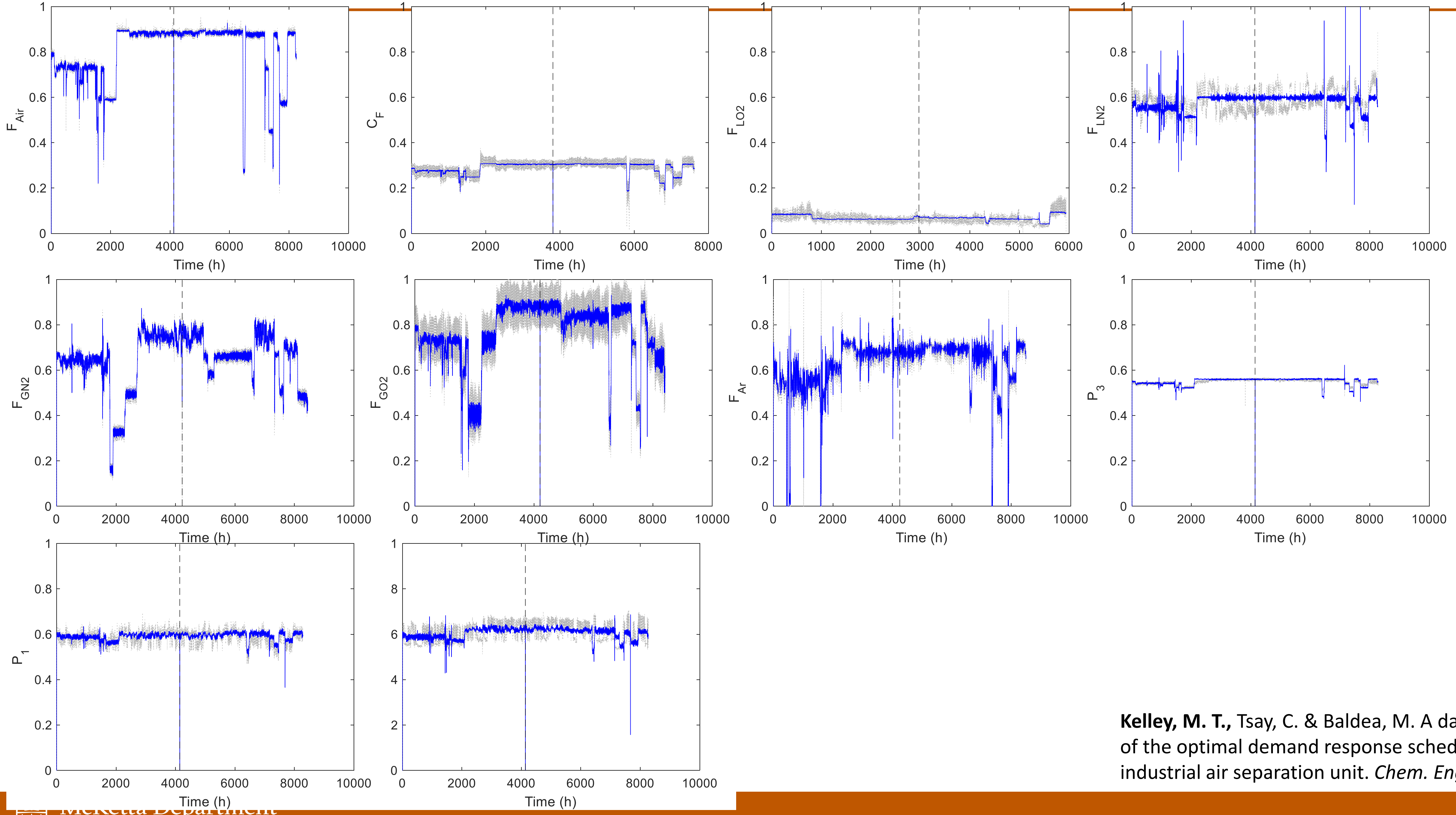

Kelley, M. T., Tsay, C. & Baldea, M. A data-driven linear formulation of the optimal demand response scheduling problem for an industrial air separation unit. *Chem. Eng. Sci. Submitted*. (2021).